SAFE CONTROL METHODS FOR NONLINEAR DYNAMICAL SYSTEMS

By

HANNAH M. SWEATLAND

A DISSERTATION PRESENTED TO THE GRADUATE SCHOOL
OF THE UNIVERSITY OF FLORIDA IN PARTIAL FULFILLMENT
OF THE REQUIREMENTS FOR THE DEGREE OF
DOCTOR OF PHILOSOPHY

UNIVERSITY OF FLORIDA

2024

To my parents, Tod and Michelle

ACKNOWLEDGMENTS

I thank my adviser, Dr. Warren Dixon, for his mentorship. Dr. Dixon has provided me with invaluable guidance, encouragement, and life lessons over the past four years. I am also profoundly thankful to my dissertation committee members, Dr. Dan Ferris, Dr. Scott Banks, and Dr. Emily Fox, for their advice and insights. Without Dr. Ferris, I would never have pursued a PhD. I would like to express my appreciation for my family and friends for their love, motivation, and much needed distractions from research. Additionally, I would like to thank my colleagues in the Nonlinear Controls and Robotics Laboratory and external collaborators for the time, assistance, and expertise they have provided. Lastly, I would like to thank Brendan Sutton for his support and endless patience. This dissertation would not have been possible without the guidance and encouragement of these individuals, and for that, I am profoundly grateful.

TABLE OF CONTENTS

LIST OF TABLES

LIST OF FIGURES

Figure page

LIST OF ABBREVIATIONS

ACC	Adaptive Cruise Control
aDCBF	Adaptive Deep Neural Network Control Barrier Function
CBF	Control Barrier Function
CLF	Control Lyapunov Function
DNN	Deep Neural Network
FES	Functional Electrical Stimulation
HOCBF	High-Order Control Barrier Function
ICCBF	Input Constrained Control Barrier Function
IRB	Institutional Review Board
Lb	Lyapunov-based
ND	Neurological Disorder
NN	Neural Network
PBC	Passivity-Based Control
PCH	Port-Controlled Hamiltonian
QP	Quadratic Program
ResNet	Residual Neural Network
RISE	Robust Integral of the Sign of the Error
SOS	Sum-of-Squares

LIST OF SYMBOLS

=	equal to
$\neq$	not equal to
$\triangleq$	defined as
$\in$	an element of
$\mathbb{R}^n$	n-dimensional Euclidean space
$\mathbb{R}^{n\times m}$	the space of $n \times m$ dimensional matrices
$f : S_1 \to S_2$	a function f mapping a set S_1 into a set S_2
$\forall$	for all
$\exists$	there exists
$\subset$	a proper subset of
$\subseteq$	a subset of
$\sup$	supremum, the least upper bound
$\inf$	infimum, the greatest lower bound
$A^\top(x)$	the transpose of a matrix A (of a vector x)
sgn $(\cdot)$	the signum function
$\emptyset$	empty set

Abstract of Dissertation Presented to the Graduate School
of the University of Florida in Partial Fulfillment of the
Requirements for the Degree of Doctor of Philosophy

SAFE CONTROL METHODS FOR NONLINEAR DYNAMICAL SYSTEMS

By

Hannah M. Sweatland

December 2024

Chair: Warren E. Dixon
Major: Mechanical Engineering

Safety is an essential element in all control applications. This dissertation will explore how the safety of a control system can be defined and methods that can be used to provide safety guarantees. In the literature, set invariance and safety are often used synonymously, since the invariance of a safe set of states guarantees that system trajectories will never escape to an unsafe state. Invariance can be achieved by converting constraints on the state into constraints on the control input. In other cases, safety can be achieved by ensuring compliance of the system to external disturbances by requiring that the system can only dissipate energy. This dissertation extends currently available control strategies that can yield safety through two means: set invariance and passivity. The first is a control barrier function (CBF) method that allows for the use of an optimization-based controller to yield invariance while also adhering to other design specifications. The other is a passivity-based control (PBC) approach which uses a constructive design method to yield a safe controller. This Ph.D. dissertation consists of a literature review and research developments relating to safe control methods for nonlinear dynamical systems that are, in many cases, less restrictive than constructive Lyapunov-based methods.

Chapter 1 provides a general background and a literature review of safe control methods, including methods to ensure safety such as CBFs and PBC methods. Section 1.1 defines safety from a control systems perspective and provides background. In

Sections 1.2 and 1.3, I discuss how CBFs and PBC have been used to ensure safety of control systems and some limitations of previous works. Section 1.5 discusses works involving safety for human-robot interaction, including works on functional electrical stimulation (FES)-cycling systems. Some mathematical notation and other preliminaries are also briefly discussed.

Chapter 2 develops a high-order control barrier function (HOCBF) method for differential inclusions that can be applied to systems with more general dynamics than possible using previous HOCBF works. The effectiveness of the developed approach is demonstrated on a motorized rehabilitative cycle. An allowable set of motor controllers is designed to constrain the crank position to a time-varying user-defined safe range. Because of the uncertain and nonlinear dynamics of the system, robust control methods are borrowed from Lyapunov theory to develop worst-case controllers that render the intersection of a series of sets forward invariant. The implemented controller is designed so that it provides minimal assistance within the safe range, maximizing the efforts of the rider (facilitating more effective therapy), while guaranteeing forward invariance of the safe set.

In Chapter 3, adaptive deep neural network (DNN) CBFs (aDCBFs) are developed to ensure safety while learning the system's uncertain dynamics in real-time. The goal of this chapter is to ensure safety while reducing the conservative behavior often introduced when bounding the model uncertainty in CBF works. This chapter provides the first result combining CBFs with an adaptive DNN that updates in real-time, eliminating the need for pre-training. The DNN adaptation law is not based on the tracking error as in all previous Lyapunov-based (Lb)-DNN literature. Instead, a least squares adaptation law is designed by constructing an identification error. Since computing an identification error requires state-derivative information, an interlaced approach is used where a secondary state-derivative estimator is combined with the adaptive DNN to generate the adaptation laws. A combined Lyapunov-based analysis yields guarantees on the

DNN parameter estimation. The convergent upper-bound of the parameter estimation error is then used to formulate candidate CBF-based constraints in an optimization-based control law to guarantee the forward invariance of the safe set, while reducing the conservative behavior often seen in robust approaches. As a result, during intermittent loss of feedback, the identified DNN can be used to make open-loop predictions that are then used to reformulate CBF-based constraints to guarantee safety. Thus, the developed method can be used for safe operation of uncertain systems in environments with feedback occlusion zones, where intermittent loss of feedback typically occurs.

Chapter 4 combines the ideas of PBC and multiple CBFs to design an optimization-based controller that renders the closed-loop system passive and a safe set forward invariant despite an external disturbance, which can be especially important in human-machine interaction. By using a quadratic program (QP) to enforce both passivity and safety constraints, a set of allowable controllers is developed, generalizing the control design while providing performance guarantees. While the developed passivity constraint resembles a Lyapunov constraint, PBC and Lyapunov-based control are separate concepts with separate applications. Previous results combining PBC and CBFs require the initial design of a passive nominal controller and provide conditions for which the passivity of that specific nominal controller is not disrupted by a safety constraint, while the developed technique produces a set of passivating and safety-ensuring controllers. The developed approach results in a forward invariant safe set that is robust to the external disturbance.

In Chapter 5, the previous chapters are summarized. Additionally, potential future work is presented based on Chapters 2, 3, and 4.

CHAPTER 1
LITERATURE REVIEW AND DISSERTATION OUTLINE

1.1 Safety

Safety-critical systems are present in all industries and include numerous devices such as spacecrafts, automobiles, pacemakers, and nuclear power plants. The failure or malfunction of one of these safety-critical systems can result in death or serious injury to to the people using them or damage to surrounding equipment or environment, but the notion of safety tends to be somewhat abstract. Inherently, it is desirable for a system to be "safe", but there is often a question of how exactly to define safety and what must be done to achieve it. A precise definition of safety was introduced in [1], where *safety* is said to be a property that states something bad will not happen. Safety is a counterpart to *liveness*, which is a property that states something good will happen. An example of a liveness property is asymptotic stability, where a system's state eventually reaches a stable equilibrium point. The definitions for safety and liveness were formalized in [2] and [3]. In these results, if a safety property does not hold, then at some point a "bad thing" must happen, and there is an identifiable time that it occurs. A safety property cannot specify that a "bad thing" does not happen at a particular time, instead, if it occurs at any time, the execution is not safe. Similarly, a liveness property cannot guarantee that a "good thing" happens at a certain time, only that it eventually happens. This dissertation focuses on how "bad" events are defined and prevented in control systems.

An important type of safety property called invariance is discussed in works such as [4–7] where a set is said to be invariant if trajectories that start within an invariant safe set will never reach the complement of the set, where "bad things" happen. The initial study of safety in the context of dynamical systems is credited to Mitio Nagumo in [4], dating back to the 1940s. In [4], necessary and sufficient conditions for set invariance are developed. Given a dynamical system $\dot{x} = f(x)$ with $x \in \mathbb{R}^n$, if the safe

set $\mathcal{C}$ is the superlevel set of a smooth function $h : \mathbb{R}^n \to \mathbb{R}$, which can also be written as $\mathcal{C} = \{x \in \mathbb{R}^n : h(x) \geq 0\}$, and if $\frac{\partial h}{\partial x} \neq 0$ for all x such that $h(x) = 0$, then based on the derivative of h on the boundary of $\mathcal{C}$,

$$\mathcal{C} \text{ is invariant} \Leftrightarrow \dot{h}(x) \geq 0, \forall x \in \partial\mathcal{C}.$$

A similar analysis is performed in [5] and [8], which each arrive at the same conclusion for the conditions for invariance.

In dynamical systems, safety is can be verified by invariance of a set of some permitted states. A subset of the state space is said to be *invariant* if the inclusion of the state at some time implies the inclusion in both the future and the past. More commonly used in the literature, the set of permitted states is *forward invariant* if at some point in time it contains the system's state, then it contains the state for all future times. This idea can also be applied to cases in which there is a control input; a set is *controlled invariant* or viable if the trajectory can be kept inside a set via a proper control action, for all initial conditions inside the set [6]. Contractivity is a strong form of forward invariance that is also introduced in [6]. A *contractive set* is a forward invariant set where when a solution starts from its boundary, it immediately leaves the boundary and evolves toward its interior. If liveness is equated to asymptotic stability, and safety is equated to forward invariance, then historically, liveness has received more attention in control theory.

Another common way of ensuring safety in dynamical systems is through a passivity analysis. Instead of considering safety as a forward invariance problem, passivity-based approaches view safety as an energy-transfer problem. *Passive systems* are often desirable due to their compliant behavior stemming from the fact that they can only dissipate energy and cannot generate any energy of their own [9]. This means that they yield to external inputs. Specifically in the context of human-robot interaction, passivity can be used to ensure the machine yields to inputs from the human operator. A passive

machine will not overpower the person in contact with it and therefore will not transfer undue torques to the person [10].

1.2 Control Barrier Functions

1.2.1 History

Control barrier functions (CBFs) are the first method that will be investigated in this dissertation to ensure the safety of a dynamic system. CBFs play a role in safety similar to control Lyapunov functions (CLFs) in liveness. Instead of constructively designing a specific controller (as is done in Lyapunov-based control), CLFs and CBFs define sets of controllers satisfying conditions that ensure stability and forward invariance, respectively. Nearly twenty years ago, researchers began to investigate barrier certificates as a way to formally prove the safety of nonlinear systems [11–13]. Barrier certificates separate the state space into safe and unsafe parts. The early work in [12] use barrier certificates as a way to identify contradictions between model and experimental data. In these papers, the unsafe set $\mathcal{C}_u$ is chosen to be the complement of the safe set $\mathcal{C}$ with a set of initial conditions $\mathcal{C}_0$ and a function $B : \mathbb{R}^n \to \mathbb{R}$, where $B(x) \leq 0$ for all $x_0 \in \mathcal{C}_0$ and $B(x) > 0$ for all $x \in \mathcal{C}_u$. The function B is a barrier certificate if $\dot{B}(x) \leq 0 \Rightarrow \mathcal{C}$ is invariant. The conditions in [12] ultimately reduce to Nagumo's conditions in [4]. Barrier certificates were further studied in [14] and were extended to stochastic settings in [15]. As means to broaden safety guarantees beyond the boundary of the safe set, some other barrier certificate-based approaches can be described as Lyapunov-like. If the invariant level sets of a Lyapunov function are contained in the safe set, one can guarantee safety. The work in [16] uses a *barrier Lyapunov function* similar to the function B above, but with the additional requirement that it is positive definite. Again, by enforcing $\dot{B} \leq 0$ on the safe set $\mathcal{C}$, the safe set can be shown to be forward invariant. In these early works, every sublevel set of the barrier certificate is required to be invariant, which is overly restrictive for most applications.

The above works describe closed systems without control inputs. In papers such as [17–19], viability theory is investigated which extends barrier certificates to controlled dynamical system, typically of the form

$$\dot{x} = f(x) + g(x)\,u, \tag{1–1}$$

where $x \subseteq \mathbb{R}^n$ denotes the state, $u \in \mathcal{U} \subset \mathbb{R}^m$ denotes the control input, $f : \mathbb{R}^n \to \mathbb{R}^n$ denotes the drift dynamics, and $g : \mathbb{R}^n \to \mathbb{R}^{n\times m}$ denotes the known control effectiveness matrix, where $\mathcal{U} : \mathbb{R}^n \times \mathbb{R}^m \to \mathbb{R}^k$ denotes set of admissible control inputs. Dynamics of the form in (1–1) with the inclusion of the control input u require the introduction of controlled invariant sets, which are sets can be made invariant by a suitably designed controller. The first definition of a CBF is introduced in [20], which is slightly different than the definition introduced in the next subsection that is currently used in the literature. The CBF definition in [20] was formally combined with control Lyapunov functions in [21] to design controllers that ensure safety and stability simultaneously. The conditions for invariance in [17–22] reduce to finding a control input that satisfies $\dot{h}(x,u) \geq 0$, which still requires that each sublevel set of the CBF is invariant, which is more restrictive than is often necessary.

More recent works such as [23] lessen the conditions of the above works and extend Nagumo's conditions to the entirety of the safe set. In [23], the proposed CBF is unbounded at the set boundary and is defined such that

$$\inf_{x\in \mathrm{Int}(\mathcal{C})} B(x) \geq 0, \qquad \lim_{x\to\partial\mathcal{C}} B(x) = \infty. \tag{1–2}$$

The barrier function defined in (1–2) is now called a reciprocal barrier function. Reciprocal type barrier functions are not well-defined outside the operating region and can require potentially unbounded control actions to ensure invariance. While reciprocal barrier functions can be well-suited for some applications, the more refined definition of CBFs in [23, 24] is usually preferable.

1.2.2 Modern Control Barrier Functions

The goal of achieving safety while still leaving the system with as much freedom as possible motivates the modern definition of CBFs. The definition of a CBF in [23–25], sometimes called a zeroing CBF, for a safe set $\mathcal{C}$ and barrier function h is

$$\sup_{u \in \mathcal{U}} \left[L_f h(x) + L_g h(x) u \right] \geq -\alpha(h(x)) \Rightarrow \mathcal{C} \text{ is invariant,} \tag{1–3}$$

where α is an extended class $\mathcal{K}_\infty$ function and $L_f h$ and $L_g h$ are the Lie derivatives of h with respect to f and g, respectively. The condition in (1–3) is minimally restrictive because it is necessary and sufficient for compact sets. Previous to these works, the condition that $\dot{B} \leq 0$ means that solutions are not allowed to leave a sub-level set of the CBF even if the solution would still be contained in the safe set. The condition in (1–3) is true over the entire set $\mathcal{C}$ and allows trajectories to move toward the boundary at states far from the boundary of the safe set. The work in [24] provides robust safety guarantees such as asymptotic stability of the safe set in addition to forward invariance.

With the formulation of a CBF in (1–3), safety can be united with stability using pointwise optimal controllers as is done in works such as [23] and [26], among others. These controllers are usually implemented via an optimization problem that allows for some nominal (typically but not necessarily stabilizing) control input to be modified such that it ensures safety while minimizing some cost function. Suppose a feedback controller $u_{nom} : \mathbb{R}^n \to \mathbb{R}^m$ is a continuous nominal control input designed to stabilize the system. It is possible that $u_{nom} \notin K_{\text{cbf}}(x) \triangleq \{u \in U : L_f h(x) + L_g h(x) u + \alpha(h(x)) \geq 0\}$, meaning that the stabilizing control input may not be in the set of admissible safety-ensuring control inputs. Therefore, u_{nom} can be modified using an optimization problem in the form of

$$\begin{aligned} u^*(x) = \underset{u \in \mathbb{R}^m}{\text{argmin}} & Q(x, u), \\ \text{s.t. } & L_f h(x) + L_g h(x) u \geq -\alpha(h(x)) \end{aligned} \tag{1–4}$$

so that it is safe, where $Q : \mathbb{R}^n \times \mathbb{R}^m$. Because (1–4) can be solved online in real-time, the modified controller u^* can be computed at each time step during operation. In some cases, it may be favorable to define a closed-form solution to (1–4) so the controller can be implemented without the need for the use of an optimization program. When the cost function Q is selected to be $Q = \|u - u_{nom}\|^2$, as is often the case, (1–4) is a quadratic program (QP) and closed-form solution to (1–4) is given by

$$u^*(x) \begin{cases} -\frac{L_f h(x) + \alpha(h(x))}{L_g h(x)}, & L_f h(x) + L_g h(x) u + \alpha(h(x)) > 0, \\ u_{nom}, & \text{otherwise.} \end{cases} \tag{1–5}$$

1.2.3 Limitations

Though [23] focuses mainly on the applications to automotive control problems, the paper provides a foundation for many problems in safety-critical control. This version of a CBF can be applied to a variety of control systems such as multi-robot systems [27–29], walking robots [30], and human-machine interaction problems [31]. While asymptotic stability of the safe set can be guaranteed using CBFs under some conditions, the typical result of CBF-based control design is forward invariance, which is weaker than stability. Despite a weaker result, CBFs have advantages in safe control design. A CBF-based approach can allow for more freedom inside the safe set meaning that the states are not necessarily forced to follow a set trajectory as long as they are not near the boundary of the safe set, allowing for other control objectives to be considered while state constraints are enforced. CBF-based controllers have merit, but there are some limitations to be considered.

1.2.3.1 High-Order Control Barrier Functionss

CBFs are typically used to constrain systems of relative degree one, meaning that the control input shows up explicitly in the first derivative of the state that is being constrained. Constraints for systems of relative degree one typically correspond to a velocity constraint, so these CBFs may be ineffective in many robotic systems that

would benefit more from a position constraint. To broaden the potential applications of CBFs, some works such as [32] and [33] have used a backstepping approach, which have been shown to work for position-based constraints for systems of relative degree two. For systems with an arbitrarily high relative degree, recent work in [34] has developed high-order control barrier functions (HOCBFs) which are not restricted to exponential functions and can be used in systems with control affine dynamics. HOCBFs work by iteratively redefining CBF candidates until the state being constrained appears in the derivative of the CBF, eliminating problem states from the safe set.

A motorized recumbent cycle is an example of a safety-critical dynamic system and can be an effective method of rehabilitation for people with neuromuscular disorders [35]. Closed-loop motor control can help to produce safe and consistent cycling repetitions that the rider may not be able to generate under their own volition. Whenever possible, it is desirable to forgo motor assistance and have the rider pedal entirely volitionally to cause higher intensity training where the rider's heart rate and cardiac output increase [36], improving cardiovascular health. Controllers for the cycle-rider system have been designed with this idea of forced-use therapy in mind, such as the three-mode controller in [37] where the motor assistance (or resistance) is only activated when the rider's cadence exits the safe range. CBFs have been used to render a safe range of cadence values forward invariant in [31] and [38], which differs from the work in [37] because the controller gradually increases effort as the cadence approaches the boundary of the safe cadence set.

In the related results in [31, 37, 38], the cycle cadence is restricted to a user-defined range, but in some cases, it may be desirable to instead constrain the position of the cycle crank to a time-varying set of safe positions. Previously, it has not been possible to use CBFs to formulate this type of position constraint because by considering the position as an output, the system is of relative degree two. With recent developments in HOCBFs, we can now develop a controller that ensures the forward invariance of a

user-defined range of position values while minimizing the control input when the rider is able to maintain the crank's position near the midpoint of that range. Using a HOCBF to constrain the cycle crank's position has the potential to be especially useful in the case of teleoperation as in [39] or in the use of a split-crank cycle where the rider's dominant side tracks a position that is offset from the position of the non-dominant leg such as in [40].

1.2.3.2 Uncertain Dynamics

CBF-based control input constraints depend on the dynamic model of the system. As a result, uncertainties in modeling the dynamics can endanger safety. To address challenges posed by the modeling uncertainty, robust safety methods can be used, where safety guarantees are provided using the worst-case bounds on the uncertainty. However, robust methods yield an overly conservative constraint on the control input that restricts the state to an operating region that is a subset of the safe set.

Adaptive CBFs have been developed to ensure the forward invariance of a safe set through online parameter adaptation [41–44], but because the adaptive CBF approaches developed in [41] and [42] include the parameter estimation error, the state is restricted to a subset of the safe set, dependent on the upper-bound of the estimation error. Methods such as set membership identification [42], integral concurrent learning [45], and parameter-adaptive CBFs [44] reduce the conservativeness with sufficient data, but these methods involve a white-box approach where the uncertainty is required to have a known structure based on traditional modeling techniques. In contrast, recent results such as [46–48] use black-box models such as pre-trained deep neural networks (DNNs) and Gaussian processes to identify uncertain dynamics using training datasets and therefore reduce conservativeness; however, since these methods are not adaptive, they result in static models that may become obsolete over time. Moreover, they require state-derivative information and do not provide any performance guarantees.

Other recent works reduce conservativeness by combining CBFs with disturbance observers [48–51]. Disturbance observers are used to produce an estimate of the uncertainty which is then used in the CBF constraint, expanding the state's operating region when compared to a robust approach. Adaptive safety is achieved in [48] through a modular approach that can combine a pre-trained DNN model with a robust integral of the sign of the error (RISE)-based disturbance observer, eliminating conservativeness of the safe set over time. Although disturbance observers can estimate general nonlinear and time-varying uncertainties, the estimates are only instantaneous and do not involve a model that can be used for subsequent predictions. In contrast, models such as DNNs can extrapolate through unexplored regions, and thus can be employed to ensure safety under intermittent loss of feedback. Therefore, instead of using disturbance observers or pre-trained DNNs as in [48–51] it is desirable to construct adaptive CBFs using DNNs such as those in [52–56] with analytic real-time adaptation laws without the need for pre-training. Previous Lyapunov-based (Lb-) DNN adaptive controllers address the trajectory tracking problem; however, the tracking error-based adaptation laws in these results are not suitable for the adaptive safety problem since safety does not typically require tracking error convergence. Thus, to combine adaptive DNNs with CBFs, a novel weight adaptation law must be formulated to instead yield parameter estimation error convergence.

1.2.3.3 Other Considerations

Many CBF results assume that infinite control effort is available. Input constrained CBFs (ICCBFs) were formalized in [57], but were initially investigated in works such as [33, 58–60]. If a state trajectory is approaching the boundary of the safe set, there exists some input that will slow it down or reverse it so that it does not exit the set. Eventually, the state will reach a point too close to the boundary or will be approaching the boundary too quickly for a reasonable or achievable control input to maintain invariance. In the presence of input constraints, only a subset of the safe set may be

rendered forward invariant. To compute this subset of the safe set, several methods could be used such as a Hamilton-Jacobi partial differential equation over the state space [61] or a sum-of-squares (SOS)-based semi-definite program that uses the Positivestellensatz theorem [62, 63]. Both of these methods scale poorly with the increasing dimension of the state-space. Some of the works regarding ICCFs focus on only specific classes of systems such as Euler-Lagrange systems [58] or mechanical systems on a manifold [33]. The ICCBFs in [57] are considered a generalization of HOCBFs (meaning they can also be applied to systems of higher relative degree) and work similarly to HOCBFs by iteratively redefining CBF candidates until the intersection of the safe sets defined by the CBF recursions can be rendered forward invariant by the available input. These ICCBF methods need further investigation into their robustness to noise and perturbations, as well as potential methods to efficiently automate the search for ICCBFs.

For systems with multiple constraints, multiple CBFs often need to be defined, but theoretical results to ensure the invariance of sets defined by multiple CBFs are limited. Works such as [29] and [64], combine CBFs using min or max operations. The work in [65] provides a method for synthesizing forward invariance-ensuring controllers for continuous-time differential inclusions with flow constraints on the state and control input, but only investigate continuous-time dynamics. Many real-life dynamical system have a combination of continuous-time and discrete time behaviors. Systems that can be modeled as a combination of continuous and discrete dynamics are considered to be hybrid dynamical systems. These systems are described by differential inclusions or ordinary differential equations called the flow map that model the continuous evolution of the state paired with a set of flow states where flows occur and by difference equations modeling the jumps paired with the jump map describing the set of states where those discrete events occur. A hybrid systems approach can be used to model a wide range of systems including switched systems. The work in [66] can be used to enforce multiple

CBF constraints for the continuous-time portions of a hybrid dynamical system, but does not provide any guidance on the discrete part of the dynamics. While results in [67] and [68] can be used to prove the forward invariance or asymptotic stability of sets defined by a scalar CBF in the context of hybrid systems, there are few results for noncompact safe sets or safe sets defined by multiple CBFs. In [69], an approach is developed to establish the forward invariance of a safe set defined by multiple barrier functions for uncontrolled hybrid dynamics. There are results available to aid in the design of controllers that ensure the forward invariance of sets defined by multiple CBFs for systems with continuous dynamics [66] and the forward invariance of sets defined by single CBFs for systems with hybrid dynamics [31], but there are currently no results at the intersection of those two groups, where the safe set of a system with hybrid dynamics is defined by multiple CBFs.

1.3 Passivity-Based Control Methods

1.3.1 History

Another method of ensuring the safety of a system is through passivity theory, which can be used as an alternative to a Lyapunov-based stability analysis commonly seen in nonlinear control. Passivity notions can be traced back to Lagrange and Dirichlet in the late 1700s and early 1800s who showed that the stable equilibria of mechanical systems correspond to the minima of the potential function. Modernly, the use of passivity in control theory has been motivated by the use of passivity in circuit theory and electrical network theory, which began in the 1950s. In early works such as [70] and [71], the distinction between active and passive networks is that active networks may contain internal energy sources, while passive ones do not. Analogies can be drawn between this case and more general control systems, where passive control systems only store or release the energy provided to them.

Passivity is broadly defined as a nonnegativity condition on the system's input energy. The Kalman-Yakubovich-Popov Lemma, also known as the Positive Real Lemma,

is an important result that can be used to establish the passivity of linear systems based on its transfer function [72–75]. A system's transfer function is positive real, and therefore passive, if and only if, a certain set of matrix equations has a nonnegative definite solution. While the Positive Real Lemma applies only to linear systems, works such as [76–78] are some of the first to extend similar ideas to nonlinear systems. An approach similar to the Positive Real Lemma for nonlinear systems is developed in [78], which shows that a system is passive if an only if there exists a scalar function of the state which is nonnegative. The approach in [78] can be applied to nonlinear systems with the restriction that the state equation of the system should only involve the control vector linearly.

The requirements of passive nonlinear systems are more precisely outlined in [79]. If a system is passive, the power absorbed by the system over any period of time $[0, t]$ must be greater than or equal to the increase in the energy stored in the system (represented by $V(x)$) over the same period, that is

$$\int_0^t u(s)\, y(s)\, ds \geq V(x(t)) - V(x(0)), \tag{1–6}$$

where $x \in \mathbb{R}^n$ is the state, $u \in \mathbb{R}^m$ is the control input, $y \in \mathbb{R}^m$ is the output, and $V : \mathbb{R}^n \to \mathbb{R}_{\geq 0}$ is a positive semidefinite storage function. If (1–6) holds with strict inequality, then the difference between the absorbed energy and increase in the stored energy must be the energy dissipated in the resistive components of the network. For every $t \geq 0$, it must be true that the instantaneous power inequality $u(t)\, y(t) \geq \dot{V}(x(t))$ holds. In other words, the flow of energy to the system must be greater than or equal to the rate of change of the energy being stored in the system. Specific cases of passivity can be considered when there is no dissipation or strict dissipation when the input and/or output are not identically zero.

In the subsequent chapters, the definition of passivity in [79] is used. For the passivity of a system with dynamic model represented by

$$\dot{x} = f(x, u), \tag{1–7}$$

$$y = h(x, u), \tag{1–8}$$

where $f : \mathbb{R}^n \times \mathbb{R}^m \to \mathbb{R}^n$ denotes a locally Lipschitz function, $h : \mathbb{R}^n \times \mathbb{R}^m \to \mathbb{R}^m$ denotes the continuous output function, $f(0, 0) = 0$, and $h(0, 0) = 0$.

Definition 1.1. [79, Definition 6.3] The system in (1–7) and (1–8) is passive if there exists a continuously differentiable positive semi-definite storage function $V(x)$ such that

$$u^\top y \geq \dot{V} = \frac{\partial V}{\partial x} f(x, u), \forall (x, u) \in \mathbb{R}^n \times \mathbb{R}^m.$$

Moreover, the system is said to be

- lossless if $u^\top y = \dot{V}$,
- input-feedforward passive if $u^\top y \geq \dot{V} + u^\top \varphi(u)$ for some function φ,
- input strictly passive if $u^\top y \geq \dot{V} + u^\top \varphi(u)$ and $u^\top \varphi(u) > 0$, $\forall u \neq 0$,
- output-feedback passive if $u^\top y \geq \dot{V} + y^\top \rho(y)$ for some function ρ,
- output strictly passive if $u^\top y \geq \dot{V} + y^\top \rho(y)$ and $y^\top \rho(y) > 0$, $\forall y \neq 0$.

In all cases, the inequality should hold for all (x, u).

If a system is output-feedback passive, the term $y^\top \rho(y)$ can represent an excess or shortage of passivity. If $y^\top \rho(y) > 0$ for all $u \neq 0$, there is an excess of passivity because the energy supplied is greater than the increase in the stored energy unless the output $y(t)$ is identically zero. If $y^\top \rho(y) < 0$ for all $u \neq 0$, there is a shortage of passivity in the system.

Passivity of a dynamic system is a desirable property for a variety of reasons. One of the main motivations for studying passivity in the context of control theory is its close relationship with stability. This is first mentioned in [76], where passivity is deemed

a sufficient condition for stability. The relationship between passivity and stability is shown in Section 6.4 of [79]. A system is 0-input asymptotically stable if it is strictly passive or output strictly passive and zero-state observable. These stability results hold globally if its storage function is radially unbounded. Furthermore, a passive system can be stabilized by output feedback $u = -ky$, and the passivity of each component of an interconnected system ensures that the overall interconnected system is passive, as well [80, 81], regardless of system nonlinearities. These passivity properties hold for series, parallel, and feedback interconnections, enabling the analysis of complex large-scale systems in a component-wise fashion. Additionally, because passivity is an input-output property, the system's dynamics do not necessarily need to be explicitly known which can be beneficial in the case of human-robot interaction where a dynamic model for the behavior of the operator is not available. Passivity is a diverse tool that can be used to handle issues such as input saturation, time delays, and switching between control inputs.

1.3.2 Applications

Beginning in the 1980s, passivity started to play a bigger role in robotics applications, including robust [82, 83] and adaptive [84–86] control of manipulators. Passivity-based control (PBC) was introduced in [87] in the context of adaptive control of rigid manipulators with its roots tracing back to circuit and electronic systems theory. While typical control schemes for nonlinear systems are signal-based, PBC is energy-based, viewing controls in terms of an energy balance between interconnections and can be used in systems that can be modeled as an Euler-Lagrange system [88], port-controlled Hamiltonian (PCH) system [89], switched system [90], or hybrid system [68]. The concept of PBC has been applied to the control of electric motors [91, 92], chemical processes [93, 94], bipedal locomotion [95], and teleoperation [96], among others.

Feedback passive systems can be made passive with respect to an input/output pair with preliminary feedback. In [97], the system in (1–7)-(1–8) is said to be feedback

equivalent to passive if there exists a feedback law $u = \alpha(x) + \beta(x)\nu$ such that the system with new input ν is strictly passive. Passivation methods allow for passive system tools to be used for systems that may are not initially passive. Related to passivity, modifications of the energy function and dissipation rate are often called energy-shaping and damping injection, respectively, and can be used to ensure stable closed-loop behavior that is robust to disturbances [98–100]. These methods are well-suited for PCH systems, which focus on the geometric description of systems as an interconnection of their subsystems based on Hamiltonian equations [89]. Works such as [94, 101, 102] use an energy-shaping plus damping injection approach to stabilize robotic manipulators, chemical process, and multi-agent systems.

Because of the interconnection properties of passivity, a PBC approach is well-suited for the stabilization of bilateral teleoperators. In bilateral teleoperation, a follower robot imitates the motion of a leader robot, while simultaneously interacting with a remote environment. The control objective is to ensure motion tracking between the leader and follower robots, often with a secondary goal of having the force acting on the follower system being accurately transmitted to the leader. A common issue in the control of bilateral teleoperators is time delays between subsystems which often introduce a non-negligible time delay on the signals between agents, which can destabilize an otherwise stable system [103]. Passivity-based approaches to address time delays are investigated in [104, 105], where control schemes are derived to overcome the constant delay while ensuring passivity from input torques to their joint velocities. The approaches in [104, 105] are often victim of position drift and sluggish response at high delays. Other works such as [96, 104–110] demonstrate how PBC can be used to stabilize bilateral teleoperators with time delays. Output synchronization of networked passive systems in the presence of constant and time-varying delays were studied in [111, 112] and demonstrate that under some mild assumptions the synchronization of networked passive systems is robust to unknown delays. While

these works were limited to network passive systems, the same results can be applied to systems that are feedback equivalent to passive [97, 113]. Control schemes built on these concepts have been developed to improve performance based on position feedback, impedance matching, robustness to delays, and other objectives [110].

In [90, 114–117], dissipativity and passivity properties are investigated for switched systems. Since switched control systems are a class of hybrid systems, more analysis is done for PBC of hybrid systems in [68, 118–122]. In [122], a general notion of dissipativity is presented for a class of hybrid systems that is linked with detectability to conclude asymptotic stability for large-scale interconnections of hybrid systems. Many works have investigated passivity in the context of hybrid systems such as [121, 123, 124]. More recently, explicit definitions of passivity for hybrid systems similar to those in Definition 1.1 are presented in [68, Chapter 9]. Additionally, conditions for the synthesis of passivity-based feedback laws and for guaranteeing pre-asymptotic stability of a point or set based on the passivity of the continuous and/ or discrete dynamics are provided in [68].

Like forward invariance, a passivity result is again generally considered to be weaker than stability because it does not guarantee convergence to an equilibrium point. However, because passivity is robust to time delays, interconnections between systems, and unknown external disturbances, a passivity result can be advantageous in some cases.

1.4 Combining Control Barrier Functions with Passivity-Based Control

Though PBC and CBFs have typically been regarded as independent concepts, both PBC and CBFs have implications in safe control and can be combined to stabilize systems interacting with an unknown external disturbance while satisfying prescribed state constraints. As discussed in Section 1.2, in CBF works, safety refers to a more specific mathematical notion, where a system is considered to be safe if it is restricted to a forward invariant set of safe states [125]. As discussed in Section 1.3, in the context

of PBC, there is no rigid mathematical definition of what is considered safe. Instead, in PBC, safety generally refers to ensuring robust stability with respect to the system's environment [126]. While PBC and CBF-based methods are typically unable to prevent all adverse events from occurring, each approach introduces different notions of a safe control action, each of which can be important to enforce.

When merging passivity and state constraints, the literature developed for multiple CBFs in [29, 64, 65] can be a powerful tool. By reformulating the passivity constraint into a CBF-like constraint on the control input, optimization techniques can be used to synthesize a set of controllers that yield overall passivity of the system. Construction of the specific controller that yields passivity or forward invariance of the safe set is not required. Instead, an optimization problem such as the one in (1–4) can be used to select a control input from a set of safe passivating controllers for each point in the state space, enabling easier integration with potential CBF-based state constraints.

Several works have explored combining the concepts of PBC and CBFs [127–131]. Both [127] and [128] use optimization-based methods to passivate nonpassive control actions, and [130] and [131] introduce control storage functions and control dissipation functions as aids to design stabilizing controllers for receding horizon control problems. In [127], the energy tank framework introduced in [126] is used to model the flow of energy in the system. In each of these works, optimization techniques are used only to enforce passivity [127, 128] or dissipativity [130, 131] but do not consider any state-based safety constraints. The work in [129] develops conditions under which a passive controller remains passive after being modified by a safety-filtering QP. Despite using optimization techniques to enforce safety constraints, the result in [129] requires the initial design of a specific nominal controller that renders the system passive. Furthermore, [129] neglects the effect of the external disturbance on the evolution of the state in the design of the CBF constraint. As a result, there is a potential for these external disturbances to compromise the forward invariance of the safe set.

1.5 Safe Control Methods in Human-Robot Interaction

Some of the most safety-critical systems are those involving the close physical interaction between person and machine. Motivation exists to design minimally invasive controllers for human-robot interaction that ensure safety while allowing the human to operate with minimal interference [31, 38, 39, 132–139]. In the literature on human-robot interaction, CBFs and PBC are commonly used to ensure safe interaction between industrial robots and their human operators. In industrial settings, it is typically important to prevent robots and their human counterparts from coming in direct contact to prevent injuries. The work in [132, 133] uses CBFs to restrict the operating region of industrial robots to prevent the robot from colliding with a person. In [132, 133, 138, 140, 141], PBC is used to control robots that must maintain certain position or velocity tracking objectives while also ensuring passivity with respect to external perturbations that may arise from a human or the environment.

Closed-loop control of robotic systems that interact with humans should have a way to resolve conflicting inputs between a human and robot, and should do so in a stable manner to avoid larger forces being transmitted to the operator. Controllers that ensure passivity in the human-robot system can help to yield safe performance due to their compliant behavior. Many works share the philosophy that passivity implies safety [142, 143]. While passivity is a good property to have because it is necessary to ensure a stable interaction with any unknown environment [9, 144], passivity alone may not be “safe” in the context of human-machine interaction. Therefore, control laws should be robust providing asymptotic stability guarantees while being passive specifically with respect to the human’s input [145]. A common assumption in human-robot interaction literature is that the operators behave passively [146], and because of this assumption, as long as the controlled robot is energetically passive, the interaction between robot and human will be stable [147].

Rehabilitative robotics is a specific type of human-robot interaction where robots are used to help in physical therapy methods for people with neurological disorders (NDs). The limiting factor in many rehabilitative robotics applications is that they move the individual through a rigid predetermined trajectory instead of allowing the user to move under their own control which can lead to a phenomenon called learned helplessness where the individual will begin to rely too much on motorized assistance instead of their own volitional efforts [148]. Assist-as-needed or forced-use controllers allow the user to maintain some control authority letting them better practice appropriate movement patterns and relearn normal motion. In [134, 135], CBFs are used for movement planning and motor control, respectively, for lower limb exoskeletons, and in works such as [149, 150], passivity is used to design assist-as-needed controllers that transfer some control authority back to the user.

A motorized recumbent cycle is an example of a safety-critical dynamic system and can be an effective method of rehabilitation for people with NDs [35]. Closed-loop motor control can help to produce safe and consistent cycling repetitions that the rider may not be able to generate under their own volition. Whenever possible, it is desirable to forgo motor assistance and have the rider pedal entirely volitionally to cause higher intensity training where the rider's heart rate and cardiac output increase [36], improving cardiovascular health. Controllers for the cycle-rider system have been designed with this idea of forced-use therapy in mind, such as the three-mode controller in [151–153] where the motor assistance (or resistance) is only activated when the rider's cadence exits the safe range. Works such as [31, 38, 39, 136] have used CBFs to constrain the cadence error of a motorized rehabilitative cycle to some prescribed range. In these papers, the some nominal controller, often zero [31, 38], remains unchanged while the error is near the center of the safe set. As the rider's cadence begins to exit the safe range, the controller starts to assist or resist the rider to keep the trajectory inside the safe set. The approaches in [31, 38, 39, 136] differ from the work in [151–153] because

the controller is gradually activated with increasing effort as the cadence approaches the boundary of the safe cadence set instead of discontinuously switching between assistive, passive, and resistive modes. Though the controller in [151] is shown to cause the cadence error to exponentially converge to the boundary of the desired set, the controller was unable to ensure forward invariance of the desired cadence set, and in experiments, the cycle spent nearly 50% of the time operating outside of the desired cadence region.

Several of these works, namely [38, 136], only use motor input, while [31, 39] incorporate FES before resorting to motor assistance as a way to increase power output from the rider. The addition of FES control adds switched inputs to the system and requires switching or hybrid systems approach to conclude forward invariance or stability. The cycle is modeled as a hybrid system in [31] and is constrained by only one CBF. While a hybrid systems analysis yields some robustness properties and asymptotic stability of the safe set with reduced gain conditions than would be achieved with a switched systems analysis, similar results would not be possible for systems with constraints defined by multiple CBFs because of current gaps in theoretical results.

CBF results such as [31, 38, 39, 136] are only able to enforce cadence constraints, representative of a system of relative degree one. HOCBFs could be used for position constraints on the cycle, which would be especially useful in the case of split-crank cycling where the two sides of the cycle are decoupled and controlled separately or in the case of teleoperation where a leader (hand-) cycle sets the desired trajectory for the follower cycle.

1.6 Outline

This dissertation focuses on the design of safe controllers through the use of CBFs in Chapters 2, 3, and 4 and passivity-based analyses in Chapter 4 to ensure that desired state constraints are met and to ensure stable interaction with an unknown

environment, respectively. While controllers developed using constructive Lyapunov-based methods are safe in the sense that they are asymptotically or exponentially stable, they are potentially overly conservative. The approaches in this dissertation aim to ensure the weaker notion of safety of the system through the less conservative methods of CBFs and PBC that yield forward invariance and passivity, respectively.

Chapter 2 provides a HOCBF approach for differential inclusions without flow constraints which can be applied to an even wider range of dynamic systems than previous works such as [34]. To illustrate the functionality of the result, I use the developed HOCBF approach to design a motor controller for a rehabilitative cycle. In the related results such as [31, 37, 38] the cycle cadence is restricted to a user-defined range, which is representative of a system of relative degree one. In some cases, it may be desirable to instead constrain the position of the cycle crank to a time-varying set of safe position errors. Previously, it has not been possible to use CBFs to formulate this type of position constraint because by considering the position as an output, the system is of relative degree two. With recent developments in HOCBFs, a controller can now be developed that ensures the forward invariance of a user-defined range of position error values while minimizing the control input when the rider is able to maintain the crank's position in the midpoint of that range. Using a HOCBF to constrain the cycle crank's position has the potential to be especially useful in the case of teleoperation as in [39] or in the use of a split-crank cycle where the rider's dominant side tracks a position that is offset from the position of the non-dominant leg such as in [40]. The developed method can be applied to systems with more general dynamics than those in [34] and includes a term that provides the safe set with some robustness to perturbations. The HOCBF method in this chapter allows us to constrain the cycle crank to a prescribed range about the time-varying desired position. I use theory from previous work in [66] to prove the forward invariance of the set defined by the developed HOCBF approach and an additional CBF-based constraint on the cycle's cadence. The motor controller in

this chapter uses minimal motor control effort when the position error is close to zero, with increasing control effort as the error approaches the boundary of the user-defined allowable set. This approach favors the rider's volitional efforts when they are able to stay at a near-zero error without assistance while still ensuring forward invariance of the safe set. An experiment was performed on one healthy subject to validate the developed motor controller. For the selected error range of ± 30 degrees, the controller was able to constrain the position to the prescribed error for the duration of the test while minimizing control effort when the rider pedaled volitionally.

Chapter 3 overcomes the problems discussed in Section 1.2.3.2 by developing an adaptive deep neural network (DNN)-based CBFs that ensures safety while learning the dynamics of an uncertain system. This chapter provides the first result combining CBFs with an adaptive DNN that updates in real-time, eliminating the need for pre-training. The DNN adaptation law is not based on the tracking error as in all previous Lb-DNN literature. Instead, a least squares adaptation law is designed by constructing an identification error. Since computing an identification error requires state-derivative information, an interlaced approach is used where a secondary state-derivative estimator is combined with the adaptive DNN to generate the adaptation laws. A combined Lyapunov-based analysis yields convergence guarantees on the DNN parameter estimation. The convergent upper-bound of the parameter estimation errors is then used to formulate candidate CBF-based constraints in an optimization-based control law to guarantee the forward invariance of the safe set, while reducing the conservative behavior often seen in robust approaches. As a result, during intermittent loss of feedback, the identified DNN can be used to make open-loop predictions that are then used to reformulate CBF-based constraints to guarantee safety. Thus, the developed method can be used for safe operation of uncertain systems in environments with feedback occlusion zones, where intermittent loss of feedback typically occurs. Comparative simulation

results are presented to demonstrate the performance of the developed method on two control systems with baseline results in [23] and [48].

In Chapter 4, CBFs and passivity are combined to design an optimization-based controller that renders the closed-loop system passive and a safe set forward invariant despite an external disturbance. By using a QP to enforce both passivity and safety constraints, a set of allowable controllers is developed, generalizing the control design while providing performance guarantees. While the developed passivity constraint resembles a Lyapunov constraint, PBC and Lyapunov-based control are separate concepts with separate applications. Previous results combining PBC and CBFs require the initial design of a passive nominal controller and provide conditions for which the passivity of that specific nominal controller is not disrupted by a safety constraint, while the developed technique produces a set of passivating and safety-ensuring controllers. The developed approach results in a forward invariant safe set that is robust to the external disturbance. Additionally, we provide a method to determine the feasibility of the synthesized controller using sum of squares programming. Simulation results on a planar two-link robot disturbed by an interaction torque injected by a human operator demonstrate the ability of the developed approach to achieve both passivity and safety objectives.

1.7 Notation

For notational brevity, all explicit dependence on time, t, is omitted except for when it is necessary for clarity. For example, given the trajectory $x : \mathbb{R}_{\geq 0} \to \mathbb{R}^n$, the equation $\dot{x} = Ax + Bu$ should be interpreted as $\dot{x}(t) = A(t)x(t) + B(t)u(t)$. For vectors $x, y \in \mathbb{R}^n$, the gradient of a function, denoted $\nabla f(x, y)$, is defined as $\left[\frac{\partial f(x,y)}{\partial x_1}^\top, ..., \frac{\partial f(x,y)}{\partial x_n}^\top\right]^\top$. The inner product of two vectors is defined as $\langle (x_1, x_2, ..., x_n), (y_1, y_2, ..., y_n) \rangle = x_1y_1 + x_2y_2 + x_3y_3 + ... + x_ny_n$. Let $\mathbb{R}_{\geq 0} \triangleq [0, \infty)$, $\mathbb{R}_{>0} \triangleq (0, \infty)$, and $\mathbb{R}^{n\times m}$ represent the space of $n \times m$ dimensional matrices. The identity matrix of size n is denoted by I_n. The p-norm is denoted by $\|\cdot\|_p$, $\|\cdot\|$ is the 2-norm, and $\|\cdot\|_F$ is the Frobenius norm defined as

$\|\cdot\|_F \triangleq \|\text{vec}(\cdot)\|$, where vec $(\cdot)$ denotes the vectorization operator, which satisfies the property vec $(ABC) = \left(C^\top \otimes A\right)$ vec (B) [154, Proposition 7.1.9] and $\otimes$ denotes the Kronecker product. Let the notation $[d]$ be defined as $[d] \triangleq \{1, 2, \ldots, d\}$. Given a function $B : \mathbb{R}^n \to \mathbb{R}^d$, the components are indexed as $B(x) \triangleq (B_1(x), B_2(x), ..., B_d(x))$ and the inequality $B(x) \leq 0$ means that $B_i(x) \leq 0$ for all $i \in [d]$. For a set $A \subset \mathbb{R}^n$, the boundary of X is denoted ∂X, the closure of X is denotes $\overline{X}$, the interior of X is denoted Int (X), and an open neighborhood about X is denoted $\mathcal{N}(X)$. A set-valued mapping $M : X \rightrightarrows \mathbb{R}^m$ associates every point $x \in X$ with a set $M(x) \subset \mathbb{R}^m$. The mapping G is called locally bounded if, for every $x \in \mathcal{S}$, there exists a neighborhood $\mathcal{N}_X(x) \triangleq \mathcal{N}(x) \cap \mathcal{S}$ such that $G(\mathcal{N}_X(x))$ is bounded, and G is outer semicontinuous if Graph$_X(G) \triangleq \{(x, u) \in \mathcal{S} \times \mathbb{R}^m : u \in G(x)\}$ is relatively closed in $\mathcal{S} \times \mathbb{R}^m$. A function $f : X \to \mathbb{R}$ is called inf-compact if for every $\lambda \in \mathbb{R}$, the sublevel set $\mathcal{L}_f(\lambda) \triangleq \{x \in X : f(x) \leq \lambda\}$ is compact.

Given a controller $\kappa : \mathbb{R}^n \to \mathbb{R}^m$ with $\kappa(x) \in \Psi(x)$ for all $x \in \mathbb{R}^n$, we refer to the closed-loop dynamics defined by $\dot{x} = f(x) + g(x)u$ and κ as $f_{cl}(x) \triangleq f(x) + g(x)\kappa(x)$. A solution to the closed-loop dynamics $t \mapsto x(t)$ is complete if dom$x$ is unbounded and maximal if there is no solution y such that $x(t) = y(t)$ for all $t \in$ dom$x$, where dom$x$ is a proper subset of dom$y$. The set $\mathcal{S}$ is forward pre-invariant for the closed-loop dynamics $\dot{x} = f_{cl}(x)$ if, for each $x_0 \in \mathcal{S}$ and each maximal solution x starting from x_0, $x(t) \in \mathcal{S}$ for all $t \in$ dom$x$ [155, Definition 2.5]. The set is forward invariant for the closed-loop dynamics if it is forward pre-invariant and additionally, for each $x_0 \in \mathcal{S}$, every maximal solution x starting from x_0 is complete [155, Definition 2.6].

1.8 Preliminaries

1.8.1 Deep Neural Network Model

For simplicity in the illustration, a fully-connected DNN will be described here. The following control and adaptation law development can be generalized for any network architecture Φ with a corresponding Jacobian Φ'. The reader is referred

to [156] and [157] for extending the subsequent development to ResNets and LSTMs, respectively. Given some matrix $A \triangleq [a_{i,j}] \in \mathbb{R}^{n\times m}$, where $a_{i,j}$ denotes the element in the i^{th} row and j^{th} column of A, the vectorization operator is defined as $\mathrm{vec}(A) \triangleq [a_{1,1},\ldots,a_{n,1},\ldots,a_{1,m},\ldots,a_{n,m}]^\top \in \mathbb{R}^{nm}$. Let $\sigma \in \mathbb{R}^{L_{\text{in}}}$ denote the DNN input with size $L_{\text{in}} \in \mathbb{Z}_{>0}$, and $\theta \in \mathbb{R}^p$ denote the vector of DNN parameters (i.e., weights and bias terms) with size $p \in \mathbb{Z}_{>0}$. Then, a fully-connected feedforward DNN $\Phi(\sigma,\theta)$ with output size $L_{\text{out}} \in \mathbb{Z}_{>0}$ is defined using a recursive relation $\Phi_j \in \mathbb{R}^{L_{j+1}}$ given by

$$\Phi_j \triangleq \begin{cases} V_j^\top \phi_j(\Phi_{j-1}), & j \in [k], \\ V_j^\top \sigma_a, & j = 0, \end{cases} \tag{1–9}$$

where $\Phi(\sigma,\theta) = \Phi_k$, and $\sigma_a \triangleq \begin{bmatrix} \sigma^\top & 1 \end{bmatrix}^\top$ denotes the augmented input that accounts for the bias terms, $k \in \mathbb{Z}_{>0}$ denotes the total number of hidden layers, $V_j \in \mathbb{R}^{L_j \times L_{j+1}}$ denotes the matrix of weights and biases, and $L_j \in \mathbb{Z}_{>0}$ denotes the number of nodes in the j^{th} layer for all $j \in \{0,\ldots,k\}$ with $L_0 \triangleq L_{\text{in}} + 1$ and $L_{k+1} = L_{\text{out}}$. The vector of smooth activation functions is denoted by $\phi_j : \mathbb{R}^{L_j} \to \mathbb{R}^{L_j}$ for all $j \in [k]$. If the DNN involves multiple types of activation functions at each layer, then ϕ_j may be represented as $\phi_j \triangleq \begin{bmatrix} \varsigma_{j,1} & \ldots & \varsigma_{j,L_j-1} & 1 \end{bmatrix}^\top$, where $\varsigma_{j,i} : \mathbb{R} \to \mathbb{R}$ denotes the activation function at the i^{th} node of the j^{th} layer. For the DNN architecture in (1–9), the vector of DNN weights is $\theta \triangleq \begin{bmatrix} \mathrm{vec}(V_0)^\top & \ldots & \mathrm{vec}(V_k)^\top \end{bmatrix}^\top$ with size $p = \Sigma_{j=0}^{k} L_j L_{j+1}$. The Jacobian of the activation function vector at the j^{th} layer is denoted by $\phi_j' : \mathbb{R}^{L_j} \to \mathbb{R}^{L_j \times L_j}$, and $\phi_j'(y) \triangleq \frac{\partial}{\partial z}\phi_j(z)\big|_{z=y}$, $\forall y \in \mathbb{R}^{L_j}$. Let the Jacobian of the DNN with respect to the weights be denoted by $\Phi'(\sigma,\theta) \triangleq \frac{\partial}{\partial \theta}\Phi(\sigma,\theta)$, which can be represented using $\Phi'(\sigma,\theta) = \begin{bmatrix} \Phi_0', & \Phi_1', & \ldots, & \Phi_k' \end{bmatrix}$, where $\Phi_j' \triangleq \frac{\partial}{\partial \mathrm{vec}(V_j)}\Phi(\sigma,\theta)$ for all $j \in [k]$. Then, using (1–9) and the property $\frac{\partial}{\partial \mathrm{vec}(B)}\mathrm{vec}(ABC) = C^\top \otimes A$ yields

$$\Phi_0' = \left(\prod_{l=1}^{\overset{\curvearrowleft}{k}} V_l^\top \phi_l'(\Phi_{l-1}) \right) (I_{L_1} \otimes \sigma_a^\top), \tag{1–10}$$

and

$$\Phi_j' = \left(\prod_{l=j+1}^{\overset{\curvearrowleft}{k}} V_l^\top \phi_l' \left(\Phi_{l-1} \right) \right) \left(I_{L_{j+1}} \otimes \phi_j^\top \left(\Phi_{j-1} \right) \right), \tag{1–11}$$

for all $j \in [k]$. In (1–10) and (1–11), the notation $\prod^{\curvearrowleft}$ denotes the right-to-left matrix product operation, i.e., $\prod_{p=1}^{\overset{\curvearrowleft}{m}} A_p = A_m \dots A_2 A_1$ and $\prod_{p=a}^{\overset{\curvearrowleft}{m}} A_p = I$ if $a > m$, and $\otimes$ denotes the Kronecker product.

1.8.2 Differential Inclusions and Hybrid Systems

Many systems can be modeled as a hybrid dynamical system, which is a system that exhibits both continuous- and discrete-time behavior. The model of a hybrid system requires descriptions of both the continuous and discrete dynamics and the regions where these dynamics apply. The general model of an open-loop hybrid system $\mathcal{H} \triangleq (C_u, F, D_u, G)$ with state $x \in \mathbb{R}^n$ and control input $u \in \mathbb{R}^m$ is written as [67]

$$\mathcal{H} : \begin{cases} \dot{x} \in F\left(x, u\right), & (x, u) \in C_u, \\ x^+ \in G\left(x, u\right), & (x, u) \in D_u, \end{cases} \tag{1–12}$$

where $F : \mathbb{R}^n \times \mathbb{R}^m \rightrightarrows \mathbb{R}^n$ represents the flow map, $C \subset \mathbb{R}^n \times \mathbb{R}^m$ denotes the flow set where the state evolves according to the continuous dynamics, $G : \mathbb{R}^n \rightrightarrows \mathbb{R}^n$ denotes the jump map, and $D \subset \mathbb{R}^n$ denotes the jump set where the discrete dynamics occur. Note that $\dot{x} \in F\left(x\right)$ is a differential inclusion and $x^+ \in G\left(x, u\right)$ is a difference inclusion, where $\dot{x}$ and x^+ describe the continuous and discrete dynamics, respectively. The set-valued nature of F and G can capture multiple possibilities at a given time, helping to model potential disturbances or other model uncertainty. For a hybrid controller $\kappa \triangleq (\kappa_C, \kappa_D) : \mathbb{R}^n \to \mathbb{R}^{m_C} \times \mathbb{R}^{m_D}$ the closed-loop hybrid system $\mathcal{H}_\kappa \triangleq (C, F, D, G)$ is given by

$$\mathcal{H} : \begin{cases} \dot{x} \in F_{cl}\left(x\right) \triangleq F\left(x, \kappa\right), & x \in C, \\ x^+ \in G_{cl}\left(x\right) \triangleq G\left(x, \kappa\right), & x \in D, \end{cases} \tag{1–13}$$

where $C \triangleq \{x \in \mathbb{R}^n : (x, \kappa_C) \in C\}$ and $D \triangleq \{x \in \mathbb{R}^n : (x, \kappa_D) \in D\}$. The hybrid arc ϕ is a solution to the closed-loop hybrid system $\mathcal{H}_\kappa$ defined on a hybrid time domain dom$\phi \subset \mathbb{R}_{\geq 0} \times \mathbb{N}$. The solution to $\mathcal{H}_\kappa$ denoted ϕ is parameterized by the ordinary time variable $t \in \mathbb{R}_{\geq 0}$ and discrete jump variable $j \in \mathbb{N}$. This dissertation focuses on analysis tools for the continuous-time portion of the dynamics in (1–12) and (1–13).

CHAPTER 2
HIGH-ORDER CONTROL BARRIER FUNCTION FOR CONSTRAINING POSITION IN MOTORIZED REHABILITATIVE CYCLING

2.1 Introduction

CBFs have commonly been used to encode the safety requirements of a dynamical system and to constrain the control input to guarantee forward invariance of a safe set. HOCBFs are a method of ensuring the safety of a system of high relative degree. The method developed in this chapter can be applied to a variety of nonlinear systems with more general dynamics than previous works, and is demonstrated on a motorized rehabilitative cycle of relative degree two. A motor controller is designed to constrain the crank position to a time-varying user-defined safe range. Because of the uncertain and nonlinear dynamics of the system, robust control methods are borrowed from Lyapunov theory to develop worst-case controllers that render the intersection of a series of sets forward invariant. The controller is designed so that it provides minimal assistance within the safe range, maximizing the efforts of the rider and facilitating more effective therapy.

2.2 General System

This section describes the HOCBF approach from a general perspective. The technique is inspired by the development in [34], but our work applies to a more general class of dynamics and therefore requires the application of alternative theoretical results. We consider here a specialization of our development in [66] to differential inclusions without flow constraints. A differential inclusion is modeled as

$$\dot{x} \in F(x, u) \tag{2–1}$$

where $F : \mathbb{R}^n \times \mathbb{R}^m \rightrightarrows \mathbb{R}^n$ is a set-valued mapping that associates every point $(x, u) \in \mathbb{R}^n \times \mathbb{R}^m$ with a set $F(x, u) \subset \mathbb{R}^n$. The set-valued nature of the dynamics in (2–1) can be used to model uncertainty, which is useful for robust control (see [158] for more information on set-valued mappings and differential inclusions). We assume that F is

locally bounded, outer semicontinuous, and has nonempty and convex images [66, Sec. 2].

CBFs are defined to guarantee the existence of control inputs that ensure forward invariance (i.e., safety) of a given set of states $\mathcal{S} \subset \mathbb{R}^n$. The following definition of a vector-valued CBF from [66] permits the use of multiple barrier functions to define a set of safe states.

Definition 2.1. [66, Definition 1] A vector-valued function $B : \mathbb{R}^n \to \mathbb{R}^d$ with components $B(x) = (B_1(x), B_2(x), \ldots, B_d(x))$ is called a CBF candidate defining the safe set $\mathcal{S} \subset \mathbb{R}^n$ if $\mathcal{S} = \{x \in \mathbb{R}^n : B_i(x) \leq 0,\ \forall i \in \{1, \ldots, d\}\}$. Also let $\mathcal{S}_i \triangleq \{x \in \mathbb{R}^n : B_i(x) \leq 0\}$ and $M_i \triangleq \{x \in \partial\mathcal{S} : B_i(x) = 0\}$ for each $i \in \{1, \ldots, d\}$.

Definition 2.2. [66, Definition 2] A continuously differentiable CBF candidate $B : \mathbb{R}^n \to \mathbb{R}^d$ defining the set $\mathcal{S} \subset \mathbb{R}^n$ is a CBF for F and $\mathcal{S}$ on a set $\mathcal{O} \subset \mathbb{R}^n$ with respect to a function $\gamma : \mathbb{R}^n \to \mathbb{R}^d$ if 1) there exists a neighborhood of the boundary of $\mathcal{S}$ such that $\mathcal{N}(\partial\mathcal{S}) \subset \mathcal{O}$, 2) for each $i \in [d]$, $\gamma_i(x) \geq 0$ for all $x \in \mathcal{N}(M_i) \setminus \mathcal{S}_i$, and 3) the set

$$K_c(x) \triangleq \{u \in \mathbb{R}^m : \Gamma_i(x, u) \leq -\gamma_i(x),\ \forall i \in [d]\} \tag{2–2}$$

is nonempty for all $x \in \mathcal{O}$, where for each $i \in \{1, \ldots, d\}$,

$$\Gamma_i(x, u) \triangleq \sup_{f \in F(x,u)} \langle \nabla B_i(x), f \rangle . \tag{2–3}$$

Based on theoretical conditions for forward invariance, the set-valued mapping K_c defines a set of control inputs that ensure safety. More specifically, the following corollary of Theorem 2 in [66] shows that, when B is a CBF and some additional conditions are satisfied, continuous controllers selected from the mapping K_c render the safe set $\mathcal{S}$ forward invariant.

Corollary 2.1. *Suppose $B : \mathbb{R}^n \to \mathbb{R}^d$ is a CBF for F and $\mathcal{S}$ on a set $\mathcal{O} \subset \mathbb{R}^n$ with respect to a function $\gamma : \mathbb{R}^n \to \mathbb{R}^d$. Let $\mathcal{D} \triangleq \mathcal{O} \cup \mathcal{S}$, and suppose the control law $\kappa : \mathbb{R}^n \to \mathbb{R}^m$ is continuous on $\mathcal{D}$ with $\kappa(x) \in K_c(x)$ for all $x \in \mathcal{O}$. If one of the following conditions hold:*

2.1.1) $\mathcal{S}$ is compact,

2.1.2) the closed-loop dynamics $F_{cl}(x) \triangleq F(x, \kappa(x))$ are bounded on $\mathcal{S}$, or

2.1.3) F_{cl} has linear growth on $\mathcal{S}$, namely, there exists $c > 0$ such that, for all $x \in \mathcal{S}$, $\sup_{v \in F_{cl}(x)} |v| \leq c(|x| + 1)$,

then $\mathcal{S}$ is forward invariant for the closed-loop dynamics $\dot{x} \in F_{cl}(x)$.

In practice, a constructive method is needed for choosing controllers $\kappa(x) \in K_c(x)$. Such selections can be made using an optimization-based controller given generically by

$$\kappa^*(x) \triangleq \underset{u \in \mathbb{R}^m}{\arg\min} \ |u - u_{nom}(x)|^2 \tag{2–4}$$
$$s.t.\ \mathcal{C}_i(x, u) \leq 0, \ \forall i \in \{1, \ldots, d\},$$

where $u_{nom} : \mathbb{R}^n \to \mathbb{R}^m$ is a continuous nominal control input. By choosing $\mathcal{C}(x, u) \triangleq \Gamma(x, u) + \gamma(x)$, we have $\kappa^*(x) \in K_c(x)$ for each $x \in \mathcal{O}$. The following specialization of Theorem 3 in [66] provides conditions for when κ^* is a continuous function.

Corollary 2.2. *Given $\mathcal{O} \subset \mathbb{R}^n$, let $\mathcal{C} : \mathbb{R}^n \times \mathbb{R}^m \to \mathbb{R}^d$ be continuous on $\mathcal{O} \times \mathbb{R}^m$, and suppose $u \mapsto \mathcal{C}_i(x, u)$ is convex for each $x \in \mathcal{O}$ and each $i \in \{1, \ldots, d\}$. Suppose $u_{nom} : \mathbb{R}^n \to \mathbb{R}^m$ is continuous and the mapping $K^\circ(x) \triangleq \{u \in \mathbb{R}^m : \mathcal{C}_i(x, u) < 0, \ \forall i \in \{1, \ldots, d\}\}$ is nonempty for every $x \in \mathcal{O}$. Then $\kappa^* : \mathcal{O} \to \mathbb{R}^m$ in (4–9) is continuous.*

HOCBFs are used in situations when the control input does not appear in the function Γ_i defined in (2–3), typically due to the fact that B_i does not depend on a state whose dynamics contain the control input. In this case, it may not be possible to render the set $\mathcal{S}_i \triangleq \{x \in \mathbb{R}^n : B_i(x) \leq 0\}$ forward invariant, and we seek a subset of $\mathcal{S}_i$ that can be made forward invariant. The subset is obtained constructively by recursively defining a new CBF candidate that constrains the system to operate in a region where B_i is a CBF, i.e., where the set $K_i(x) \triangleq \{u \in \mathbb{R}^m : \Gamma_i(x, u) \leq -\gamma_i(x)\}$ is nonempty for an appropriately selected function γ_i.

To simplify the description of the HOCBF approach, we turn our attention to a scalar CBF candidate $B_1 : \mathbb{R}^n \to \mathbb{R}$. The following assumption corresponds to the CBF candidate for a system with a relative degree greater than one [34, Definition 6].

Assumption 2.1. For CBF candidate i, the expression defining Γ_i does not depend on the control input, i.e., there is $\Gamma_i : \mathbb{R}^n \to \mathbb{R}$ such that $\sup_{f \in F(x,u)} \langle \nabla B_i(x), f \rangle = \Gamma_i(x)$ for all $x \in \mathbb{R}^n$ and $u \in \mathbb{R}^m$.

Under Assumption 2.1 and for a fixed γ_1, there are two possibilities at a given state $x \in \mathbb{R}^n$: either $K_1(x) = \mathbb{R}^m$ or $K_1(x) = \emptyset$. When $K_1(x)$ is empty at certain key states (particularly, those near the boundary of $\mathcal{S}_1$), we cannot render $\mathcal{S}_1$ forward invariant, and we seek a subset of $\mathcal{S}_1$ that can be made forward invariant. To do so, we recursively define new CBF candidates which will ultimately define a vector-valued CBF as in Definition 2.2. The following assumption is needed to ensure that the recursive CBF is continuously differentiable.

Assumption 2.2. The functions Γ_i and γ_i are continuously differentiable.

Definition 2.3. For CBF candidate $B_i : \mathbb{R}^n \to \mathbb{R}$, let $\gamma_i : \mathbb{R}^n \to \mathbb{R}$ be such that $\gamma_i(x) \geq 0$ for all $x \in \mathcal{N}(\mathcal{S}_i) \setminus \mathcal{S}_i$ and let Assumptions 2.1 and 2.2 hold. The recursion of B_i is defined as

$$B_{i+1}(x) \triangleq \Gamma_i(x) + \gamma_i(x) + \epsilon_i, \tag{2–5}$$

where $\epsilon_i > 0$ is a user-selected constant.

Remark 2.1. It is problematic if trajectories reach states where $\Gamma_i(x) > 0$, since this condition would indicate a potential for the trajectory to continue moving away from the safe set. For certain acceptable choices of γ_i (e.g., $\gamma_i(x) = 0$ for all $x \in \mathbb{R}^n$), it is possible that $\Gamma_i(x) > 0$ at points just outside of the set $\mathcal{S}_{i+1}$. The constant ϵ_i is included in (2–5) to ensure that $\Gamma_i(x) + \gamma_i(x) \leq 0$ in a region outside of $\mathcal{S}_{i+1}$, thereby providing robustness to perturbations from the safe set.

The recursive CBF candidate B_{i+1} is used to restrict the system to operate in the set $\mathcal{S}_{i+1} = \{x \in \mathbb{R}^n : B_{i+1}(x) \leq 0\}$ where $\Gamma_i(x) \leq -\gamma_i(x)$. In other words, we have

that $K_i(x) = \{u \in \mathbb{R}^m : \Gamma_i(x) \leq -\gamma_i(x)\} = \mathbb{R}^m$ for all $x \in \mathcal{S}_{i+1}$. For the new CBF candidate, the function Γ_{i+1}, defined according to (2–3), may or may not depend on the control input. The procedure is to define multiple recursions until either one obtains a CBF, or the set $\mathcal{S} \triangleq \cap_{i=1}^{k} \mathcal{S}_i$ is empty. The following theorem shows how a CBF for the intersection $\mathcal{S} \triangleq \cap_{i=1}^{k} \mathcal{S}_i$ is found when a CBF is obtained after $k > 1$ recursions.

Theorem 2.1. *Consider a CBF candidate $B_1 : \mathbb{R}^n \to \mathbb{R}$ defining the set $\mathcal{S}_1$. For some $k > 1$ and each $i \in \{1, \ldots, k-1\}$, let $B_{i+1} : \mathbb{R}^n \to \mathbb{R}$ be the recursion of B_i defined according to Definition 2.3. Suppose that $\mathcal{S} \triangleq \cap_{i=1}^{k} \mathcal{S}_i$ is nonempty, $\gamma_k : \mathbb{R}^n \to \mathbb{R}$ is continuous with $\gamma_k(x) \geq 0$ for all $x \in \mathcal{N}(M_k) \setminus \mathcal{S}_k$, and there exists a set $\mathcal{O}_k \supset \mathcal{N}(\mathcal{S})$ such that*

$$K_k(x) \triangleq \{u \in \mathbb{R}^m : \Gamma_k(x, u) \leq -\gamma_k(x)\} \tag{2–6}$$

is nonempty for every $x \in \mathcal{O}_k$. Then there is a set $\mathcal{O} \supset \mathcal{N}(\mathcal{S})$ such that $B(x) \triangleq (B_1(x), \ldots, B_k(x))$ is a CBF for F and $\mathcal{S}$ on $\mathcal{O}$ with respect to $\gamma(x) \triangleq (\gamma_1(x), \ldots, \gamma_k(x))$, and $K_c(x) = K_k(x)$ for all $x \in \mathcal{O}$, where

$$K_c(x) \triangleq \{u \in \mathbb{R}^m : \ \Gamma_k(x, u) \leq -\gamma_k(x), \ \Gamma_i(x) \leq -\gamma_i(x) \ i \in \{1, \ldots k-1\}\}.$$

Proof. By the recursive definition in (2–5), the function $B(x) \triangleq (B_1(x), \ldots, B_k(x))$ is a CBF candidate defining the set $\mathcal{S}$. For $x \in \mathcal{S}$ and $1 \leq i < k$, $\Gamma_i(x) \leq -\gamma_i(x) - \epsilon_i$ since $B_{i+1}(x) \leq 0$. Using continuity of B_i, Γ_i, and γ_i, and because $\mathcal{O}_k$ contains a neighborhood of $\mathcal{S}$, there is a set $\mathcal{O}$ such that $\mathcal{N}(\mathcal{S}) \subset \mathcal{O} \subset \mathcal{O}_k$ and for which, for any $1 \leq i < k$, $\Gamma_i(x) \leq -\gamma_i(x)$ for all $x \in \mathcal{O}$. Thus, for any $x \in \mathcal{O}$, $K_c(x) = K_k(x)$. Since K_k is nonempty on $\mathcal{O}$, it follows that K_c is also nonempty on $\mathcal{O}$, which implies that B is a CBF. □

Remark 2.2. In addition to the HOCBF candidate $B(x) = (B_1(x), \ldots, B_k(x))$ defining the set $\mathcal{S} \triangleq \cap_{i=1}^{k} \mathcal{S}_i$, there may be additional CBF candidates $B_v : \mathbb{R}^n \to \mathbb{R}^d$ defining the set $\mathcal{S}_v \subset \mathbb{R}^n$. The conclusions of Theorem 2.1 hold for the CBF candidate $\tilde{B}(x) \triangleq (B(x), B_v(x))$ by replacing the assumption that K_k in (2–6) is nonempty with the

assumption that the set $K_k(x) \cap K_v(x)$ is nonempty for all x in some set $\mathcal{O}_k \supset \mathcal{N}(\tilde{\mathcal{S}})$, where $\tilde{\mathcal{S}} \triangleq \mathcal{S} \cap \mathcal{S}_v$ and K_v is defined by B_v and an appropriately selection function γ_v according to (2–2). The key difference is that $\mathcal{O}_k$ need only contain a neighborhood of the smaller set $\tilde{\mathcal{S}}$.

Since we have established the HOCBF approach for the general dynamics in (2–1), the following sections provide a specific example of how this development can be applied for a person riding a motorized recumbent cycle for rehabilitation.

2.3 Cycle Dynamic Model

The Euler-Lagrange dynamics of the motorized cycle-rider system are [159]

$$M(q)\ddot{q} + V(q,\dot{q})\dot{q} + G(q) + P(q,\dot{q}) + \tau_b(\dot{q}) + \tau_d(t) = \tau_{vol}(t) + \tau_e(t), \tag{2–7}$$

where $q \in \mathcal{Q}$ denotes the measurable crank angle, $\dot{q} \in \mathbb{R}$ denotes the calculable rider cadence (i.e., the crank velocity), and $\ddot{q} \in \mathbb{R}$ denotes the crank acceleration. The set $\mathcal{Q} \subseteq \mathbb{R}$ denotes all possible crank angles. The continuously differentiable inertial forces from the combination of the cycle and the rider's legs are denoted by $M : \mathbb{R} \to \mathbb{R}_{>0}$. The centripetal-Coriolis, gravitational, and viscoelastic tissue forces are denoted by $V : \mathbb{R}^2 \to \mathbb{R}$, $G : \mathbb{R} \to \mathbb{R}$, and $P : \mathbb{R}^2 \to \mathbb{R}$, respectively. The unknown viscous damping torque is denoted by $\tau_b : \mathbb{R} \to \mathbb{R}$. The torque due to unknown disturbances (typically from muscle spasticity) is denoted by $\tau_d : \mathbb{R}_{\geq 0} \to \mathbb{R}$, and the torque produced by volitional efforts of the rider is denoted by $\tau_{vol} : \mathbb{R}_{\geq 0} \to \mathbb{R}$. The torque produced by the electric motor is defined as $\tau_e \triangleq c_e u$, where $c_e > 0$ is the known electric motor control constant that relates the input current $u : \mathbb{R}_{\geq 0} \to \mathbb{R}$ to the motor output torque.

The open-loop dynamics of the motorized cycle-rider system in (2–7) can be rewritten as a continuous time system where F_u is the flow map (see [159] and [38])

$$\dot{z} \in \begin{bmatrix} z_2 \\ M^{-1}(z_1)\,\tau_f(z) \\ 1 \end{bmatrix} + \begin{bmatrix} 0 \\ M^{-1}(z_1) \\ 0 \end{bmatrix} \tau_e \triangleq F_u(z,u), \tag{2–8}$$

where the state $z = [z_1, z_2, z_3]^T$ is defined as $z \triangleq [q, \dot{q}, t]^T$, and the auxiliary term $\tau_f : \mathbb{R}^3 \to \mathbb{R}$ is defined as

$$\tau_f(z) \triangleq \tau_{vol}(t) - \tau_d(t) - V(z)\,z_2 - G(z_1) - P(z) - \tau_b(z_2).$$

The dynamics in (2–8) are unknown because of the unknown input by the rider, the disturbance torques, and the parametric uncertainty in the dynamics. However, each of these physical quantities can be upper bounded by known constants, as described in [159]. The boundedness of each of these terms and other properties from [159] are provided below to facilitate the subsequent control development.

Property 1. The unknown terms in (2–8) can be bounded as $\underline{c}_I \leq M(z_1) \leq \bar{c}_I$, $|V_p(z)| \leq c_V |z_2|$, $|G(z_1)| \leq c_G$, $|P(z)| \leq c_{P1} + c_{P2}|z_2|$, $|\tau_b(z_2)| \leq c_b |z_2|$, $\tau_d \leq c_d$, and $\tau_{vol} \leq c_{vol}$ where $\underline{c}_I$, $\bar{c}_I$, c_V, c_G, c_{P1}, c_{P2}, c_b, c_d, $c_{vol} \in \mathbb{R}_{>0}$ are known constants.

Property 2. $\frac{1}{2}\dot{M}(z_1) = V(z)$.

Property 3. The set-valued mapping $F_u : \mathbb{R}^3 \times \mathcal{U} \rightrightarrows \mathbb{R}^3$ is outer semicontinuous, locally bounded, and convex-valued [31].

2.4 Control Design

A crank position control (versus a cadence control) objective is motivated by motorized cycling applications such as teleoperation and the use of a split-crank cycle. In teleoperation, the desired trajectory of the cycle crank is defined by the angular position of a separate leader cycle [39]. Split-crank cycling is a form of asymmetric rehabilitation where the two sides of the cycle are physically decoupled and controlled independently, preventing the rider from relying too heavily on one leg [40]. Typical split-crank control schemes have the dominant leg track a position that is 180 degrees

offset from the nondominant leg. Because of the symmetry of the cycle, the dynamic model in Section 2.3 can also be used to model a single side of the cycle.

2.4.1 Control Objective

Unlike our previous work in [31] where a CBF was used to constrain the cycle system to a desired cadence range, the control objective is to restrict the position of the cycle crank to a prescribed error range while it follows a desired time-varying position. To quantify this objective, we define the crank position error as

$$e \triangleq z_{1d}(t) - z_1, \tag{2–9}$$

where $z_{1d}(t)$ is the desired angle of the crank. We define $e_L < 0 < e_H$ as user-selected allowable position errors, and the goal is to constrain the position of the crank to a safe set $\mathcal{S} = \{z \in \mathbb{R}^3 : e_L \leq e \leq e_H\}$. The absolute values of e_L and e_H are not required to be equal, so the safe set may be asymmetric about $e = 0$. We then aim to create a controller for the system that renders the allowable set of states forward invariant while using the least amount of motorized input as possible when the state is within the safe set, necessitating the rider's voltional efforts. When the rider begins to stray from a near-zero position error, the motor will assist. We apply the HOCBF approach in Section 2.2 to this motorized cycle-rider system.

2.4.2 Barrier Function Design

The electric motor control input is designed to ensure the safety of the set $\mathcal{S}_1 = \{z \in \mathbb{R}^3 : e_L \leq e \leq e_H\}$ by designing the barrier function candidate $B_1 : \mathbb{R} \to \mathbb{R}$ to be

$$B_1(z) \triangleq \frac{1}{2}\left(\frac{e^2}{\beta(z)} - 1\right), \tag{2–10}$$

where

$$\beta(z) \triangleq \begin{cases} e_L^2 & e \leq 0 \\ e_H^2 & e > 0 \end{cases}.$$

Based on the definition of $\beta(z)$, an equivalent expression for $\mathcal{S}_1$ is

$$\mathcal{S}_1 = \left\{ z \in \mathbb{R}^3 : B_1(z) \leq 0 \right\}. \tag{2–11}$$

As discussed in Section 2.2, one of the requirements for the function B_1 to be a CBF is for the set

$$K_1(z) = \{ u \in \mathbb{R} : \Gamma_1(z, u) \leq -\gamma_1(z) \}$$

to be nonempty for all z in some neighborhood $U(\partial S_1)$, where $\gamma_1(z)$ is a given function such that $\gamma_1(z) \geq 0$ for all $z \in U(S_1) \setminus S_1$. In this case, we can select

$$\gamma_1(z) \triangleq k_{b1} M^{-1}(z_1) B_1(z), \tag{2–12}$$

where $k_{b1} > 0$ is a control gain. The definition in (2–12) satisfies the condition that $\gamma_1(z) \geq 0$ for all $z \in U(S_1) \setminus S_1$ because $M^{-1}(z_1)$ is always positive. Although (2–12) contains the uncertain term $M(z_1)$, γ_1 is not needed for the controller implementation. Based on (2–3), Γ_1 is given by

$$\Gamma_1(z) = \frac{e}{\beta(e)} \dot{z}_{1d} - \frac{e}{\beta(e)} z_2. \tag{2–13}$$

Given (2–12) and (2–13), Γ_1 and γ_1 satisfy Assumptions 2.1 and 2.2.

Because the control input does not appear in (2–13), the set $\mathcal{S}_1$ cannot be rendered forward invariant, and we seek a subset of $\mathcal{S}_1$ that can be made forward invariant. We must iteratively define a new CBF candidate based on (2–5) as

$$B_2(z) \triangleq M(z_1) \frac{e}{\beta(e)} \dot{z}_{1d} - M(z_1) \frac{e}{\beta(e)} z_2 + k_{b1} B_1(z) + \epsilon_1. \tag{2–14}$$

The ϵ_1 term is included in (2–14) to provide some robustness to perturbations. This recursively defined barrier function candidate defines a new safe set

$$\mathcal{S}_2 \triangleq \left\{ z \in \mathbb{R}^3 : B_2(z) \leq 0 \right\}. \tag{2–15}$$

Remark 2.3. The CBF in (2–14) is defined as in (2–5) and is then multiplied by $M(z_1)$. Since $M(z_1) > 0$, it is possible to include the $M(z_1)$ term because the set of states $\mathcal{S}_2$ defined in (2–15) is equivalent to the set of states $z \in \mathbb{R}^3$ such that $M^{-1}(z_1) B_2(z) \leq 0$. The $M(z_1)$ term is included in (2–14) to simplify the subsequent analysis by compensating for the unknown $M^{-1}(z_1)$ terms in (2–8).

Similar to the analysis in Section 2.4.2, the function B_2 is a CBF if there exists a set $\mathcal{O}_2 \supset U(\partial \mathcal{S}_2)$ such that the set

$$K_2(z) = \{u \in \mathbb{R} : \Gamma_2(z, u) \leq -\gamma_2(z)\}, \tag{2–16}$$

is non-empty for all $z \in \mathcal{O}_2$, where $\gamma_2(z)$ is defined as

$$\gamma_2(z) \triangleq \begin{cases} k_{b2}\left(\overline{c}_I \Gamma_1(z) + k_{b1} B_1(z) + \epsilon_1\right) & \text{if } \Gamma_1 \geq 0 \\ k_{b2}\left(\underline{c}_I \Gamma_1(z) + k_{b1} B_1(z) + \epsilon_1\right) & \text{otherwise} \end{cases},$$

where $k_{b2} > 0$ is a control gain. The control input u appears in Γ_2, so another recursive barrier function is not needed.

Remark 2.4. As discussed in Section 2.2, the function γ_2 should be nonnegative on a neighborhood outside the boundary of the safe set. A natural choice that satisfies this condition is the function B_2. However, because the $M(z_1)$ term in (2–14) is uncertain, we use the bound of $M(z_1)$ from Property 1 to define γ_2 such that $\gamma_2(z) \geq k_{b2} B_2(z)$ for all $z \in \mathbb{R}^3$, which implies that $\gamma_2(z) \geq 0$ for all $z \in U(\mathcal{S}_2) \setminus \mathcal{S}_2$.

There are uncertainties in the dynamics of the system, so the inequality in (2–16) cannot be directly computed. Instead we turn to Lyapunov-based robust control techniques where we develop a worst-case bound of the unknown terms in Γ_2. Properties 1-3 are used to show that the unknown terms can be bounded as

$$\Gamma_2(z, u) \leq -\tau_e \frac{e}{\beta(z)} + C(z), \tag{2–17}$$

for all $z \in \mathbb{R}^3$,$u \in \mathbb{R}$, and for positive constants c_1 and c_2 where

$$C(z) \triangleq c_1 + c_2 |e|. \tag{2–18}$$

To facilitate the control design, we define a function $\chi(z) \triangleq k_1 + k_2 |e|$ and select k_1 and k_2 such that

$$C(z) \leq \chi(z) \; \forall e \in \mathbb{R}. \tag{2–19}$$

Based on the gain conditions in (2–19), the inequality in (2–17) can be further bounded as

$$\Gamma_2(z,u) \leq -\frac{c_e}{\beta(e)} eu + \chi(z), \tag{2–20}$$

for all $z \in \mathbb{R}^3$, $u \in \mathbb{R}$. A new regulation map $\bar{K}_2 : \mathbb{R} \rightrightarrows \mathbb{R}$ is defined based on the bound in (2–20) as

$$\bar{K}_2(z) \triangleq \left\{ u \in \mathbb{R} : -\frac{c_e}{\beta(e)} eu + \chi(z) \leq -\gamma_2(z) \right\}. \tag{2–21}$$

Proposition 2.1. *If the gains k_1 and k_2 are selected according to (2–19), then, for any $z \in \mathbb{R}^3$ and $u \in \bar{K}_2(z)$, it follows that $u \in K_2(z)$.*

Proof. When the gains k_1 and k_2 are selected according to (2–19), $\Gamma_2(z,u) \leq -\frac{c_e}{\beta(e)} eu + \chi(z)$. The set $\bar{K}_2(z)$ in (2–21) defines the set of control inputs such that $-\frac{c_e}{\beta(e)} eu + \chi(z) \leq -\gamma_2(z)$, implying that $\Gamma_2(z,u) \leq -\gamma_2(z)$. Therefore, any $u \in \bar{K}_2$ also satisfies the inequality in (2–16). □

A new safe set $\mathcal{S}$ is defined as the intersection of the two previously defined sets

$$\mathcal{S} \triangleq \mathcal{S}_1 \cap \mathcal{S}_2, \tag{2–22}$$

which is defined by the CBF candidate $B(z) \triangleq (B_1(z), B_2(z))$. The cadence state z_2 is unbounded in the set $\mathcal{S}$. To resolve this problem, we follow the analysis in [31] to design a separate CBF to restrict the cycle's cadence to a user-defined safe set.

To add a cadence constraint, we will define the cadence error $e_v \triangleq z_2 - z_{2d}$, where $z_{2d} > 0$ is a constant setpoint. We will limit the cycle's cadence to the safe set $\mathcal{S}_v = \{z \in \mathbb{R}^3 : e_{v_L} \leq e_v \leq e_{v_H}\}$ where $e_{v_L} \leq 0 \leq e_{v_H}$ are user-selected constants. The safe cadence set is encoded by a CBF candidate

$$B_v(z) \triangleq \frac{1}{2} M(z_1) \left(\frac{e_v^2}{\beta_v(z)} - 1 \right), \tag{2–23}$$

where

$$\beta_v(z) \triangleq \begin{cases} e_{v_L}^2 & e_v \leq 0 \\ e_{v_H}^2 & e_v > 0 \end{cases}.$$

The safe set will be defined as the intersection of the set defined by the HOCBF approach in (2–22) and the safe set of cadences defined by (2–23) as

$$\tilde{\mathcal{S}} \triangleq \mathcal{S} \cap \mathcal{S}_v. \tag{2–24}$$

This additional CBF construction necessitates the addition of a second CBF-based constraint to the QP in Section 2.4.3. Such a constraint was developed in [31] for the dynamics in (2–8), where [31] included an additional functional electrical stimulation (FES) control input. The constraint derivation is the same in the absence of FES and is given by the following mapping [31, Eq. 18]

$$\bar{K}_v(z) \triangleq \left\{ u \in \mathbb{R} : \chi_v(z) + \frac{c_e}{\beta(z)} e_v u \leq -\gamma_v(z) \right\}, \tag{2–25}$$

where $\chi_v(z) \triangleq k_{v1} + k_{v2}|e_v| + k_{v3} e_v^2$, and the control gains k_{v1}, k_{v2}, and k_{v3} are positive constants selected according to [31, Eq. 16]. The function γ_v is defined as $\gamma_v(z) \triangleq k_{c1} \left(\frac{e_v^2}{\beta_v(z)} - 1 \right)$,where $k_{c1} > 0$ is a control gain.

2.4.3 Controller Design

While electric motor assistance may be intermittently required in rehabilitative cycling, greater physiological benefits are achieved when assistance is only provided

when the rider is unable to meet cycling objectives on their own [160]. Otherwise, the rider should be expected to pedal under their own volition. The over-reliance on motor assistance can lead to learned helplessness [149], so in the below forced-use approach, the motor control input is designed to be minimized when the rider is able to maintain a position near the desired position volitionally.

The implementable form of the motor controller can be written as the following QP:

$$\begin{aligned} u^{*}(z) = \underset{u \in \mathbb{R}}{\arg\min} \, & |u - u_{nom}(z)|^{2} \\ \text{s.t.} \quad & -\frac{c_e}{\beta(z)} e u + \chi(z) \leq -\gamma_2(z), \\ & \frac{c_e}{\beta_v(z)} e_v u + \chi_v(z) \leq -\gamma_v(z), \end{aligned} \tag{2–26}$$

where $u^{*} : \mathbb{R}^{3} \to \mathbb{R}$ denotes the motor control input and $u_{nom} : \mathbb{R}^{3} \to \mathbb{R}$ is any continuous nominal controller. For the purpose of the experiment in Section 2.6, the nominal controller is defined as $u_{nom}(z) \triangleq 0$ and the controller is completely off whenever possible. The nominal controller can be defined as some positive or negative constant so that the motor provides some amount of assistance or resistance, respectively, as long as this constant does not violate the safety constraint. A number of other types of nominal controllers can be used depending on the goal of the exercise.

Remark 2.5. When there is only one constraint on the motor controller (i.e., the position constraint in (2–21)), a closed-form solution to (2–26) can be developed from [31, Eq. 8] as $u^{*}(z) = -\frac{b(z)}{a(z)}$ when $a(z) u_{nom} + b(z) > 0$, where $a(z) \triangleq -\frac{c_e}{\beta(z)} e$ and $b(z) \triangleq \chi(z) + \gamma_2(z)$, and as $u^{*}(z) = u_{nom}(z)$ otherwise. The closed-form solution without the cadence constraint is feasible and locally Lipschitz continuous according to Lemma 1 of [31] if $e = 0$ implies that $a(z) u_{nom} + b(z) < 0$ when $a(z) = 0$. Equivalently, k_1, k_{b1}, and k_{b2} should be selected such that $k_1 + k_{b2}\left(\epsilon_1 - \frac{1}{2} k_{b1}\right) < 0$. When the cadence constraint is included in the motor controller, the analysis becomes more complicated and SOS programming can be used to verify feasibility as in [66, Section V].

2.5 Forward Invariance

The closed-loop system F_{cl} defined by the open-loop dynamics F_u in (2–8) and the controller u^* in (2–26) is

$$\dot{z} \in F_u\left(z, u^*\left(z\right)\right) \triangleq F_{cl}\left(z\right). \tag{2–27}$$

Define the set of safe control inputs as $K\left(z\right) \triangleq K_2\left(z\right) \cap K_v\left(z\right)$, where K_v is defined as in [31, Eq. 10], and define an additional set $\bar{K}\left(z\right) \triangleq \bar{K}_2\left(z\right) \cap \bar{K}_v\left(z\right)$ as the intersection of the mappings in (2–21) and (2–25). We define a mapping of the interior of $\bar{K}$ using the constraints in (2–26) as

$$\bar{K}^{\circ}\left(z\right) \triangleq \{u \in \mathbb{R} : -\frac{c_e}{\beta\left(e\right)} e u + \chi\left(z\right) < -\gamma_2\left(z\right), \ \frac{c_e}{\beta\left(z\right)} e_v u + \chi_v\left(z\right) < -\gamma_v\left(z\right)\}.$$

For the controller in (2–26) to be feasible and continuous, the set $\bar{K}^{\circ}$ must be nonempty, which we assume in the subsequent theorem. The nonemptiness of $\bar{K}^{\circ}$ can be verified using sum of squares programming [66, Section V].

The following theorem shows that by implementing the QP in (2–26), the position and cadence tracking errors are contained in the desired operating range (i.e., the safe set is forward invariant). The desired operating range is defined by user-selected bounds on the position and cadence of the cycle crank with an additional constraint on the cadence imposed by the HOCBF that is necessary to prevent the position from reaching a state outside of the safe set.

Theorem 2.2. *Consider the motorized cycle-rider system in* (2–8)*. If $\bar{K}^{\circ}$ is nonempty on $\mathcal{O}_2 \supset \mathcal{N}(\tilde{\mathcal{S}})$, then the safe set $\tilde{\mathcal{S}}$ is forward invariant for the closed-loop dynamics defined by F_u and u^* in* (2–27)*, provided that the gain conditions in* (2–19) *and [31, Eq. 16] are met.*

Proof. The function $\tilde{B}\left(z\right) \triangleq \left(B_1\left(z\right), B_2\left(z\right), B_v\left(z\right)\right)$ is a CBF candidate defining the set $\tilde{\mathcal{S}}$. Since $\bar{K}^{\circ}$ is nonempty, $\bar{K}_2$ is nonempty. By Proposition 2.1, $\bar{K}_2 \subset K_2$ if the gain conditions in (2–19) are met, so K_2 is nonempty. Similarly, by [31, Prop. 1], $\bar{K}_v \subset K_v$

if the gains are selected according to [31, Eq. 16]. Therefore, if $\bar{K}$ is nonempty, K is nonempty on $\mathcal{O}_2 \supset \mathcal{N}(\tilde{\mathcal{S}})$. Recalling Remark 2.2, we apply Theorem 2.1 to conclude that there exists a set $\mathcal{O}_2 \supset \mathcal{N}(\tilde{\mathcal{S}})$ such that $\tilde{B}(z)$ is a CBF for F_u and $\tilde{\mathcal{S}}$ on $\mathcal{O}_2$ with respect to the function $\tilde{\gamma}(z) \triangleq (\gamma_1(z), \gamma_2(z), \gamma_v(z))$.

The motor controller u^* is defined in (2–26), and has continuous constraints defined by $\mathcal{C}_1(z,u) \triangleq -\frac{c_e}{\beta(z)}eu + \chi(z) + \gamma_2(z)$ and $\mathcal{C}_2(z,u) \triangleq \frac{c_e}{\beta(z)}e_v u + \chi_v(z) + \gamma_v(z)$ so that $u^*(z) \in K(z)$. By definition, the nominal controller u_{nom} is continuous. The functions $\mathcal{C}_1$ and $\mathcal{C}_2$ are convex in the control input u, so by Corollary 2.2, the controller u^* in (2–26) is continuous. To prove the forward invariance of $\tilde{\mathcal{S}}$, we first prove the closed-loop dynamics given in (2–27) are bounded on $\tilde{\mathcal{S}}$. From Property 1, it can be concluded that F_{cl} is bounded on any set for which z_2 and u^* are bounded. The errors e and e_v take bounded values in $\tilde{\mathcal{S}}$, and thus the state z_2 is bounded. The rate at which the desired position changes $\dot{z}_{1d}$ is bounded by assumption, so it follows that the functions Γ_1, γ_2, and γ_v take bounded values on $\tilde{\mathcal{S}}$. From the boundedness of e, e_v, γ_2, and γ_v and the continuity of u^*, the controller u^* is bounded on $\tilde{\mathcal{S}}$. By Property 1 unknown terms in F_u are bounded by known constants, and by Property 3, the flow map $F_u : \mathbb{R}^3 \times \mathcal{U} \rightrightarrows \mathbb{R}^3$ is locally bounded, ensuring that compact inputs to the mapping will result in compact outputs. Therefore, the closed-loop dynamics are bounded on $\tilde{\mathcal{S}}$, and by Corollary 2.1.2, $\tilde{\mathcal{S}}$ is forward invariant. □

2.6 Experiments

Experiments were conducted to validate the performance of the proposed motor controller in (2–26). The results of the experiments were compared to uncontrolled volitional pedaling. The developed controller was evaluated by its ability to constrain the position of the cycle's crank to a desired position error range and reduce the variance in the cycle crank position compared to volition-only pedaling. Two HOCBF configurations were tested to demonstrate the relationship between the selected safe set and resulting motor input. Experiments were performed on three able-bodied subjects, who gave

written informed consent as approved by the Institutional Review Board at the University of Florida (IRB201600881). Participants 1 and 2 were female, Participant 3 was male, and all ranged in age from 22 to 26 years old.

2.6.1 Experimental Testbed

The experimental testbed consisted of a commercially available recumbent cycle that was modified to have a 250 W, 24 V motor coupled to the drive chain. Orthotic boots were attached to each of the pedals to couple the rider's feet to the crank. An optical encoder with an angular resolution of 20,000 pulses per revolution was mounted to the crank to measure position and cadence. The encoder output was measured using a data acquisition board (Quanser QPIDe) at a sampling rate of 1000 Hz for a duration of 180 s. Real-time control software was run on a desktop computer (Windows 10, QUARC, Matlab/ Simulink). A closed-form solution was found for the QP in (2–26) so that the controller could be run without the need for MATLAB's optimization tools. Although the controller could be implemented without a closed-form solution using Matlab's `quadprog` function, the closed-form solution is less computationally expensive and can be run in real-time. Further details on the experimental setup are available in [152].

An additional experiment was performed on a split-crank cycling testbed like the one in [151]. The left and right sides of the split-crank cycle are mechanically decoupled and controlled separately. Due to the decoupling, the opposing leg does not offset gravitational effects during up-stroke and down-stroke, leading to larger position errors compared to the single-crank cycle [151]. Because the split-crank cycle is symmetric by design, the cycle dynamics in (2–7) can be used to model a single side of the split crank cycle-rider system, without loss of generality. Therefore, the developed HOCBF approach can also be used to constrain the position error on the split-crank cycle.

2.6.2 Procedure

Protocol A is used to validate the developed controller on one participant by demonstrating forward invariance of the safe set of position states even if no volitional effort is provided. Protocol B is designed to investigate whether the HOCBF-based controller in (2–26) reduces the variance in the crank's position compared to volition-only pedaling. Protocol C was performed only on Participant 1 and tests volitional pedaling and the developed HOCBF method on a split-crank cycle [151].

For each protocol, the subject was seated on the cycle and adjustments were made to the seat to prevent knee hyperextension during pedaling. The rider's feet were strapped into orthotic boots. The participant was asked to begin pedaling to bring the cycle's cadence up to 50 RPM, at which point the controller was turned on. For the duration of the trial, the inverted measured position error was displayed for the rider to see. Based on the definition of the position error in (2–9), it was more intuitive for the rider to view the inverted value of the measured position error. The tests for Protocols A and B were 180 s including an initial ramp-up period. The test for Protocol C was 120 s including an initial ramp-up period. To ensure the presented data is representative of steady-state operation, transient data is removed in post-processing. In Protocol A only, the rider was asked not to pedal volitionally for a period of 30 s to demonstrate how the motor controller functions in the absence of volitional effort. For each experiment in Protocols B and C, once the ramp-up period was over, the rider was asked to pedal volitionally and attempt to follow the desired trajectory as closely as possible (i.e., maintain the position error at a near-zero value) for the remaining time.

Protocol A was performed on Participant 1. The purpose of Protocol A is to demonstrate that the controller in (2–26) can render the safe set forward invariant for each of the participants even if the participant provides no volitional effort. A warm-up trial was performed before data was recorded. The warm-up trial allowed the participant to get used to the cycle and controller. The control gains were tuned during this warm-up

trial to ensure the gain condition in (2–19) was met and that the rider was comfortable. The rider was shown a live plot of the inverted position error with a visible indication of the setpoint at 50 RPM and was asked to try to maintain a near-zero position error for the majority of the trial. At 120 s, the rider was asked to withdraw volitional effort and let the motor take over for 30 s. The acceptable low and high position errors e_L and e_H were set to -30 degrees and $+30$ degrees, respectively. The the position error limits were selected based on data from previous volitional pedaling tests. The desired position changed at a rate of 50 RPM, and the lower and upper allowable cadence errors were set to $e_{v_L} = -30$ RPM and $e_{v_H} = 30$ RPM, encoding a cadence range of $20 - 80$ RPM. The cadence limits were chosen to be large so that the majority of the control effort would come from the position constraint, not the cadence constraint. The position and cadence error limits can be tightened or relaxed based on the goal of the cycling exercise.

Protocol B was performed for each of the three participants. For each of the participants in Protocol B, the volitional pedaling trial was performed first of the three trials (two HOCBF trials and one volition-only trial). The order of the two HOCBF trials were randomly selected. The riders were asked to track a desired position z_{1d} that changed at a rate of 50 RPM. The nominal controllers were set to $u_{nom} = 0$ for each trial. For the one of the HOCBF trials (hereafter HOCBF$_{20}$), the acceptable low and high errors e_L and e_H were set to -20 degrees and $+20$ degrees, respectively, and for the other HOCBF trial (hereafter HOCBF$_{30}$), the acceptable low and high errors e_L and e_H were set to -30 degrees and $+30$ degrees. For both HOCBF trials, the lower and upper allowable cadence errors were selected be the same as in Protocol A. For each of the trials in Protocol B, the rider was shown a live plot of the inverted position error with a visible indication of the setpoint at 50 RPM. A warm-up trial was performed for each controller so the controller could be tuned and the rider could become accustomed to

the controller. During the warm-up trials, the control gains were tuned to ensure the forward invariance of the safe set. None of the warm-up trials were recorded.

Protocol C was performed with only Participant 1 to validate the use of the developed controller on the split-crank cycle. Due to the lack of gravitational offset from the opposite leg during split-crank cycling, it is difficult to produce consistent cycling repetitions volitionally. For Protocol C, the HOCBF$_{30}$ safe set was used, where the acceptable low and high errors e_L and e_H were again set to -30 degrees and $+30$ degrees. Because of how difficult it is to pedal volitionally on the split-crank cycle, Protocol C was only tested for one minute after the ramp-up period, instead of two minutes as in Protocols A and B. The participant was unable to complete a volitional effort only comparison test.

Remark 2.6. When the HOCBF method was implemented in the experiment, the terms $\gamma_2(z)$ and $\gamma_v(z)$ in (2–26) were replaced with $\gamma_2(z)^3$ and $\gamma_v(z)^3$, respectively. This selection improves feasibility on the interior of the safe set by allowing the state to evolve more freely near the center of the safe set. The cubic function can be used because meets the requirements for the constraint function outlined in Theorem 2.1.

2.6.3 Results

The position error and motor current for Protocol A are shown in Figure 2-1. For the duration of the trial, the position error did not exit the prescribed safe position range. The minimum position error was -20.83 degrees while the maximum position error was 16.75 degrees. While the rider was able to maintain a near-zero position error, the motor input remained at the nominal control input of zero. At points where the position error approached the upper boundary of the safe region, the motor resisted the rider, driving the error down. For the period of the test where the rider withdrew volitional efforts, the motor input increased, assisting the rider and successfully maintaining a position error inside the safe set. For the duration of the trial, the cadence error did not approach the boundary of the allowable cadence range at ± 30 RPM. The minimum cadence error

was -5.56 RPM, and the maximum cadence error was 4.26 RPM. It was determined computationally that the control input was never impacted by the cadence constraint during the trial. Based on these results, further investigation may enable the removal of the cadence constraint, simplifying the closed-form solution and feasibility analysis of the controller as discussed in Remark 2.5.

Table 2-1 shows relevant statistics for each participant under Protocol B, including the average and standard deviation of the position error, minimum and maximum position error, and time outside safe set during steady-state operation for the HOCBF trials. The torque terms in Table 2-1 are included to differentiate the resistive motor torque that made pedaling more difficult for the rider, and the assistive motor torque, which implies work was done by the motor and not the rider. Resistive torque is defined as the negative component of $\int u^* dt$, and assisitive torque is defined as the positive component of $\int u^* dt$. Controller HOCBF$_{20}$ produced the lowest standard deviation in position error between the three methods but required the greatest motor assistance. Because the safe range of position errors was larger for HOCBF$_{30}$, the standard deviation of errors was larger but still ensured forward invariance of the safe set with less motor effort. In the two HOCBF trials across all participants, the error state never escaped the safe set. Data from the duration of the HOCBF$_{20}$ test for Participant 2 can be seen in Figure 2-2.

Table 2-2 shows relevant statistics for Protocol C. The safe set in Protocol C was defined to be the same as the safe set in Protocol B HOCBF$_{30}$. Despite the fact that the allowable error range is defined to be the same in Protocol B, the average and standard deviation of the position error using the HOCBF approach in Protocol C are much greater than Protocol B HOCBF$_{30}$. Furthermore, the assistive torque used for the HOCBF approach in Protocol C is almost five times greater than Protocol B HOCBF$_{30}$, despite the trial being half as long. The motor is active more regularly in the split-crank configuration because of the increased effect of gravity. Despite the challenges that

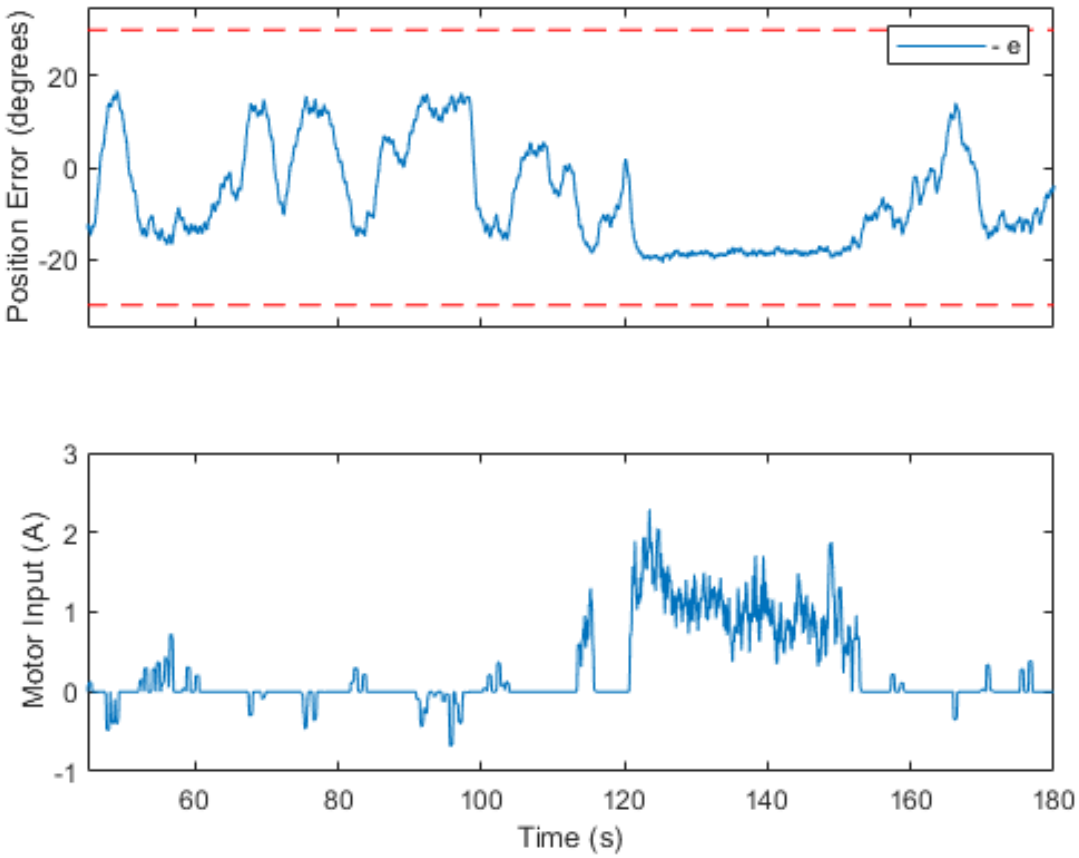

Figure 2-1. Inverted position error (top) and motor current (bottom) for an able-bodied rider for Protocol A. The horizontal lines are representative of the upper and lower desired error range. The ramp-up phase is excluded. The motor current input was filtered with a 0.5 s moving average.

arise due to the lack of gravitational offset from the decoupled opposite side of the crank, the developed HOCBF approach is able to keep the position error inside the safe set for the entire duration of the test.

2.6.4 Discussion

The experimental results show that the HOCBF approach was successful in assisting three riders in maintaining a position error of less than ± 20 or ± 30 degrees on the single-crank cycle and one rider in maintaining a position error of less than ± 30 degrees on the split-crank cycle. Across the three participants, the developed HOCBF approach reduced the standard deviation of the single-crank cycle's position error an

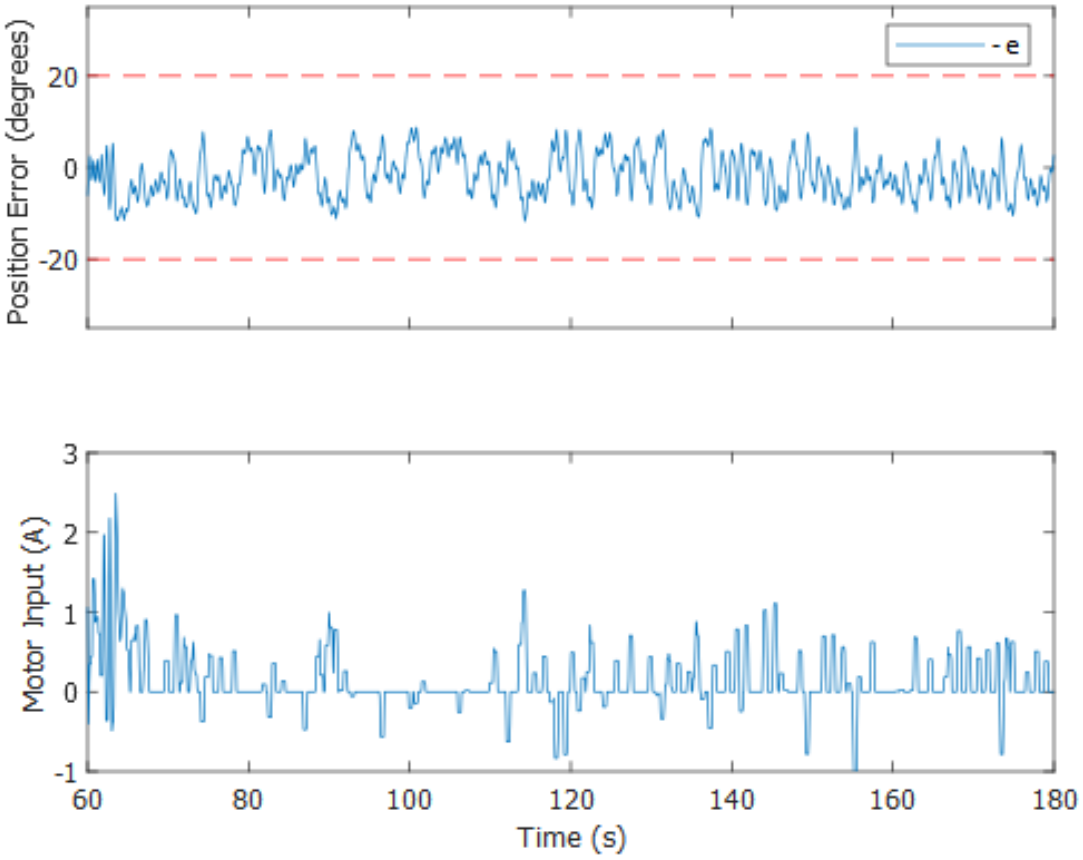

Figure 2-2. Inverted position error (top) and motor current (bottom) for Participant 2 under Protocol A $HOCBF_{20}$. The horizontal lines are representative of the upper and lower desired error range. The ramp-up phase is excluded. The motor current input was filtered with a 0.5 s moving average.

Table 2-1. Protocol B: Results during steady-state operation on single-crank cycle for 60 s to 180 s.

		Participant Number			
Controller	Metric	1	2	3	Avg.
HOCBF_{20}	Avg. e [degrees]	4.10	1.84	2.96	2.97
	SD of e [degrees]	3.70	4.56	4.13	4.13
	Min./Max. e [degrees]	-8.61/10.83	-8.76/11.73	-7.57/10.52	-8.31/11.03
	Assistive Torque [A·s]	15.90	25.24	22.55	21.23
	Resistive Torque [A·s]	-0.65	-8.52	-2.09	-3.75
	Avg. $\lvert u^* \rvert$ [A]	0.14	0.14	0.17	0.15
	Time Outside $\mathcal{S}$ [s]	0	0	0	0
HOCBF_{30}	Avg. e [degrees]	-1.04	-0.82	1.14	-0.24
	SD of e [degrees]	7.59	6.40	8.15	7.38
	Min./Max. e [degrees]	-15.00/15.96	-14.15/14.12	-16.88/18.90	-15.34/16.33
	Assistive Torque [A·s]	1.25	4.11	17.46	7.61
	Resistive Torque [A·s]	-1.12	-2.76	-6.32	-3.4
	Avg. $\lvert u^* \rvert$ [A]	0.001	0.01	0.09	0.03
	Time Outside $\mathcal{S}$ [s]	0	0	0	0
Volition-Only	Avg. e [degrees]	4.69	-0.49	4.18	2.1
	SD of e [degrees]	12.48	10.27	10.84	11.38
	Min./Max. e [degrees]	-44.22/35.41	-39.31/28.11	-27.90/37.88	-41.76/31.76

Table 2-2. Protocol C: Results during steady-state operation on split-crank cycle for 60 s to 120 s.

		Participant Number
Controller	Metric	1
HOCBF_{30}	Avg. e [degrees]	17.03
	SD of e [degrees]	6.85
	Min/Max e [degrees]	6.21/27.78
	$\int (u^*)^+ \, dt$ (Assistive Torque) [A·s]	101.00
	$\int (u^*)^- \, dt$ (Resistive Torque) [A·s]	0
	Avg. $\lvert u^* \rvert$ [A]	1.70
	Time Outside $\mathcal{S}$ [s]	0

average of 35.14% and 63.70% for HOCBF$_{20}$ and HOCBF$_{30}$, respectively. Figures 2-1 and 2-2 show how the motor input varies as the position error changes. The control input is inactive near the center of the safe set and ramp up as the position error gets closer to the boundary of $\mathcal{S}$. The nominal control range can be widened or narrowed by the operator by increasing or decreasing the allowable position error. In Protocol B, HOCBF$_{20}$ had a small allowable position range of ± 20 degrees, while HOCBF$_{30}$ had a larger allowable position range of ± 30 degrees. As can be seen in Table 2-1, average motor input over the duration of the trial decreased as the allowable position range was increased, which is to be expected. Results from Protocol C, which can be seen in Table 2-2, show that the developed approach is also able to constrain the cycle crank position on a split-crank cycle, which typically suffer from a larger position variation than the single-crank cycle. With an increase in control effort compared to the single-crank cycle, developed approach constrained the split-crank's position error to a range of ± 30 degrees, despite the lack of gravitational offset from the opposite side.

2.7 Conclusion

This chapter develops a new HOCBF approach for nonlinear dynamical systems. The technique can be applied to a more general class of dynamics than previous works, and provides the safe set with more robustness to perturbations. The approach was applied to a motorized rehabilitation cycle, and a motor controller is developed to constrain the cycle's crank to an allowable range about the desired time-varying position. Previous works using CBFs on this system were only able to constrain the crank's cadence. In an effort to improve therapy outcomes, the control scheme is designed in such a way that it provides minimal assistance near the center of the safe set, with increasing control effort as the cycle crank approaches the boundary of the safe range, causing the rider to rely less heavily on motor assistance. The safe set is shown to be forward invariant provided certain gain conditions are met. Preliminary experimental results on a single individual demonstrate the designed controller's

ability to maintain the position of the crank to a prescribed safe range while minimizing assistance when the rider is able to do so volitionally. It can be seen in Figures 2-1 and 2-2 that although the error trajectory never leaves the safe set, it also never reaches states near the boundary of the safe set, which is a good example of conservativeness due to uncertain dynamics as discussed in Section 1.2.3.2. Although this conservative behavior is not problematic in the case of the cycling problem, conservativeness can impact performance in other applications. Therefore, the next chapter investigates a method to expand the state's operating region by generating an estimate of the system's uncertain dynamics.

CHAPTER 3
ADAPTIVE DEEP NEURAL NETWORK-BASED CONTROL BARRIER FUNCTIONS

3.1 Introduction

Safety constraints of nonlinear control systems are commonly enforced through the use of control barrier functions (CBFs). Uncertainties in the dynamic model can disrupt forward invariance guarantees or cause the state to be restricted to an overly conservative subset of the safe set. In this chapter, adaptive deep neural networks (DNNs) are combined with CBFs to produce a family of controllers that ensure safety while learning the system's dynamics in real-time without the requirement for pre-training. By basing the least squares adaptation law on a state derivative estimator-based identification error, the DNN parameter estimation error is shown to be uniformly ultimately bounded. The convergent bound on the parameter estimation error is then used to formulate CBF-constraints in an optimization-based controller to guarantee safety despite model uncertainty. Furthermore, the developed method is applicable for use under intermittent loss of state-feedback. Comparative simulation results demonstrate the ability of the developed method to ensure safety in an adaptive cruise control problem and when feedback is lost, unlike baseline methods.

3.2 Problem Formulation

3.2.1 Dynamic Model and Control Objective

Consider the nonlinear dynamic system modeled by

$$\dot{x} = f(x) + g(x)\, u, \tag{3–1}$$

where $x \in \mathbb{R}^n$ denotes the state, $f : \mathbb{R}^n \to \mathbb{R}^n$ denotes an unknown continuously differentiable function, $u \in \Psi \subset \mathbb{R}^m$ denotes the control input, and $g : \mathbb{R}^n \to \mathbb{R}^{n\times m}$ denotes the known control effectiveness matrix, where $\Psi : \mathbb{R}^n \rightrightarrows \mathbb{R}^m$ denotes the set of admissible control inputs. The control objective is to design a controller that ensures the forward invariance of a safe set $\mathcal{S} \subset \mathbb{R}^n$ despite the uncertainty in (3–1). Forward

invariance is a common safety objective as trajectories beginning inside a forward invariant safe set will never reach an unsafe region.

CBFs are a method used to encode a system's safety requirements. Using the development in [65], multiple scalar-valued CBF candidates can be used to define the safe set.

Definition 3.1. [65, Definition 1] A vector-valued function $B : \mathbb{R}^n \to \mathbb{R}^d$ is a CBF candidate defining a safe set $\mathcal{S} \subset \mathbb{R}^n$ if $\mathcal{S} = \{x \in \mathbb{R}^n : B(x) \leq 0\}$, where $B(x) \triangleq (B_1(x), B_2(x), \ldots, B_d(x))$. Also let $\mathcal{S}_i \triangleq \{x \in \mathbb{R}^n : B_i(x) \leq 0\}$ and $M_i \triangleq \{x \in \partial\mathcal{S} : B_i(x) = 0\}$ for each $i \in [d]$.

The state constraints defined by the CBF candidate can then be translated to constraints on the control input, through the introduction of a performance function $\gamma : \mathbb{R}^n \to \mathbb{R}^d$. The design parameter γ limits the worst-case growth of B to ensure forward invariance of $\mathcal{S}$ based on conditions derived in [69].

Definition 3.2. A continuously differentiable CBF candidate $B : \mathbb{R}^n \to \mathbb{R}^d$ defining the set $\mathcal{S} \subset \mathbb{R}^n$ is a CBF for (3–1) and $\mathcal{S}$ on a set $\mathcal{O} \subset \mathbb{R}^n$ with respect to a function $\gamma : \mathbb{R}^n \to \mathbb{R}^d$ if 1) there exists a neighborhood of the boundary of $\mathcal{S}$ such that $\mathcal{N}(\partial\mathcal{S}) \subset \mathcal{O}$, 2) the function γ is such that, for each $i \in [d]$, $\gamma_i(x) \geq 0$ for all $x \in \mathcal{N}(M_i) \setminus \mathcal{S}_i$, and 3) the set

$$K_c(x) \triangleq \left\{u \in \Psi(x) : \nabla B^\top(x)\left(f(x) + g(x)u\right) \leq -\gamma(x)\right\} \tag{3–2}$$

is nonempty for every $x \in \mathcal{O}$.

Since $f(x)$ is unknown, the inequality defining K_c in (3–2) cannot be guaranteed to be satisfied without using a conservative bound on the dynamics that would restrict the state's operating region to a subset of the safe set. Thus, there is motivation to develop an estimate of the uncertain dynamics to expand the operating region. DNNs are a powerful tool that can be used to produce a real-time approximation of $f(x)$.

3.2.2 Deep Neural Network (DNN) Approximation

Based on the universal function approximation theorem, DNNs can be used to approximate continuous functions that lie on a compact set [161]. Lyapunov-based methods have been developed to update the layer weights of a number of neural network (NN) architectures including fully-connected DNNs [52], long short-term memory NNs [157], deep recurrent NNs [56], and deep residual NNs (ResNets) [156].

On a compact set $\Omega \subset \mathbb{R}^n$, the uncertain dynamics in (3–1) can be modeled as

$$f(x) = \Phi(x, \theta^*) + \varepsilon(x), \tag{3–3}$$

where $\Phi : \mathbb{R}^n \times \mathbb{R}^p \to \mathbb{R}^n$ denotes the selected DNN architecture, $\theta^* \in \mathbb{R}^p$ denotes a vector of ideal weights defined as $\theta^* = \arg \min_{\theta} \sup_{x \in \Omega} \left(\|f(x) - \Phi(x, \theta)\|^2 + \sigma \|\theta\|^2 \right)$, where $\sigma \in \mathbb{R}_{>0}$ is a regularizing constant, and $\varepsilon : \mathbb{R}^n \to \mathbb{R}^n$ denotes the unknown function reconstruction error. By the universal function approximation property, for any prescribed $\bar{\varepsilon} \in \mathbb{R}_{>0}$, there exist ideal DNN weights such that $\sup_{x \in \Omega} \|f(x) - \Phi(x, \theta^*)\| \leq \bar{\varepsilon}$. The function approximation error in (3–3) satisfies $\sup_{x \in \Omega} \|\varepsilon(x)\| \leq \bar{\varepsilon}$ on the compact domain Ω. The subsequent CBF analysis ensures the input to the DNN, x, remains in the forward invariant safe set $\mathcal{S} \subseteq \Omega$ for all time, so the universal function approximation property can be applied.

The DNN has a nested nonlinearly parameterized structure, so traditional adaptive control techniques used for linearly parameterized systems are not applicable. To help overcome the complexities introduced by the nonlinearities, a first-order Taylor series approximation can be used to estimate $\Phi(x, \theta^*)$ as [52]

$$\Phi(x, \theta^*) = \Phi\left(x, \hat{\theta}\right) + \Phi' \tilde{\theta} + \Delta_O^2\left(\left\|\tilde{\theta}\right\|\right), \tag{3–4}$$

where $\hat{\theta} \in \mathbb{R}^p$ denotes a vector composed of the adaptive estimates the DNN layer weights that are generated using the subsequently designed adaptation laws, $\Phi' \in \mathbb{R}^{n \times p}$ denotes the Jacobian of the DNN architecture defined as $\Phi' \triangleq \frac{\partial \Phi\left(x, \hat{\theta}\right)}{\partial \hat{\theta}}$, $\tilde{\theta} \in \mathbb{R}^p$ denotes

the weight estimation error defined as $\tilde{\theta} \triangleq \theta^* - \hat{\theta}$, and $\Delta_O^2 : \mathbb{R}^p \to \mathbb{R}^n$ denotes higher-order terms. The following assumption is made to facilitate the subsequent analysis.

Assumption 3.1. There exists a known constant $\overline{\theta} \in \mathbb{R}_{>0}$ such that the unknown ideal weights can be bounded as $\|\theta^*\| \leq \overline{\theta}$ [162, Assumption 1]. Additionally, there exists a known constant $\Xi \in \mathbb{R}_{>0}$ such that $\|f(x) - \Phi(x,\theta)\|^2 + \sigma \|\theta\|^2$ is convex with respect to θ for all $\theta \in \mathcal{B} \triangleq \{\vartheta \in \mathbb{R}^p : \|\theta^* - \vartheta\| \leq \Xi\}$.

Remark 3.1. In Assumption 3.1, local convexity of the regularized loss function $\|f(x) - \Phi(x,\theta)\| + \sigma \|\theta\|^2$ is assumed to facilitate convergence to a local minimum in the subsequent analysis. A number of theoretical results in deep learning literature that indicate that for some DNN architectures such as deep residual neural networks (ResNets), every local minimum is a global minimum [163–166]. Furthermore, the regularizing term $\sigma \|\theta\|^2$ assists in convexifying the loss function and mitigating practical issues in deep learning such as overfitting [167, Chapter 7].

Substituting the DNN estimate in (3–3) and Taylor series approximation in (3–4) into the left-hand side of the inequality in (3–2) yields

$$\dot{B}(x,u) = \nabla B^\top(x) \left(\Phi\left(x, \hat{\theta}\right) + \Phi' \tilde{\theta} + \Delta + g(x)\, u \right), \tag{3–5}$$

where $\Delta \in \mathbb{R}^n$ is defined as $\Delta \triangleq \Delta_O^2\left(\left\|\tilde{\theta}\right\|\right) + \varepsilon(x)$. Although the DNN approximation alone is less conservative than bounding the entire uncertainty, (3–5) is still composed of the unknown terms $\tilde{\theta}$ and Δ. Assumption 3.1 could be used to bound $\tilde{\theta}$ in the CBF constraint in (3–5), but instead we introduce an adaptive identifier in the following subsection to further reduce conservative behavior due to the uncertainty in $\tilde{\theta}$.

3.2.3 Adaptive DNN-Based Identifier Design

All previous Lb-DNN-based adaptive control results update the DNN weights using the tracking error [52, 55, 56, 156, 157, 168]; however, the objective in those results is to track a desired trajectory. To achieve adaptive safety, the adaptive weight updates need to be performed with system identification as the objective. Therefore, a least squares

weight adaptation law is introduced to adaptively identify the system dynamics based on an identification error. Performing least squares-based real-time identification is challenging for continuous-time systems because it requires state-derivative information which is often unknown or noisy. Therefore, the identification error is quantified using the high-gain state-derivative estimator

$$\dot{\hat{x}} = \hat{f} + g(x)\,u + k_x\tilde{x}, \qquad \dot{\hat{f}} = k_f\left(\dot{\tilde{x}} + k_x\tilde{x}\right) + \tilde{x}, \tag{3–6}$$

where $\hat{x}, \hat{f} \in \mathbb{R}^n$ denote the observer estimates of x and f, respectively, $k_x, k_f \in \mathbb{R}_{>0}$ are positive constant observer gains, and observer errors $\tilde{x}, \tilde{f} \in \mathbb{R}^n$ are defined as $\tilde{x} \triangleq x - \hat{x}$ and $\tilde{f} \triangleq f(x) - \hat{f}$, respectively. Although state feedback is available and therefore $\tilde{x}$ is known, $\dot{\tilde{x}}$ is unknown. An implementable form of $\hat{f}$ can be found by integrating both sides of $\dot{\hat{f}}$ in (3–6) to yield $\hat{f}(t) = \hat{f}(t_0) + k_f\tilde{x}(t) - k_f\tilde{x}(t_0) + \int_{t_0}^{t}(k_f k_x + 1)\,\tilde{x}(\tau)\,d\tau$. Taking the time derivative of the definitions of $\tilde{x}$ and $\tilde{f}$ and substituting (3–6) yields

$$\dot{\tilde{x}} = \tilde{f} - k_x\tilde{x}, \qquad \dot{\tilde{f}} = \dot{f} - k_f\tilde{f} - \tilde{x}, \tag{3–7}$$

where $\dot{f}(x) \triangleq \nabla f^{\top}(x)\,\dot{x}$. The following lemma is provided to establish the boundedness of $\dot{f}$ based on the continuous differentiablility of f under common assumptions in CBF literature.

Lemma 3.1. *Consider the function f, a continuous controller $\kappa \in \Psi$ and the set $\mathcal{S} \subset \mathbb{R}^n$. Based on the continuous differentiability of f, the continuity κ, and the boundedness of x on $\mathcal{S}$, the signals f and κ are bounded on $\mathcal{S}$. Therefore, there exists a known constant $\bar{\dot{f}} \in \mathbb{R}_{>0}$ such that $\left\|\dot{f}(x)\right\| \leq \bar{\dot{f}}$ for all $x \in \mathcal{S}$.*

Proof. The safe set $\mathcal{S}$ is compact because it is a closed subset of the compact set Ω. Because of the continuity of f and the fact that $\mathcal{S}$ is compact, there exists a known constant $\overline{f} \in \mathbb{R}_{\geq 0}$ such that $\|f(x)\| \leq \overline{f}$ for all $x \in \mathcal{S}$. The controller κ and control effectiveness g are continuous and therefore bounded for all $x \in \mathcal{S}$. Thus, because $\dot{x} = f(x) + g(x)\,\kappa(x)$, it follows that $\dot{x}$ is bounded for all $x \in \mathcal{S}$ based on the boundedness

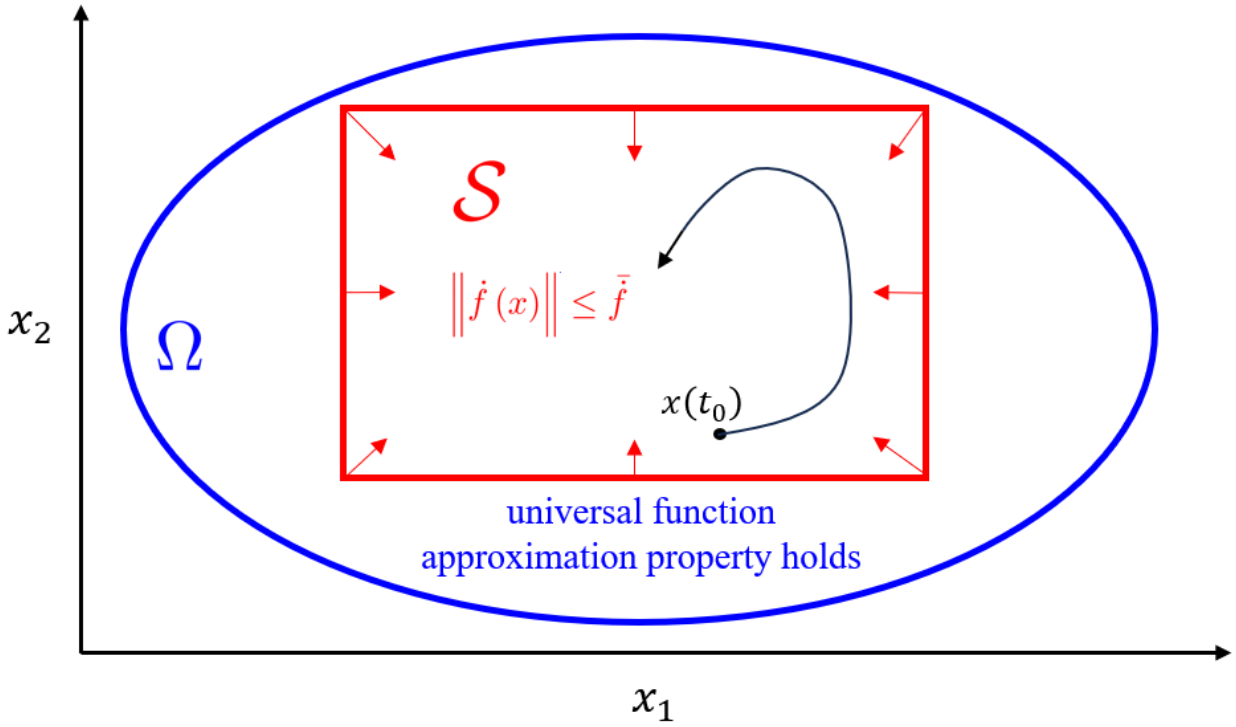

Figure 3-1. An illustration of the sets Ω and $\mathcal{S}$ in $\mathbb{R}^2$. On the blue set Ω the universal function approximation property holds. Flows generated by the CBF are constrained to the red set $\mathcal{S}$, where $\left\|\dot{f}(x)\right\| \leq \bar{\dot{f}}$.

of f, x, and κ on $\mathcal{S}$. The function f is continuously differentiable, so ∇f is bounded on $\mathcal{S}$. Therefore, since $\dot{f}(x) = \nabla f^{\top}(x)\dot{x}$, there exists a constant $\bar{\dot{f}} \in \mathbb{R}_{>0}$ such that $\left\|\dot{f}(x(t))\right\| \leq \bar{\dot{f}}$ for all $x \in \mathcal{S}$. □

Figure 3-1 provides a visualization of the sets Ω and $\mathcal{S}$. The CBF constraints restrict the state trajectories to the safe set $\mathcal{S}$, where $\left\|\dot{f}(x)\right\| \leq \bar{\dot{f}}$. Because $\mathcal{S} \subseteq \Omega$, the universal function approximation property of DNNs holds on $\mathcal{S}$.

Based on the subsequent analysis, the DNN adaptation law $\dot{\hat{\theta}} \in \mathbb{R}^p$ is defined as

$$\dot{\hat{\theta}} = \text{proj}\left(\Gamma\left(-k_\theta\hat{\theta} + \Phi'^{\top}\left(x,\hat{\theta}\right)\left(\hat{f} - \Phi\left(x,\hat{\theta}\right)\right)\right)\right), \tag{3–8}$$

where $k_\theta \in \mathbb{R}_{>0}$ denotes a constant gain and the projection operator proj $(\cdot)$ is defined as in [169, Appendix E] and ensures that $\hat{\theta}(t) \in \mathcal{B}$. The term $\Gamma \in \mathbb{R}^{p\times p}$ denotes a symmetric

positive-definite time-varying least squares adaptation gain matrix that is a solution to

$$\frac{d}{dt}\Gamma^{-1} = -\beta\left(t\right)\Gamma^{-1} + \Phi'^{\top}\left(x,\hat{\theta}\right)\Phi'\left(x,\hat{\theta}\right), \tag{3–9}$$

with the bounded-gain time-varying forgetting factor $\beta : \mathbb{R}_{\geq 0} \to \mathbb{R}_{\geq 0}$ designed as $\beta\left(t\right) \triangleq \beta_0\left(1 - \frac{\|\Gamma\|}{\kappa_0}\right)$, where $\beta_0, \kappa_0 \in \mathbb{R}_{>0}$ are user-defined constants that denote the maximum forgetting rate and the bound prescribed on $\|\Gamma\|$, respectively. The adaptation gain matrix is initialized to be positive-definite such that $\|\Gamma\left(t_0\right)\| < \kappa_0$, and $\Gamma\left(t\right)$ remains positive-definite for all $t \in \mathbb{R}_{\geq 0}$ [170]. Because $\Gamma\left(t\right)$ is positive-definite, there exists a constant $\kappa_1 \in \mathbb{R}_{>0}$ such that $\lambda_{\min}\left(\Gamma\left(t\right)\right) \geq \kappa_1$ for all $t \in \mathbb{R}_{\geq t_0}$. If $\Phi'\left(x,\hat{\theta}\right)$ satisfies the persistence of excitation (PE) condition, meaning there exist constants $\varphi_1, \varphi_2 \in \mathbb{R}_{>0}$ such that $\varphi_1 I_p \leq \int_{t_1}^{t_1+T} \Phi'^{\top}\left(x\left(\tau\right),\hat{\theta}\left(\tau\right)\right)\Phi'\left(x\left(\tau\right),\hat{\theta}\left(\tau\right)\right)d\tau \leq \varphi_2 I_p$ for all $t_1 \in \mathbb{R}_{\geq 0}$ and $T \in \mathbb{R}_{>0}$, it can be shown that $\beta_1 > 0$ [170, Sec. 4.2], where $\beta_1 \in \mathbb{R}_{\geq 0}$ is a constant such that $\beta \geq \beta_1$.

3.3 Stability Analysis

Taking the time derivative of $\tilde{\theta}$, adding and subtracting f, and substituting (3–3) and (3–4) into (3–8), the parameter estimation error dynamics are

$$\dot{\tilde{\theta}} = -\text{proj}\left(\Gamma\left(k_\theta\tilde{\theta} + \Phi'^{\top}\left(x,\hat{\theta}\right)\left(\Phi'\tilde{\theta} + \Delta - \tilde{f}\right) - k_\theta\theta^*\right)\right). \tag{3–10}$$

The subsequent Lyapunov-based stability analysis demonstrates the convergence properties of (3–7) and (3–10).

To facilitate the subsequent stability analysis, let $z \triangleq \left[\tilde{x}^{\top}\ \tilde{f}^{\top}\ \tilde{\theta}^{\top}\right]^{\top} \in \mathbb{R}^{2n+p}$ denote the concatenated state vector. Let the Lyapunov function candidate $V : \mathbb{R}^{2n+p} \to \mathbb{R}$ be defined as

$$V\left(z\right) \triangleq \frac{1}{2}\tilde{x}^{\top}\tilde{x} + \frac{1}{2}\tilde{f}^{\top}\tilde{f} + \frac{1}{2}\tilde{\theta}^{\top}\Gamma^{-1}\tilde{\theta}, \tag{3–11}$$

which can be bounded as

$$\lambda_1\left\|z\right\|^2 \leq V\left(z\right) \leq \lambda_2\left\|z\right\|^2, \tag{3–12}$$

where $\lambda_1 \triangleq \min\left\{\frac{1}{2}, \frac{1}{2\kappa_0}\right\}$, $\lambda_2 \triangleq \max\left\{\frac{1}{2}, \frac{1}{2\kappa_1}\right\}$. Taking the time-derivative of (3–11), substituting (3–7), (3–9), and (3–10), and applying the property of projection operators $-\tilde{\theta}^\top \Gamma^{-1} \text{proj}(\mu) \leq -\tilde{\theta}^\top \Gamma^{-1} \mu$ [169, Lemma E.1.IV], yields

$$\begin{aligned}\dot{V} \leq & -k_x \|\tilde{x}\|^2 - k_f \left\|\tilde{f}\right\|^2 + \tilde{f}^\top \dot{f} \\ & - \left(\frac{\beta_1}{2\kappa_0} + k_\theta\right) \left\|\tilde{\theta}\right\|^2 - \frac{1}{2}\tilde{\theta}^\top \Phi'^\top \left(x, \hat{\theta}\right) \Phi'\left(x, \hat{\theta}\right) \tilde{\theta} \\ & + \tilde{\theta}^\top \Phi'^\top \left(x, \hat{\theta}\right) \left(\tilde{f} - \Delta\right) + k_\theta \tilde{\theta}^\top \theta^*. \end{aligned} \tag{3–13}$$

Because f and Φ are continuously differentiable $\|\Delta\| \leq c_1$ and $\left\|\Phi'\left(x, \hat{\theta}\right)\right\|_F \leq c_2$ when $z \in \mathcal{D} \triangleq \{\zeta \in \mathbb{R}^{2n+p} : \|\zeta\| \leq \chi\}$, where $c_1, c_2, \chi \in \mathbb{R}_{>0}$ are known constants. Recall that by Lemma 3.1, there exists a known bound $\overline{\dot{f}} \in \mathbb{R}_{>0}$ such that $\left\|\dot{f}\right\| \leq \overline{\dot{f}}$ for all $x \in \mathcal{S}$. Using Young's Inequality and Assumption 3.1, $\tilde{\theta}^\top \Phi'^\top \left(x, \hat{\theta}\right)\left(\tilde{f} - \Delta\right) \leq c_2 \left\|\tilde{\theta}\right\|^2 + \frac{c_2}{2}\left\|\tilde{f}\right\|^2 + \frac{c_2 c_1^2}{2}$, $\tilde{f}^\top \dot{f} \leq \frac{\overline{\dot{f}}}{2}\left\|\tilde{f}\right\|^2 + \frac{\overline{\dot{f}}}{2}$, and $k_\theta \tilde{\theta}^\top \theta^* \leq \frac{k_\theta}{2}\left\|\tilde{\theta}\right\|^2 + \frac{k_\theta}{2}\overline{\theta}^2$, so (3–13) can be further bounded as

$$\dot{V} \leq -\lambda_3 \|z\|^2 + C - \frac{1}{2}\tilde{\theta}^\top \Phi'^\top \left(x, \hat{\theta}\right) \Phi'\left(x, \hat{\theta}\right) \tilde{\theta}, \tag{3–14}$$

where $\lambda_3 \triangleq \min\left\{k_x,\ k_f - \frac{\overline{\dot{f}}}{2} - \frac{c_2}{2},\ \frac{\beta_1}{2\kappa_0} + \frac{k_\theta}{2} - c_2\right\}$ and $C \triangleq \frac{\overline{\dot{f}} + c_2 c_1^2 + k_\theta \overline{\theta}^2}{2}$. Additionally, let $\mathcal{Q} \triangleq \left\{\zeta \in \mathbb{R}^{2n+p} : \|\zeta\| \leq \sqrt{\frac{\lambda_1}{\lambda_2}\chi^2 - \frac{C}{\lambda_3}}\right\}$, which is defined to initialize z in the subsequent analysis. The initial condition $x(t_0)$ is considered to be in the interior of $\mathcal{S}$ to ensure $\mathcal{I}$ is not measure-zero, thus ruling out solutions that instantly escape $\mathcal{S}$. The following theorem provides conditions under which the adaptation law in (3–8) yields parameter estimation error convergence.

Theorem 3.1. *Let $t \mapsto x(t)$ be such that $x(t_0) \in \text{int}(\mathcal{S})$ and there exists a time interval $\mathcal{I} \triangleq [t_0, t_{\mathcal{I}})$ such that $x(t) \in \mathcal{S}$ for all $t \in \mathcal{I}$. If Assumption 3.1 is satisfied, κ is continuous, and $\chi > \sqrt{\frac{\lambda_2 C}{\lambda_1 \lambda_3}}$, then the weight update law in (3–8) ensures that $\left\|\tilde{\theta}(t)\right\| \leq \tilde{\theta}_{UB}(t)$ for all $t \in \mathcal{I}$, where*

$$\tilde{\theta}_{UB}(t) \triangleq \sqrt{\frac{\lambda_2}{\lambda_1}\|z(t_0)\|^2 e^{-\frac{\lambda_3}{\lambda_2}t} + \frac{\lambda_2 C}{\lambda_1 \lambda_3}\left(1 - e^{-\frac{\lambda_3}{\lambda_2}t}\right)},$$

provided $z(t_0) \in \mathcal{Q}$, $\hat{\theta}(t_0) \in \mathcal{B}$, *and* $\lambda_3 > 0$.

Proof. From the Lyapunov function candidate in (3–11) and the inequalities in (3–12) and (3–14), $\dot{V}$ can be further bounded as $\dot{V} \leq -\frac{\lambda_3}{\lambda_2} V + C$, for all $z \in \mathcal{D}$ and $t \in \mathcal{I}$ if the gain condition is satisfied. Solving the differential inequality over the time interval $\mathcal{I}$ yields

$$V(z(t)) \leq V(z(t_0)) e^{-\frac{\lambda_3}{\lambda_2} t} + \frac{\lambda_2 C}{\lambda_3} \left(1 - e^{-\frac{\lambda_3}{\lambda_2} t}\right), \tag{3–15}$$

for all $z \in \mathcal{D}$. From (3–11) and (3–15), it follows that

$$\|z(t)\| \leq \sqrt{\frac{\lambda_2}{\lambda_1} \|z(t_0)\|^2 e^{-\frac{\lambda_3}{\lambda_2} t} + \frac{\lambda_2 C}{\lambda_1 \lambda_3} \left(1 - e^{-\frac{\lambda_3}{\lambda_2} t}\right)}, \tag{3–16}$$

for all $z \in \mathcal{D}$ and $t \in \mathcal{I}$. To ensure $z(t) \in \mathcal{D}$ for all $t \in \mathcal{I}$, further upper-bounding (3–16) yields $\|z(t)\| \leq \sqrt{\frac{\lambda_2}{\lambda_1} \|z(t_0)\|^2 + \frac{\lambda_2 C}{\lambda_1 \lambda_3}}$ for all $t \in \mathcal{I}$. Since $\mathcal{D} = \{\zeta \in \mathbb{R}^{2n+p} : \|\zeta\| \leq \chi\}$, $z(t) \in \mathcal{D}$ always holds if $\sqrt{\frac{\lambda_2}{\lambda_1} \|z(t_0)\|^2 + \frac{\lambda_2 C}{\lambda_1 \lambda_3}} \leq \chi$, which is guaranteed if $\|z(t_0)\| \leq \sqrt{\frac{\lambda_1}{\lambda_2} \chi^2 - \frac{C}{\lambda_3}}$, i.e., $z(t_0) \in \mathcal{Q}$. Thus, trajectories of z do not escape $\mathcal{D}$ if z is initialized in $\mathcal{Q}$. Additionally, because $\left\|\tilde{\theta}\right\| \leq \|z\|$, (3–16) implies

$$\left\|\tilde{\theta}(t)\right\| \leq \sqrt{\frac{\lambda_2}{\lambda_1} \|z(t_0)\|^2 e^{-\frac{\lambda_3}{\lambda_2} t} + \frac{\lambda_2 C}{\lambda_1 \lambda_3} \left(1 - e^{-\frac{\lambda_3}{\lambda_2} t}\right)}, \tag{3–17}$$

for all $t \in \mathcal{I}$ and $z \in \mathcal{D}$ if $z(t_0) \in \mathcal{Q}$. For the initial conditions to be feasible, $\mathcal{Q}$ is required to be non-empty, which is ensured by selecting $\chi > \sqrt{\frac{\lambda_2 C}{\lambda_1 \lambda_3}}$. □

The bound in (3–17) cannot be implemented without information about the concatenated initial state $z(t_0)$. Since the state information is available, $\hat{x}$ is initialized such that $\tilde{x}(t_0) = 0$. While $\tilde{f}$ and $\tilde{\theta}$ are unknown, each have known bounds. Recall that because of the continuity of f and the fact that $\mathcal{S}$ is a closed subset of the compact set Ω and is therefore compact, there exists a known constant $\overline{f} \in \mathbb{R}_{\geq 0}$ such that $\|f(x)\| \leq \overline{f}$ for all $x \in \mathcal{S}$. Thus, it follows that $\tilde{f}$ is bounded. The bound on $\tilde{\theta}$ is a result of the projection operator in (3–10). If $\left\|\hat{f}(t_0)\right\| \leq \overline{f}$ and $\hat{\theta}(t_0) \in \mathcal{B}$, then $\left\|\tilde{f}(t_0)\right\| \leq 2\overline{f}$ and $\left\|\tilde{\theta}(t_0)\right\| \leq \Xi$.

Therefore, there exists a known constant $\mathcal{Z} \in \mathbb{R}_{>0}$ such that $\|z(t_0)\| \leq \mathcal{Z} \triangleq \sqrt{\Xi^2 + 4\overline{f}^2}$ and (3–17) can be further bounded as

$$\left\|\tilde{\theta}(t)\right\| \leq \sqrt{\frac{\lambda_2}{\lambda_1}\mathcal{Z}^2 e^{-\frac{\lambda_3}{\lambda_2}t} + \frac{\lambda_2 C}{\lambda_1 \lambda_3}\left(1 - e^{-\frac{\lambda_3}{\lambda_2}t}\right)}, \tag{3–18}$$

for all $t \in \mathcal{I}$ and $z \in \mathcal{D}$ if $z(t_0) \in \mathcal{Q}$.

Because the bound in (3–18) may initially be more conservative than Ξ, we design a function $\chi_\theta \in \mathbb{R}_{>0}$ as

$$\chi_\theta \triangleq \min\left\{\Xi, \sqrt{\frac{\lambda_2}{\lambda_1}\mathcal{Z}^2 e^{-\frac{\lambda_3}{\lambda_2}t} + \frac{\lambda_2 C}{\lambda_1 \lambda_3}\left(1 - e^{-\frac{\lambda_3}{\lambda_2}t}\right)}\right\}, \tag{3–19}$$

such that $\left\|\tilde{\theta}(t)\right\| \leq \chi_\theta$ for all time. When the observer gains k_x and k_f are selected to be sufficiently high, $\lambda_3 = \frac{\beta_1}{2\kappa_0} + \frac{k_\theta}{2} - c_2$, which implies the rate of convergence in (3–18) depends primarily on β_1 and k_θ. Thus, when the PE condition is satisfied, $\beta_1 > 0$, resulting in a larger λ_3 which implies χ_θ converges faster and to a smaller value. When the PE condition is not satisfied, the gain k_θ helps achieve the uniform ultimate boundedness of $\tilde{\theta}$ based on sigma modification; however, selection of a larger k_θ yields a larger C, worsening parameter estimation performance. By substituting the developed upper-bound of the parameter estimation error in (3–19) into (3–5) and recalling $\|\Delta\| \leq c_1$, a new CBF notion composed of only the known signals can be defined.

Definition 3.3. A continuously differentiable CBF candidate $B : \mathbb{R}^n \to \mathbb{R}^d$ defining the set $\mathcal{S} \subseteq \Omega$ is an *adaptive DNN CBF (aDCBF)* for the dynamics in (3–1) and safe set $\mathcal{S}$ on a set $\mathcal{O} \subset \mathbb{R}^n$ with respect to $\gamma : \mathbb{R}^n \to \mathbb{R}^d$ if 1) there exists a neighborhood of the boundary of $\mathcal{S}$ such that $\mathcal{N}(\partial\mathcal{S}) \subset \mathcal{O}$, 2) for each $i \in [d]$, $\gamma_i(x) \geq 0$ for all $x \in \mathcal{N}(M_i) \setminus \mathcal{S}_i$, and 3) the set

$$K_d(x) \triangleq \left\{u \in \Psi : \left\|\nabla B^\top(x)\Phi'\right\|(\chi_\theta + c_1) + \nabla B^\top(x)\left(\Phi\left(x, \hat{\theta}\right) + g(x)u\right) \leq -\gamma(x)\right\},$$

is nonempty for all $x \in \mathcal{O}$.

The set K_d represents the set of control inputs that will render the set $\mathcal{S}$ forward invariant. A selection of K_d that minimizes some cost function can be made at each $x \in \mathcal{O}$ using an optimization-based control law. The controller $\kappa^* : \mathbb{R}^n \to \Psi$ is defined as

$$\kappa^*(x) \triangleq \underset{u \in \Psi}{\arg\min}\, Q(x,u), \quad \text{s.t. } \mathcal{C}_F(x,u) \leq 0, \tag{3–20}$$

where $Q(x,u) : \mathbb{R}^n \times \Psi \to \mathbb{R}$ is a cost function typically selected as $\|u - u_{nom}\|^2$, $u_{nom} \in \Psi$ is a nominal continuous control input, and $\mathcal{C} : \mathbb{R}^n \times \Psi \to \mathbb{R}^d$ are the constraints on the control input. By choosing $\mathcal{C}_F(x,u) \triangleq \left\|\nabla B^\top(x)\Phi'\right\|(\chi_\theta + c_1) + \nabla B^\top(x)\left(\Phi\left(x,\hat{\theta}\right) + g(x)u\right) + \gamma(x)$, the optimization problem yields a controller $\kappa^*(x) \in K_d$ for all $x \in \mathcal{O}$ assuming K_d is nonempty on the set $\mathcal{O}$. To obtain an implementable form of the controller, we impose the following conditions on the set of admissible control inputs Ψ.

Assumption 3.2. There exists a function $\psi : \mathbb{R}^n \times \mathbb{R}^m \to \mathbb{R}^s$ such that $\Psi(x) = \{u \in \mathbb{R}^m : \psi(x,u) \leq 0\}$ for all $x \in \mathbb{R}^n$. Additionally, for each $r \in [s]$, the function $u \mapsto \psi_r(x,u)$ is convex on K_d and $(x,u) \mapsto \psi(x,u)$ is continuous on $\mathcal{O} \times \mathbb{R}^m$.

The following lemma of [65, Theorem 4] provides conditions that result in a continuous κ^*.

Lemma 3.2. *[65, Theorem 4] Let $\mathcal{C} : \mathbb{R}^n \times \mathbb{R}^m \to \mathbb{R}^h$ be continuous on $\mathcal{O} \times \mathbb{R}^m$, and, for each $g \in [h]$, let $u \mapsto \mathcal{C}_g(x,u)$ be convex on the set $K(x) \triangleq \{u \in \mathbb{R}^m : \mathcal{C}_g(x,u) \leq 0, \forall g \in [h]\}$. Suppose $Q : \mathbb{R}^n \times \mathbb{R}^m \to \mathbb{R}$ is continuous and for each $x \in \mathcal{O}$, $u \mapsto Q(x,u)$ is strictly convex and inf-compact on $K(x)$. If the set $K^\circ(x) \triangleq \{u \in \mathbb{R}^m : \mathcal{C}_g(x,u) < 0, \forall g \in [h]\}$ is nonempty for every $x \in \mathcal{O}$, then $\kappa^*(x) \triangleq \underset{u \in K}{\arg\min}\, Q(x,u)$ is continuous.*

The continuity of κ^* established in Lemma 3.2 allows Lemma 3.1 and Theorem 3.1 to be used in the proof of the following theorem, which presents the main result of this chapter. The implication of the theorem is that the developed DNN-based optimization

problem in (3–20) ensures system trajectories beginning in the user-selected safe set $\mathcal{S}$ will remain in $\mathcal{S}$ for all time.

Theorem 3.2. *Suppose $B : \mathbb{R}^n \times \mathbb{R}^p \to \mathbb{R}$ is an aDCBF for the system defined by (3–1) and (3–20) defining a safe set $\mathcal{S} \subseteq \Omega$. Let $\hat{x}$, $\hat{f}$, and $\hat{\theta}$ update according to (3–6) and (3–8), respectively. Let the system be initialized such that $\hat{x}(t_0) = x(t_0)$, $\left\|\hat{f}(t_0)\right\| \leq \overline{f}$, $z(t_0) \in \mathcal{Q}$, and $\hat{\theta}(t_0) \in \mathcal{B}$. If Assumptions 3.1 and 4.1 hold, Q is selected to be continuous, and $u \mapsto Q(x,u)$ is strictly convex and inf-compact on $K_d(x)$, then the safe set $\mathcal{S}$ is forward invariant for the closed-loop dynamics defined by (3–1), the controller κ^* in (3–20), and the adaptive weight update law in (3–8), provided $\lambda_3 > 0$.*

Proof. Let $t \mapsto x(t)$ be a solution to the closed-loop dynamics f_{cl} defined by (4–1) and (3–20). Because B is an aDCBF in the sense of Definition 3.3, the set $K_d(x)$ is nonempty on $\mathcal{O} \supset \mathcal{N}(\mathcal{S})$. Thus, the optimization-based control law in (3–20) yields a controller $\kappa^* \in K_d$. Because Q is continuous and $u \mapsto Q(x,u)$ is strictly convex and inf-compact on $K_d(x)$ by assumption, Assumption 4.1 holds, $\mathcal{C}_F$ is continuous on $\mathcal{O} \times \mathbb{R}^m$, and $u \mapsto \mathcal{C}_F(x,u)$ is convex on K_d. Therefore, the conditions of Lemma 3.2 hold, thus implying κ^* is single-valued and continuous on $\mathcal{O}$. By Lemma 3.1, there exists a constant $\bar{\dot{f}}$ such that $\left\|\dot{f}\right\| \leq \bar{\dot{f}}$ for all $x \in \mathcal{S}$, so Theorem 3.1 can be used to show that the weight update law in (3–8) ensures $\left\|\tilde{\theta}\right\|$ is uniformly ultimately bounded by (3–17) for all $t \in \mathcal{I}$. Since $\left\|\hat{f}(t_0)\right\| \leq \overline{f}$, $z(t_0) \in \mathcal{D}$, $\hat{\theta}(t_0) \in \mathcal{B}$, and f is continuously differentiable, it follows that $\left\|\tilde{\theta}(t_0)\right\| \leq \Xi$, $\left\|\tilde{f}(t_0)\right\| \leq 2\overline{f}$, and $\|\Delta\| \leq c_1$. Therefore, for every $u \in \Psi$ and $t \in \mathcal{I}$, $\nabla B^\top(x)\dot{x} \leq \left\|\nabla B^\top(x(t))\Phi'\right\|(\chi_\theta + c_1) + \nabla B^\top(x(t))\left(\Phi\left(x(t), \hat{\theta}\right) + g(x(t))u\right)$, implying $\kappa^*(x(t)) \in K_d(x(t)) \subset K_c(x(t))$ for all $t \in \mathcal{I}$. Since K_d is nonempty for all $x \in \mathcal{O}$, K_c is nonempty on $\mathcal{O}$ and B is a CBF defining the set $\mathcal{S}$ in the sense of Definition 4.1. By Theorem 1 of [65], $\mathcal{S}$ is forward pre-invariant for the closed-loop dynamics defined by (4–1) and (3–20). Maximal solutions to f_{cl} are either complete or escape in finite-time by flowing [69, Proposition 3]. The safe set $\mathcal{S}$ is compact by definition, eliminating the possibility of finite-time escape from the safe set [158, Theorem 10.1.4],

which implies all maximal solutions to the closed-loop system are complete, i.e., the maximal $\mathcal{I} = [t_0, \infty)$. Thus, it follows that the safe set $\mathcal{S}$ is forward invariant. □

3.4 Safety Under Intermittent State Feedback

During intermittent loss of feedback, the state measurements are not available, so it is impossible to use any feedback mechanisms; however, because the developed DNN yields parameter estimation error guarantees, it can be used to make state predictions at times when feedback is lost. Let $k \in \mathbb{Z}_{\geq 0}$ denote the time index such that feedback is unavailable in the time interval $[t_{2k+1}, t_{2k+2})$. When feedback is not available, an open-loop estimation of the current state $\hat{X} \in \mathbb{R}^n$ can be updated according to

$$\dot{\hat{X}} = \Phi\left(\hat{X}, \hat{\theta}\left(t_{2k+1}\right)\right) + g\left(\hat{X}\right) u, \tag{3–21}$$

where the initial condition for the state estimate is $\hat{X}\left(t_{2k+1}\right) = x\left(t_{2k+1}\right)$. When feedback becomes available, $\hat{X}(t)$ is reset as $\hat{X}(t) = x(t)$ for all $(t, k) \in [t_{2k}, t_{2k+1}) \times \mathbb{Z}_{\geq 0}$.
In disturbance observer-based methods such as [48], the CBF-based constraint is reliant on the observer estimate of the dynamics and therefore on state measurements, so safety cannot be ensured when feedback is lost. In the developed approach, the constraint in (3–20) can be modified to ensure safety until feedback is restored.

3.4.1 Modified CBF Constraint Development

The open-loop estimator error $\tilde{X} \in \mathbb{R}^n$ is defined as $\tilde{X} \triangleq x - \hat{X}$; thus, $\tilde{X}\left(t_{2k+1}\right) = 0$. Exclusively for the purpose of this section, it is assumed that there exists a known constant $\bar{u} \in \mathbb{R}^n$ such that $\|u\| \leq \bar{u}$, for all $u \in \Psi$, the drift f is globally bounded and Lipschitz, and g is globally Lipschitz. Such an assumption on the boundedness of f is mild since finite-time escape is not inherent to the uncontrolled dynamics for most physical systems of practical interest. Based the assumptions on the boundedness of u and f and the continuous differentiability of Φ, there exists a Lipschitz constant

$L_U \in \mathbb{R}_{>0}$ such that

$$\left\| \Phi\left(x, \theta^*\right) - \Phi\left(\hat{X}, \theta^*\right) + \left(g\left(x\right) - g\left(\hat{X}\right)\right) u \right\| \leq L_U \left\| \tilde{X} \right\|, \tag{3–22}$$

and, additionally, there exists a constant $\Delta_U \in \mathbb{R}_{>0}$ such that

$$\left\| \Phi\left(\hat{X}, \theta^*\right) - \Phi\left(\hat{X}, \hat{\theta}\left(t_{2k+1}\right)\right) + \varepsilon\left(x\right) \right\| \leq \Delta_U. \tag{3–23}$$

Let the Lyapunov function candidate during loss of feedback $V_U : \mathbb{R}^{2n+p} \to \mathbb{R}$ be defined as $V_U \triangleq \frac{1}{2}\tilde{X}^\top \tilde{X}$. Taking the time-derivative of V_U, adding and subtracting $\Phi\left(\hat{X}, \theta^*\right)$, substituting in (3–22) and (3–23), and using Young's Inequality, it can be shown that $\dot{V}_U \leq \lambda_U V_U + \frac{\Delta_U}{2}$ when feedback is unavailable, where $\lambda_U \triangleq 2L_U + \Delta_U$. Solving for V_U yields $V_U\left(t\right) \leq \left(V\left(t_{2k+1}\right) + \delta_U\right) e^{\lambda_U\left(t - t_{2k+1}\right)} - \delta_U$ for all $\left(t, k\right) \in \left[t_{2k+1}, t_{2k+2}\right) \times \mathbb{Z}_{\geq 0}$, where $\delta_U \triangleq \frac{2\Delta_U}{2L_U + \Delta_U}$. Therefore, the open-loop estimation error dynamics can be shown to satisfy the form $\left\| \dot{\tilde{X}} \right\| \leq L_U \left\| \tilde{X} \right\| + \Delta_U$, which is exponentially unstable (cf., [171, 172]) such that

$$\left\| \tilde{X}\left(t\right) \right\| \leq \overline{\tilde{X}}\left(t\right) \triangleq \sqrt{\delta_U\left(e^{\lambda_U\left(t - t_{2k+1}\right)} - 1\right)} \tag{3–24}$$

for all $\left(t, k\right) \in \left[t_{2k+1}, t_{2k+2}\right) \times \mathbb{Z}_{\geq 0}$. The system dynamics can be bounded as $\left\|\dot{x}\right\| \leq \left\| \dot{\hat{X}} \right\| + \left\| \dot{\tilde{X}} \right\| \leq L_U \overline{\tilde{X}} + \Delta_U + \left\| \Phi\left(\hat{X}, \hat{\theta}\left(t_{2k+1}\right)\right) + g\left(x\right) u \right\|$, and if ∇B is locally Lipschitz, then $\left\| \nabla B^\top\left(x\right) - \nabla B^\top\left(\hat{X}\right) \right\| \leq \rho \overline{\tilde{X}}\left(t\right)$, where $\rho \in \mathbb{R}_{>0}$ is a positive constant. Thus, the controller in (3–20) becomes $\kappa^*\left(\hat{X}\right) \triangleq \underset{u \in \Psi}{\arg\min}\, Q\left(\hat{X}, u\right)$, s.t. $\mathcal{C}_U\left(\hat{X}, u\right) \leq 0$ in absence of state feedback, where

$$\begin{aligned} \mathcal{C}_U\left(\hat{X}, u\right) \triangleq \overline{\tilde{X}}\left(t\right) \rho \Big(& L_U \overline{\tilde{X}}\left(t\right) + \Delta_U + \left\| \Phi\left(\hat{X}, \hat{\theta}\left(t_{2k+1}\right)\right) \right. \\ & \left. + g\left(\hat{X}\right) u \right\| \Big) + \left\| \nabla B^\top\left(\hat{X}\right) \right\| \left(L_U \overline{\tilde{X}}\left(t\right) + \Delta_U \right) \\ & + \nabla B^\top\left(\hat{X}\right) \left(\Phi\left(\hat{X}, \hat{\theta}\left(t_{2k+1}\right)\right) + g\left(\hat{X}\right) u \right) + \gamma\left(\hat{X}\right). \end{aligned} \tag{3–25}$$

3.4.2 Maximum Loss of Feedback Dwell-Time Condition

As the time without feedback increases, the worst-case bound on $\tilde{X}$ grows exponentially, causing the constraint in (3–25) to shrink the system's operating region. To ensure the feasibility of the controller with the modified constraint in (3–25), a maximum loss of feedback dwell-time condition $\Delta t_k \in \mathbb{R}_{>0}$ can be developed using (3–24). In this subsection, it is additionally assumed that B is globally Lipschitz, implying that $\|\nabla B(x)\| \leq \bar{B}$, where $\bar{B} \in \mathbb{R}_{>0}$ is a known positive constant. While a global Lipschitzness requirement may appear restrictive, many safe sets of practical interest such as polytopes (i.e., sets described by the intersection of hyperplanes) can be described using globally Lipschitz CBF candidates. To ensure the existence of a safety-ensuring control input, the time without feedback must be such that the inequality

$$\mathcal{C}_U\left(\hat{X}, u\right) - \mathcal{C}^*(x, u) \leq \bar{\mathcal{C}} \tag{3–26}$$

is satisfied, where $\mathcal{C}^*(x, u) \triangleq \nabla B^\top(x)\dot{x}$ and $\bar{\mathcal{C}} \in \mathbb{R}^d$ is the user-selected maximum offset between the boundary of the safe set and the boundary of the operating region enforced by $\mathcal{C}_U$. Recall that, for the purpose of this section, the control input is assumed to be bounded such that $\|u\| \leq \bar{u}$, for all $u \in \Psi$. Substituting (3–25) into (3–26) and solving for $\Delta t_k \triangleq t_{2k+1} - t_{2k+2}$ yields a maximum loss of feedback dwell-time condition of

$$\Delta t_k \leq \frac{1}{\lambda_U} \ln\left(\frac{1}{\delta_U}\left(\left(\frac{\bar{\mathcal{C}} - 6\bar{B}\Delta_U - \mathcal{K}_U}{6L_U\bar{B}}\right)^2 + 1\right)\right), \tag{3–27}$$

where $\mathcal{K}_U \triangleq 4\bar{B}\left\|\Phi\left(\hat{X}, \hat{\theta}(t_k)\right)\right\| + 4\bar{B}\left\|g\left(\hat{X}\right)\right\|\bar{u}$.

3.5 Simulation Studies

Two simulations are provided to demonstrate the effectiveness of the developed aDCBFs. The optimization problem in (3–20) is used to define the control law with a cost function of $Q(x, u) = \|u - u_{nom}(x)\|^2$, where $u_{nom} \in \Psi$ is the nominal control input that tracks the desired trajectory.

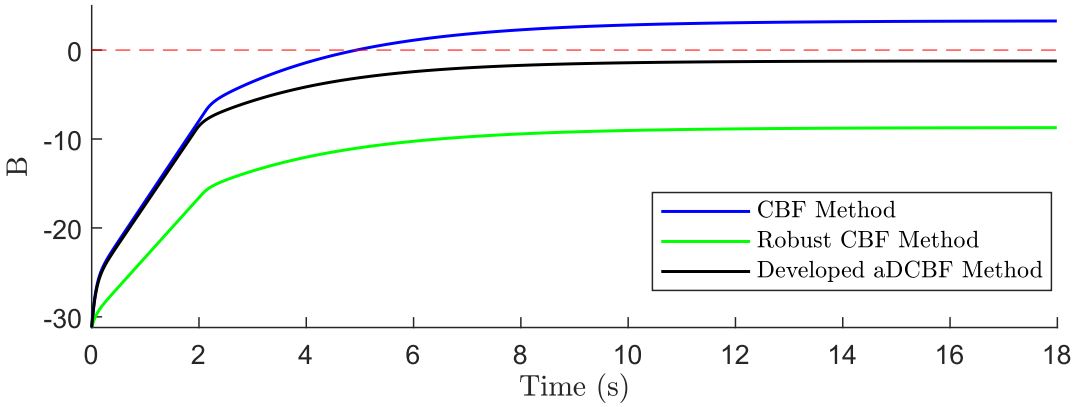

Figure 3-2. The value of the barrier functions over time for the ACC problem. A negative value of B indicates the follower vehicle remains in the safe set.

3.5.1 Adaptive Cruise Control

In this section, the developed technique is applied to an adaptive cruise control (ACC) problem [23]. Suppose there are two vehicles traveling along a straight line. The lead vehicle travels forward with a velocity $v_{\text{lead}} \in \mathbb{R}$ of $v_{\text{lead}} = 10$ m/s, while the follower vehicle trails behind the lead vehicle. The follower vehicle has dynamics in the form of

$$\begin{bmatrix} \dot{x} \\ \dot{v} \end{bmatrix} = \begin{bmatrix} v \\ -\frac{1}{m} F_r(v) + \delta(v) \end{bmatrix} + \begin{bmatrix} 0 \\ \frac{1}{m} \end{bmatrix} u,$$

where $x \in \mathbb{R}$ is the position of the vehicle in meters, $v \in \mathbb{R}$ is the velocity of the vehicle in meters per second, $m \in \mathbb{R}$ is the mass in kg, the nonlinear function $F_r : \mathbb{R} \to \mathbb{R}$ represents the vehicle's rolling resistance, the function $\delta : \mathbb{R} \to \mathbb{R}$ represents an unknown disturbance, and $u \in \mathbb{R}$ is the control input. As described in [23], the rolling resistance is modeled as $F_r(v) = f_0 + f_1 v + f_2 v^2$, where $f_0 = 0.1$ N, $f_1 = 5$ $\frac{\text{N·s}}{\text{m}}$, and $f_2 = 0.25$ $\frac{\text{N·}s^2}{\text{m}}$. The added disturbance $\delta(v) = 30 \sin(0.1v)$ represents unmodeled forces on the vehicle and the mass of the vehicle is $m = 100$ kg. In the aDCBF method, the rolling resistance function is considered to be unknown and $f(x) = -\frac{1}{m} F_r(v) + \delta(v)$ is the nonlinear function that the DNN learns. The desired velocity of the follower vehicle $v_d \in \mathbb{R}$ is set to a constant $v_d \triangleq 20$ m/s. The distance between the lead and follower

vehicles $D \in \mathbb{R}$ is defined as $D \triangleq x_{\text{lead}} - x$, where $x_{\text{lead}} \in \mathbb{R}$ is the position of the lead vehicle. The vehicles are initialized such that $v(t_0) = 16$ m/s, $v_{\text{lead}}(t_0) = 10$ m/s, and $D(t_0) = 60$ m. Because $v_{\text{lead}} < v_d$, the nominal velocity tracking controller defined as $u_{nom} \triangleq -\Phi\left(v, \hat{\theta}\right) - mk_1(v - v_d)$, where $k_1 = 10$ is a user-selected control gain, would eventually cause the follower vehicle to collide with the leader. The developed aDCBF approach is used to enforce a safe following distance. The safe set is defined as $\mathcal{S} \triangleq \{v \in \mathbb{R} : B(v) = -D + 1.8v \leq 0\}$, where 1.8 s represents the desired time headway as in [23]. A deep residual network (ResNet) is used with 2 hidden layers, a shortcut connection between each layer, and 6 neurons in each layer, for a total of 122 individual layer weights. The weights are initialized from the normal distribution $N(0, 3)$ and the DNN gains are selected as $\Gamma(t_0) = 5I_{122}$, $k_\theta = 0.001$, $\beta_0 = 2$, and $\kappa_0 = 3$. The state-derivative estimator is used to produce the secondary estimate of f uses gains of $k_x = 5$ and $k_f = 10$. Figure 3-2 shows how the controller in (3–20) with $\gamma(v) = 10B(v)$ is able to constrain the follower vehicle to a safe distance behind the lead vehicle.

Results for two comparison simulations are also provided in Figure 3-2. Using a standard CBF approach [23], the nominal controller is given access to F_r and m but does not have information about the disturbance term, meaning $u_{nom} \triangleq F_r(v) - mk_1(v - v_d)$ and the CBF constraint is defined as $\mathcal{C}(v, u) \triangleq \dot{D} + 1.8\left(-\frac{1}{m}F_r(v) + \frac{1}{m}u\right) + 10B(v)$. The unmodeled uncertainty δ pushes the state trajectory out of the safe set (B reaches a positive steady-state value of 3.15, thus violating the safe following distance requirements). If it is known that the model of F_r is imperfect, a robust CBF approach can be used, with $u_{nom} \triangleq F_r(v) - m\bar{\delta} - mk(v - v_d)$ and $\mathcal{C}(v, u) \triangleq \dot{D} + 1.8\left(-\frac{1}{m}F_r(v) + \bar{\delta} + \frac{1}{m}u\right) + 10B(v)$, where $\bar{\delta} \in \mathbb{R}_{>0}$ is a known constant such that $\|\delta\| \leq \bar{\delta}$. Although the robust approach is able to keep the trajectory inside the safe set, the use of a worst-case bound on δ results in an overly conservative set of admissible controllers, restricting the state trajectory to a subset of the safe set. Using the robust CBF approach, B reaches a steady-state value of -8.81. Adaptive CBF methods such

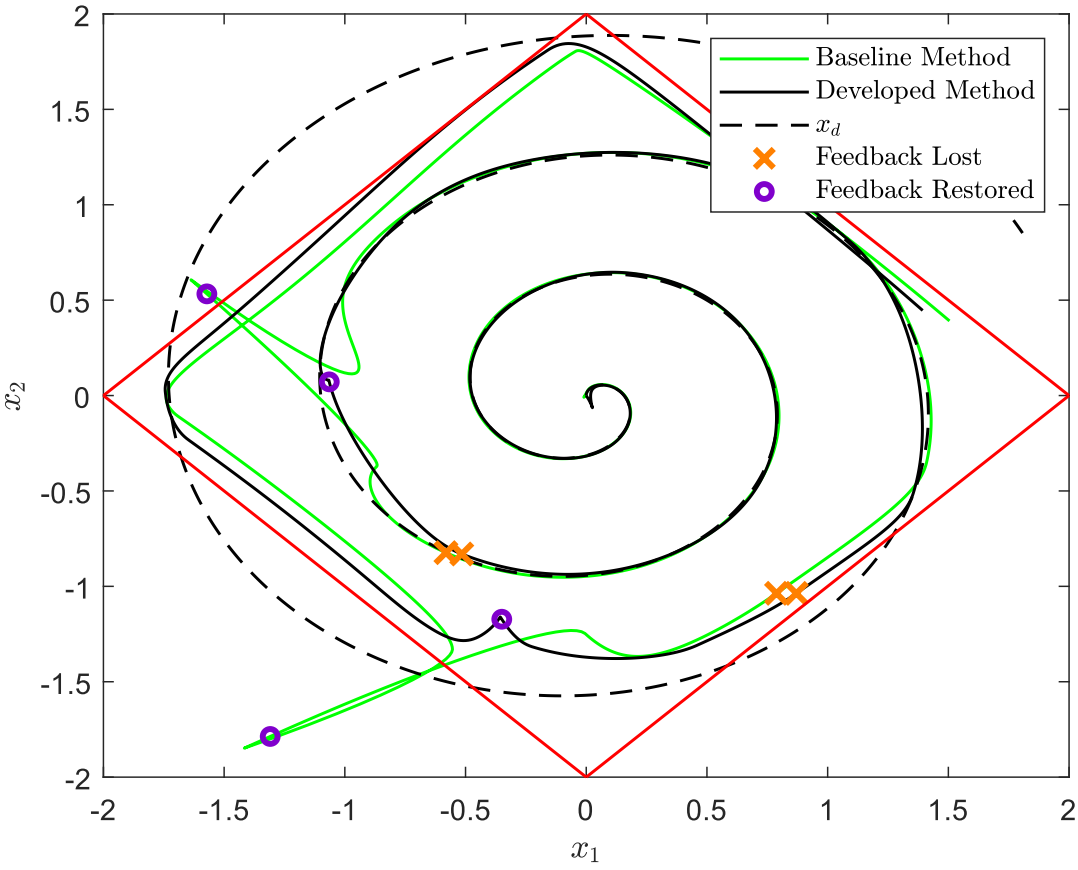

Figure 3-3. The state trajectory of the closed-loop system outlined in Section 3.5.2 using the developed aDCBF approach (black line) compared to the same control scheme without the ResNet approximation of the dynamics (green line). The orange markers corresponds to the instances state feedback is lost, and the purple markers correspond to when feedback is restored. The red line represents the boundary of the safe set.

as those in [41] and [42] cannot be directly applied to this problem because of the nonlinearly parameterized uncertainty in δ. Using the developed method, B reaches a stead state value of -1.27. The developed aDCBF method ensures safety while reducing undesirable conservative behavior by 85.6%, unlike in the baseline methods.

3.5.2 Non-Polynomial Dynamics

Consider the nonlinear dynamical system in (3–1) with $f(x) = \left[x_2 \sin(x_1) \tanh^2(x_2),\ x_1 x_2 \cos(x_2)\,\text{sech}(x_2)\right]^\top$ and $g(x) = [1,\ 1]^\top$, where $x = [x_1, x_2]^\top$.

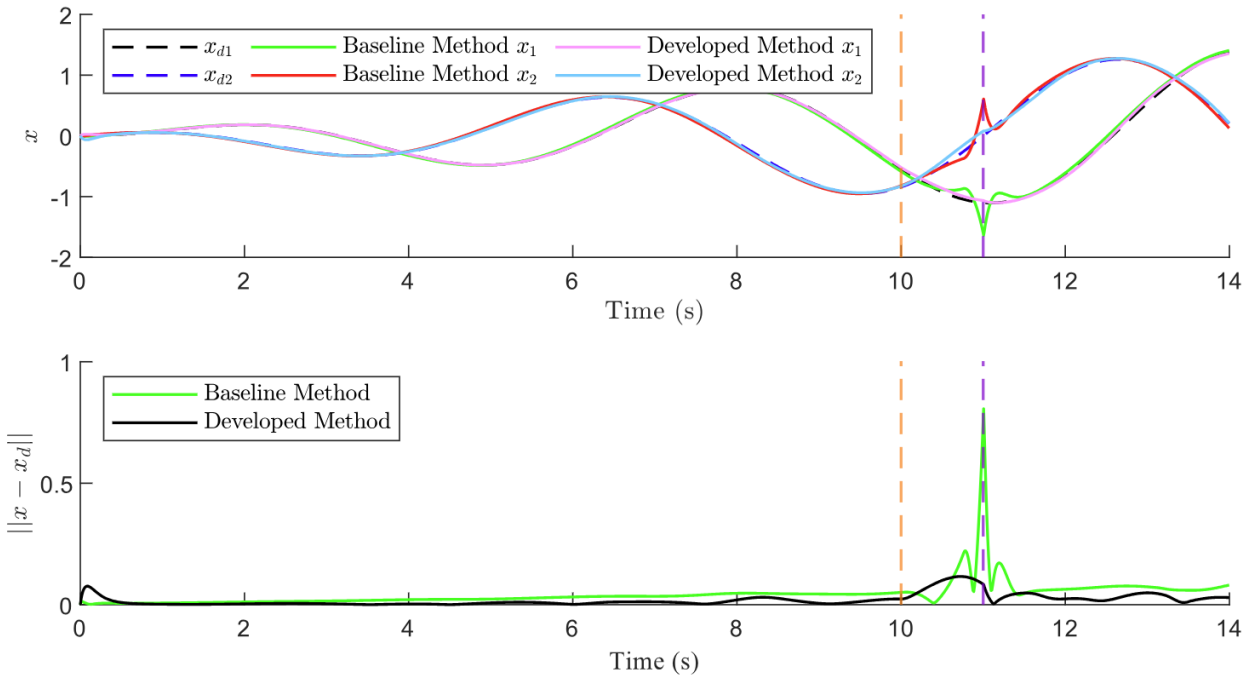

Figure 3-4. The top plot shows the desired versus actual value of each position state for the baseline and developed methods over the first 14 seconds of the simulation. The bottom plot shows the position tracking error for the two methods over the first 14 seconds of the simulation. The vertical orange dotted line shows when state feedback is lost, and the vertical purple dotted line shows when feedback is restored.

The states are initialized as $x(t_0) = [0,\ 0]^\top$ and $\dot{x}(t_0) = [0,\ 0]^\top$, and the desired trajectory is defined as $x_d(t) = 0.1t\,[\sin(t),\ \cos(t)]^\top$. We define a vector-valued CBF as $B(x) \triangleq [x_1 + x_2 - 2,\ x_1 - x_2 - 2,\ -x_1 + x_2 - 2,\ -x_1 - x_2 - 2]^\top$ which defines a diamond safe set $\mathcal{S} = \{x \in \mathbb{R}^2 : B(x) \leq 0\}$ with height and width of 4. The deep ResNet has 3 hidden layers, a shortcut connection across each hidden layer, and with 5 neurons in each layer, thus involving 174 total weights. The weights are initialized from the normal distribution $N(0, 5)$ and the DNN gains are selected as $\Gamma(t_0) = 5I_{174}$, $k_\theta = 0.001$, $\beta_0 = 2$, and $\kappa_0 = 10$. The state-derivative estimator is used to produce the secondary estimate of f using gains of $k_x = 10$ and $k_f = 5$. The nominal controller is defined as $u_{nom} = \dot{x}_d - \Phi\left(x, \hat{\theta}\right) - k_e(x - x_d)$, where $k_e = 10$. The function γ is selected as $\gamma(x) = 10B(x)$. Figure 3-3 shows the safe set and the desired and actual state trajectories. To simulate performance under intermittent state feedback, the state measurement is made unavailable for 1 second intervals beginning at 10 seconds and 15 seconds, denoted by the orange $\times$ markers in Figure 3-3. During loss of feedback, the procedure in Section 3.4 is followed, where the identified DNN is used to make a prediction of the state and the modified robust CBF constraint in (3–25) is used to ensure safety. The method developed in Section 3.4 prevents the state from escaping the safe set until the feedback is restored at 11 seconds and 16 seconds, respectively, indicated by the purple $\circ$ markers.

For the baseline method in [48], the nominal controller is $u_{nom} \triangleq \dot{x}_d - \hat{d} - k_e(x - x_d)$, where $\hat{d} \in \mathbb{R}^2$ represents the RISE-based disturbance observer estimate of f defined in [48, Eq. 6], and the CBF constraint in the optimization-based controller is $\mathcal{C}_F(x, u) \triangleq \left\|\nabla B^\top(x)\right\| \overline{f} + \nabla B^\top(x)\, g(x)\, u + \gamma(x)$. Though trajectory tracking performance is comparable to the developed approach at times when feedback is available, the state-derivative observer alone only provides an instantaneous estimate of the dynamics and fails to ensure safety in both instances of feedback loss, unlike the developed method. Figure 3-4 shows the trajectory tracking performance of the two methods. The

position tracking error for the developed method spikes at the start of the simulation, which can be accredited to the random initialization of the DNN weights. The developed weight adaptation law in (3–10) helps to enable the position error to settle in less than 0.5 seconds. When feedback is lost at 10 seconds, the position error norm grows to a maximum value of 0.116 with the developed method compared to a value of 0.807 with the baseline method, thus achieving a 85.6% performance improvement. The root mean square position error norm between 0 and 14 seconds is 0.031 with the developed method compared to 0.071 with the baseline method, thus achieving a 56.3% tracking performance improvement. The position tracking error from 14 seconds to 20 seconds is omitted from the plot because the desired trajectory in this timespan is outside of the safe set, rendering position error uninformative.

3.6 Conclusion

This chapter presented a method of ensuring the safety of an uncertain nonlinear system with the development of aDCBFs with real-time weight adaptation. The DNN adaptation law yields estimation error convergence, which is then used in an optimization-based control law that yields forward invariance of the safe set. Simulation results show improved performance compared to baseline methods and demonstrate the ability of the developed method to ensure safety in feedback-denied environments.

CHAPTER 4
OPTIMIZATION-BASED CONTROLLERS FOR PASSIVITY AND SAFETY CONSTRAINTS

4.1 Introduction

Though historically regarded as unrelated concepts, passivity-based control (PBC) and control barrier functions (CBFs) are methods used to establish the safety of control systems. In this chapter, an optimization-based PBC technique is developed which can be combined with CBF-based methods to find a set of controllers that each render a nonlinear control system energetically passive while also adhering to state constraints necessary for safety. Borrowing concepts from literature developed for multiple CBFs, passivity and safety objectives are simultaneously achieved through the use of a pointwise-optimal controller. Simulation results demonstrate the closed-loop system is passive with respect to an external disturbance despite a nonpassive nominal control input while also satisfying state constraints required for safety.

4.2 System Model

Consider a control system in the form

$$\dot{x} = f(x, \nu) + g(x)\, u, \tag{4–1}$$

where the state is denoted $x \in \mathbb{R}^n$, the control input is denoted by $u \in \Psi(x) \subset \mathbb{R}^m$, an external disturbance is denoted by $\nu \in \Phi(x) \subset \mathbb{R}^p$, and known continuous functions are denoted by $f : \mathbb{R}^n \times \mathbb{R}^p \to \mathbb{R}^n$ and $g : \mathbb{R}^n \to \mathbb{R}^{n\times m}$. The set-valued mappings $\Psi : \mathbb{R}^n \rightrightarrows \mathbb{R}^m$ and $\Phi : \mathbb{R}^n \rightrightarrows \mathbb{R}^p$ represent the admissible values for the input and external disturbance, respectively, at each state. The control input u has state-dependent constraints, so to develop an implementable controller we impose the following assumption.

Assumption 4.1. There exists a function $\psi : \mathbb{R}^n \times \mathbb{R}^m \to \mathbb{R}^k$ such that $\Psi(x) = \{u \in \mathbb{R}^m : \psi(x, u) \leq 0\}$ is nonempty.

4.3 Control Barrier Functions for State Constraints

The physical safety of a system is commonly defined by state constraints that must be satisfied. For example, a system may have position or velocity limits that must be met for obstacle avoidance. CBFs are a method of converting those state constraints into constraints on the control input. A control input found through a CBF-based analysis renders the safe set forward invariant, i.e., trajectories that begin within the safe set remain there for all time [125]. Therefore, if the state begins in a safe region, it will be unable to reach an unsafe region of the state space.

To enforce the forward invariance of the safe set, we must consider the effects of the external disturbance in (4–1). While [129] investigates the combination of passivity and state constraints, consideration of the external disturbance is omitted in the CBF development, resulting in the potential for the state to be pushed into an unsafe region of the state space by the external disturbance. Compared to previous results that combine passivity and CBFs, the subsequent development systematically considers the impact of the unknown external disturbance on the evolution of the state to ensure that it does not disrupt the forward invariance of the safe set. To do so, the following conditions are imposed on the system dynamics [65].

Assumption 4.2. The set-valued mapping $F : \mathbb{R}^n \rightrightarrows \mathbb{R}^n$ defined as $F(x) \triangleq \{f(x,\nu) : \nu \in \Phi(x)\}$ is nonempty, convex-valued, and bounded for every $x \in \mathbb{R}^n$.

Assumption 4.3. The set $\Phi(x) \subset \mathbb{R}^p$ is closed for every $x \in \mathbb{R}^n$.

We adapt the definition of a CBF presented in [65, Definition 2] to fit the dynamic system in (4–1). This definition considers a notion of vector-valued CBFs where the safe set can be defined by multiple scalar-valued functions, corresponding to multiple state constraints. A function $B : \mathbb{R}^n \to \mathbb{R}^d$ is a CBF candidate defining the safe set $\mathcal{S}$ if $\mathcal{S} = \{x \in \mathbb{R}^n : B(x) \leq 0\}$, where $B(x) \triangleq [B_1(x),\ B_2(x),\ ...,\ B_d(x)]^\top$. If B is continuous, $\mathcal{S}$ is a closed set. The scalar-valued CBF candidates denoted by $B_i : \mathbb{R}^n \to \mathbb{R}$ each define sets $\mathcal{S}_i \triangleq \{x \in \mathbb{R}^n : B_i(x) \leq 0\}$ and $M_i \triangleq \{x \in \partial\mathcal{S} : B_i(x) = 0\}$, for each $i \in [d]$.

For a continuously differentiable CBF candidate B, we define a function $\Gamma : \mathbb{R}^n \times \mathbb{R}^m \rightarrow \mathbb{R}^d$ such that for each $i \in [d]$, the i-th component of Γ is defined as $\Gamma_i(x,u) \triangleq \sup_{\nu \in \Phi(x)} \left\{ \nabla B_i(x)^\top (f(x,\nu) + g(x)\,u) \right\}$. The function Γ_i represents the worst-case growth of $B_i(x)$ for any direction in the set-valued mapping $F(x)$. We also introduce a function $\gamma : \mathbb{R}^n \rightarrow \mathbb{R}^d$ defined as $\gamma(x) \triangleq [\gamma_1(x),\ \gamma_2(x),\ ...,\ \gamma_d(x)]^\top$ which is used to constrain the rate of growth of Γ to guarantee the forward invariance of $\mathcal{S}$. The function γ is a relaxation of the extended class-$\mathcal{K}$ functions used in results such as [23]. While the use of an extended class-$\mathcal{K}$ function can help to achieve asymptotic stability of the safe set, extended class-$\mathcal{K}$ functions impose stronger conditions on the growth of Γ than are necessary to achieve forward invariance of the safe set [65, Remark 1].

Definition 4.1. ([65, Definition 2]) A continuously differentiable vector-valued CBF candidate $B : \mathbb{R}^n \rightarrow \mathbb{R}^d$ defining the set $\mathcal{S} \subset \mathbb{R}^n$ is a CBF for (4–1) and $\mathcal{S}$ on a set $\mathcal{O}_\mathcal{C} \subset \mathbb{R}^n$ with respect to a function $\gamma : \mathbb{R}^n \rightarrow \mathbb{R}^d$ if 1) there exists a neighborhood of the boundary of $\mathcal{S}$ such that $\mathcal{N}(\partial\mathcal{S}) \subset \mathcal{O}_\mathcal{C}$, 2) for each $i \in [d]$, $\gamma_i(x) \geq 0$ for all $x \in \mathcal{N}(M_i) \setminus \mathcal{S}_i$, and 3) the set

$$K_c(x) \triangleq \{u \in \Psi(x) : \Gamma(x,u) \leq -\gamma(x)\} \tag{4–2}$$

is nonempty for all $x \in \mathcal{O}_\mathcal{C}$.

Based on theoretical conditions for forward invariance in [65], the set-valued mapping K_c in (4–2) defines a set of control inputs that ensure safety. More specifically, [65] shows that, when B is a CBF and some additional conditions are satisfied, continuous controllers selected from the mapping K_c render the safe set $\mathcal{S}$ forward invariant.

4.4 Passivity-Based Control

4.4.1 Control Development

If a system is passive, the output energy of the system can be no greater than the energy that is put into the system [88]. Therefore, PBC is commonly used in systems

that interact with a potentially unknown environment as a way to ensure stable interaction between the system and environment. Based on typical definitions of passivity such as the one in [79, Definition 6.3], the system in (4–1) is said to be passive if there exists a continuously differentiable storage function $V : \mathbb{R}^n \to \mathbb{R}$ such that

$$\dot{V}(x, u, \nu) \leq \nu^\top h(x, \nu). \tag{4–3}$$

In a way similar to a Lyapunov stability analysis, this definition requires the design of a single passivating control input u that makes the inequality in (4–3) true. We modify the definition of passivity in [79] to present the notion of control passivity, resulting in a set of controllers that each render the system passive. The developed control passivity definition is compatible with optimization-based controller synthesis methods commonly used with CBFs, allowing for simpler unification of passsivity and safety constraints.

Definition 4.2. For an output $y = h(x, \nu)$, the system in (4–1) is considered to be *controllably passive* with respect to input ν and output $h : \mathbb{R}^n \times \mathbb{R}^p \to \mathbb{R}^p$ on a set $\mathcal{O}_\mathcal{P} \subseteq \mathbb{R}^n$ if there exists a continuously differentiable positive semi-definite storage function $V : \mathbb{R}^n \to \mathbb{R}$ such that the set

$$K_p(x) \triangleq \left\{ u \in \Psi(x) : \sup_{\nu \in \Phi(x)} \left\{ \dot{V}(x, u, \nu) - \nu^\top h(x, \nu) \right\} \leq 0 \right\}, \tag{4–4}$$

is nonempty for every $x \in \mathcal{O}_\mathcal{P}$, where $\dot{V}(x, u, \nu) \triangleq \nabla V(x)^\top (f(x, \nu) + g(x) u)$.

Remark 4.1. The storage function can also be vector-valued, defined as $V \triangleq [V_1, V_2, \ldots, V_a]^\top : \mathbb{R}^n \to \mathbb{R}^a$, rendering the system in (4–1) passive with respect to multiple input-output pairs. In this case, each storage function defines a constraint on the control input such that

$$\sup_{\nu \in \Phi(x)} \left\{ \dot{V}_i(x, u, \nu) - \nu_i^\top h_i(x, \nu) \right\} \leq 0, \forall i \in [a].$$

By designing the set of passivity-ensuring controllers in (4–4), controller synthesis methods commonly used with CBFs can be used to enforce passivity. Selections of K_p

ensure the system is passive in the same way selections of K_c render a safe set forward invariant.

4.4.2 Implementation

A new representation of passivity based on Definition 4.2 is developed to better integrate PBC with CBF mechanisms. To design a controller u that renders the closed-loop system passive with respect to the external disturbance, we develop a function $P : \mathbb{R}^n \to \mathbb{R}$ defined as

$$P(x) \triangleq \sup_{\nu \in \Phi(x)} \left\{ \nabla V(x)^\top f(x,\nu) - \nu^\top h(x,\nu) \right\}. \tag{4–5}$$

Note that P is finite when the system is controllably passive with storage function V. The set of passivating control inputs in (4–4) can be rewritten as

$$K_p(x) \triangleq \left\{ u \in \Psi(x) : \nabla V(x)^\top g(x)\, u \leq -P(x) \right\}. \tag{4–6}$$

Instead of designing a specific controller that renders the system passive, a selection of (4–6) can be made using an optimization-based control law in the form of

$$\begin{aligned} \kappa^*(x) \triangleq \arg\min_{u \in \mathbb{R}^m} & \; Q(x,u), \\ \text{s.t.} & \; \nabla V(x)^\top g(x)\, u \leq -P(x), \\ & \; \psi(x,u) \leq 0, \end{aligned} \tag{4–7}$$

yielding a controller that is a selection of K_p while minimizing some cost function $Q : \mathbb{R}^n \times \mathbb{R}^m \to \mathbb{R}$ and satisfying the input constraints on u.

Example 4.1. We will demonstrate a few subtleties of the above development with a simple example. Begin with the system

$$\begin{cases} \dot{x} = x + u + \nu, \\ y = x, \end{cases} \tag{4–8}$$

where the state and control input are denoted by $x, u \in \mathbb{R}$, and the external disturbance is $\nu \in \mathbb{R}$. Selections of different storage functions can produce different values of P. By selecting the storage function as $V = \frac{1}{2}x^2$, the function P is defined as $P(x) \triangleq \sup_{\nu \in \Phi(x)} \{x^2 + x\nu - \nu x\} = x^2$ which is known and the system is therefore controllably passive with respect to input-output pair (ν, x) using Definition 4.2, regardless of the boundedness of $\Phi(x)$. For an unbounded external disturbance term, the above storage function is the only possible selection that results in a finite P. If the storage function was instead chosen as $V = x^2$, the function P is $P(x) \triangleq \sup_{\nu \in \Phi(x)} \{2x^2 + 2x\nu - \nu x\} = \sup_{\nu \in \Phi(x)} \{2x^2 + x\nu\}$ which may be unbounded for an unbounded $\Phi(x)$.

4.5 Passivity-Preservation

The notion of control passivity is compatible with CBF literature and can be enforced using the same methods, meaning that passivity and safety constraints can each be used as a condition in one point-wise optimal controller. The set of passivity- and safety-ensuring control laws can be found at the intersection of K_p in (4–6) and K_c in (4–2) and is defined as $K(x) \triangleq K_p(x) \cap K_c(x)$. A selection of K that minimizes some cost function is implemented using the controller

$$\begin{aligned} \kappa^*(x) \triangleq \underset{u \in \mathbb{R}^m}{\text{arg min}}\ & Q(x, u), \\ \text{s.t. } & \Gamma(x, u) \leq -\gamma(x), \\ & \nabla V(x)^\top g(x) u \leq -P(x), \\ & \psi(x, u) \leq 0, \end{aligned} \tag{4–9}$$

where the cost function $Q : \mathbb{R}^n \times \mathbb{R}^m \to \mathbb{R}$ is often chosen as $Q = \left\| u - u_{\text{nom}}(x) \right\|^2$ to minimally modify some continuous nominal control input $u_{\text{nom}} : \mathbb{R}^n \to \mathbb{R}^m$.

Definitions 4.1 and 4.2 provide conditions for when the control system is rendered passive or a set is rendered forward invariant, respectively. The optimization problem in (4–9) yields a controller that is both passive and safe without the a priori design of a

passive nominal controller. For the system to be both passive and safe, there must be at least one control input for each $x \in \mathbb{R}^n$ that satisfies both conditions. Thus, passivity can be preserved in the presence of safety constraints using the QP in (4–9) only when the constraints are simultaneously feasible.

Although $\kappa^*(x)$ is feasible if $K(x) \neq \emptyset$, the optimization problem in (4–9) does not necessarily generate a continuous controller. The following corollary of [65, Lemma 3] provides conditions that will result in a single-valued and continuous control input.

Corollary 4.1. *([65, Lemma 3]) Let $\mathcal{C} : \mathbb{R}^n \times \mathbb{R}^m \to \mathbb{R}^d$ be continuous on $\mathcal{O} \times \mathbb{R}^m$, and, for each $j \in [k]$, let $u \mapsto \mathcal{C}_j(x,u)$ be convex on the set $K(x) \triangleq \{u \in \mathbb{R}^m : \mathcal{C}_j(x,u) \leq 0, \forall j \in [k]\}$. Suppose $Q : \mathbb{R}^n \times \mathbb{R}^m \to \mathbb{R}$ is continuous and, for each $x \in \mathcal{O}$, $u \mapsto Q(x,u)$ is strictly convex and inf-compact on $K(x)$. If the set $K^\circ(x) \triangleq \{u \in \mathbb{R}^m : \mathcal{C}_i(x,u) < 0, \forall j \in [k]\}$ is nonempty for every $x \in \mathcal{O}$, $\kappa^*(x) \triangleq \underset{u \in K}{\arg\min}\, Q(x,u)$ is single-valued and continuous.*

We impose the following assumption on the constraints in (4–9) to yield the necessary continuity properties required by Corollary 4.1. The assumption allows the main result establishing the forward (pre-)invariance of the safe set $\mathcal{S}$ and passivity of the closed-loop system from the external disturbance ν to output y to be proven.

Assumption 4.4. For all $i \in [d]$, the functions $u \mapsto \Gamma_i$ and $u \mapsto \psi(x,u)$ are convex on $K_c(x)$ for all $x \in \mathcal{O}_\mathcal{C}$, and the functions $(x,u) \mapsto \Gamma_i(x,u) + \gamma_i(x)$ and $(x,u) \mapsto \psi(x,u)$ are each continuous on $\mathcal{O}_\mathcal{C} \times \mathbb{R}^m$. The function $(x,u) \mapsto \nabla V(x)^\top g(x) u + P(x)$ is continuous on $\mathcal{O}_\mathcal{P} \times \Psi$.

The notion of forward pre-invariance allows for maximal solutions to the closed-loop system that are not complete. A solution is said to be maximal if there is no solution ϕ' such that $\phi(t) = \phi'(t)$ for all $t \in \text{dom}\phi$, where domϕ is a proper subset of domϕ', and a solution is complete if domϕ is unbounded. The following assumption helps to establish the forward invariance of $\mathcal{S}$.

Assumption 4.5. Maximal solutions to the closed-loop system defined by (4–1) and (4–9) cannot escape in finite-time inside the safe set $\mathcal{S}$.

Theorem 4.1. *Consider the system in* (4–1) *with a control input selected by the passivity- and safety-ensuring control input in* (4–9)*. Suppose Assumptions 4.1-4.4 hold, the function B is a CBF defining the set $\mathcal{S}$, the function V is a positive semi-definite storage function, and $\mathcal{O}_{\mathcal{P}} \supset \mathcal{N}(\mathcal{S})$. Let the cost function Q be continuous, $u \mapsto Q(x,u)$ be strictly convex for each $x \in \mathcal{O}_{\mathcal{P}}$, and, for each $x \in \mathcal{O}_{\mathcal{P}}$, let $u \mapsto Q(x,u)$ be strictly convex and inf-compact on $K(x)$. Additionally, let the mapping*

$$K^{\circ}(x) \triangleq \left\{ \begin{array}{c} u \in \mathbb{R}^m : \Gamma(x,u) < -\gamma(x) \\ \nabla V(x)^{\top} g(x) u < -P(x) \\ \psi(x,u) < 0 \end{array} \right\}$$

be nonempty on $\mathcal{O}_{\mathcal{P}}$. If Assumption 4.5 holds, then the resulting closed-loop system is passive with respect to V and input-output pair (ν, y), and the safe set $\mathcal{S}$ is forward invariant despite the influence of the external disturbance.

Proof. We will first show that the set $\mathcal{S}$ is forward pre-invariant for closed-loop dynamics defined by (4–1) and (4–9). Because Assumption 4.4 holds, Q is continuous, and $u \mapsto Q(x,u)$ is strictly convex and inf-compact for each $x \in \mathcal{O}_{\mathcal{P}}$, the conditions of Corollary 4.1 are satisfied, and it can be concluded that the controller κ^* in (4–9) is single-valued and continuous on $\mathcal{O}_{\mathcal{P}}$. The set-valued mapping F is outer semicontinuous by Assumptions 4.2 and 4.3, and because of the continuity of κ^*, the closed-loop dynamics defined by $F(x)$ and κ^* are continuous. By Theorem 1 of [65], the safe set is forward pre-invariant, which means that solutions cannot escape $\mathcal{S}$ but may terminate due to finite-time escape. To conclude forward invariance, it remains to be shown that maximal solutions to the closed-loop system starting from $\mathcal{S}$ are complete. Under the continuous closed-loop dynamics defined by (4–1) and (4–9), maximal solutions are either complete

or escape in finite time [69, Proposition 3]. By Assumption 4.5, the possibility of finite-time escape is eliminated, implying that all maximal solutions are complete. Therefore, the safe set $\mathcal{S}$ is forward invariant. Because $K_p \subseteq K$, the controller in (4–9) yields a controller in the set K_p. Therefore, any controller that is a selection of K ensures that the system is passive according to the definition of passivity in [79, Definition 6.3]. □

Remark 4.2. Bounded solutions avoid finite-time escape from the safe set; however, there is no guarantee that solutions to the closed-loop dynamics defined by (4–1) and (4–9) remain bounded because it is not required that $\mathcal{S}$ is designed to be bounded. There are a number of ways in which Assumption 4.5 can be satisfied. For example, finite-time escape is eliminated if $\mathcal{S}$ is compact or if $\mathcal{S}$ is closed and additionally the closed-loop dynamics defined by (4–1) and (4–9) are either bounded on $\mathcal{S}$ or have linear growth on $\mathcal{S}$.

With a passive control action and a state near the center of the safe set, $\kappa^* = u_{\text{nom}}$. As the state approaches the boundary of the safe set, or when the nominal control action leads to a nonpassive closed-loop system, the QP minimally modifies the nominal controller to meet both the passivity and state objectives. The implication of this control design is that the system will remain passive with respect to some external disturbance while operating within a forward invariant safe set defined by a vector-valued CBF. With the addition of the consideration of the external disturbance in the CBF design, the safe set is guaranteed to be forward invariant unlike in previous results, where there are no safeguards preventing the external disturbance from pushing the state into an unsafe region of the state space. Despite the energy being injected by the CBF, the system remains passive if there is a solution to (4–9).

Remark 4.3. With only one constraint in (4–9) (either the passivity, safety, or input constraint), a closed-form solution to (4–9) can be developed; however, developing a closed-form solution is more difficult to do with the inclusion of each constraint. Sum of

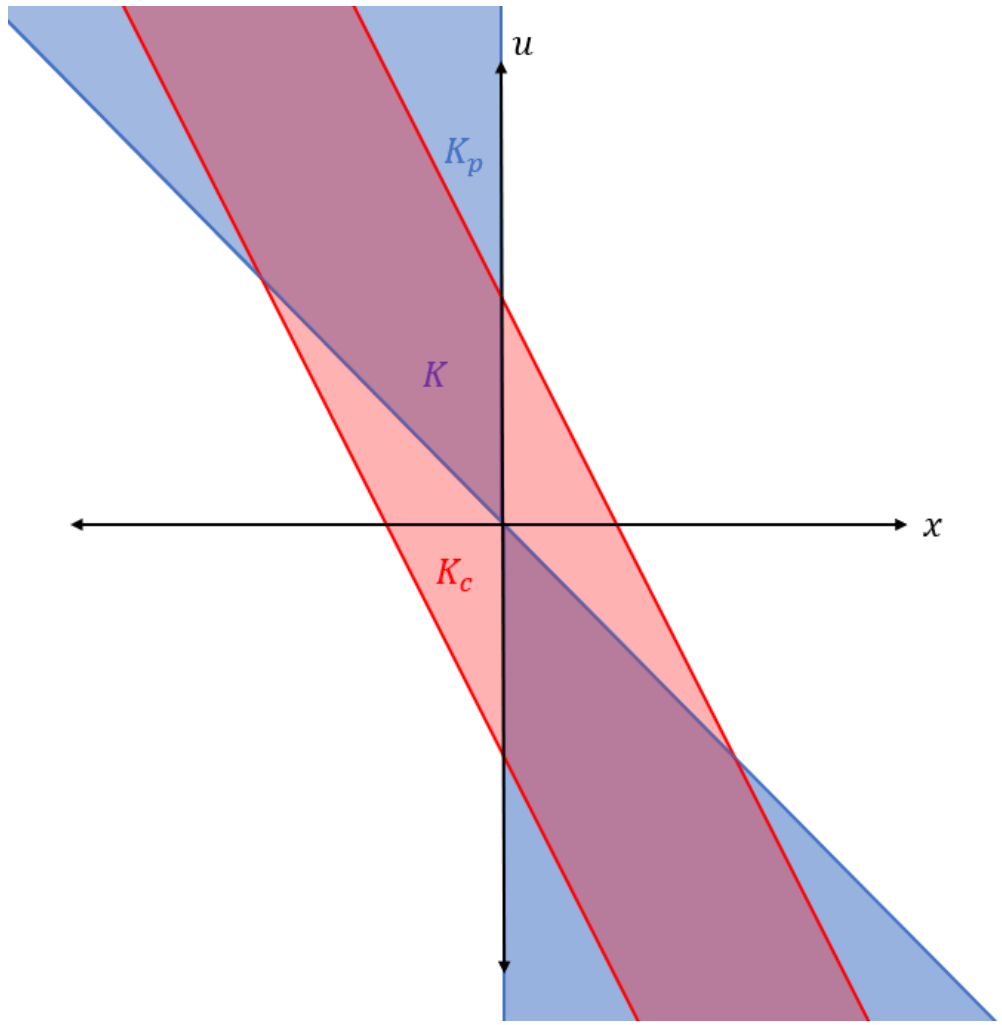

Figure 4-1. A visual representation of the sets of passivating and safety-ensuring control inputs for the toy example in (4–8). The region outlined in blue represents K_p and the pink region between the two red lines represents K_c. The purple region represents K, where K_p and K_c overlap.

squares programming can be used as in [65, Section V] to identify the set where at least one feasible solution to (4–9) exists, which is equivalent to states where K is nonempty.

Example 4.2. Continuing the example in Section 4.1, we will demonstrate the potential of the developed passivation approach to be used in combination with CBFs. Suppose the CBF is selected as $B(x) = [-x - \bar{x},\ x - \bar{x}]^\top$, restricting the state to $-\bar{x} \leq x \leq \bar{x}$, and γ is selected as $\gamma(x) = k_b B(x)$, where $k_b \in \mathbb{R}_{>0}$ is the CBF gain. From Section 4.1, it is known that a control input satisfying $xu \leq -x^2$ will passivate the system. Similarly, a control input of $-k_b(x + \bar{x}) + \bar{\nu} \leq u \leq -k_b(x - \bar{x}) - \bar{\nu}$ will yield forward invariance of

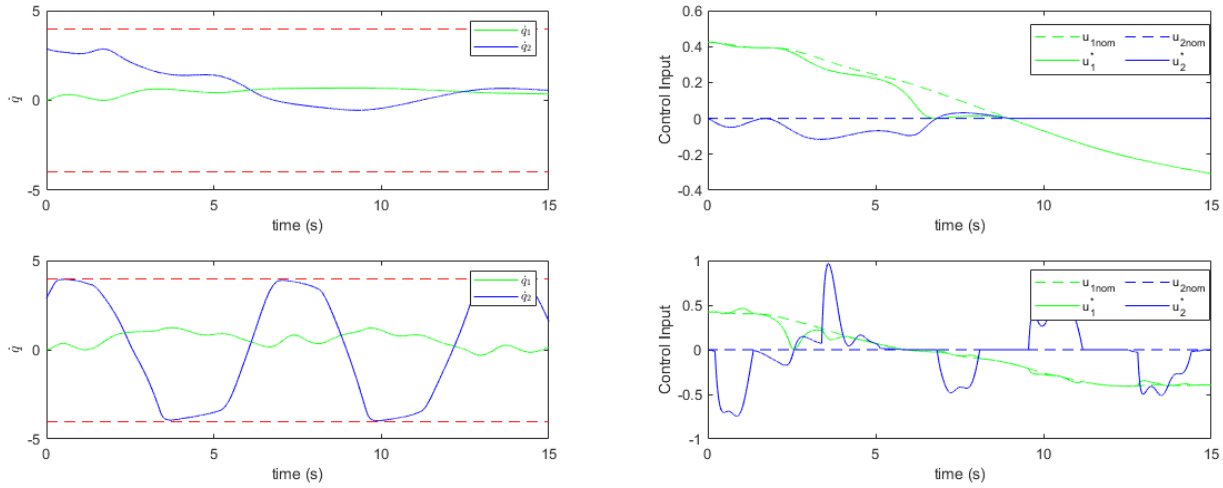

Figure 4-2. The simulated evolution of the state (left) and control input (right) of the two-link manipulator system using the developed QP-based controller. The two top plots correspond to the case where human input set to zero, and the two bottom plots show the system's behavior when there is a human input.

the safe set, where $\overline{\nu} \in \mathbb{R}_{>0}$ is a bound on $\nu \in \mathbb{R}$ such that $|\nu| \leq \overline{\nu}$. It can be verified analytically that K_c is nonempty if $-k_b\left(x+\bar{x}\right)+\bar{\nu} \leq -k_b\left(x-\bar{x}\right)-\overline{\nu}$, which is true if k_b and $\bar{x}$ are selected such that $k_b\bar{x} \geq \bar{\nu}$. As can be seen in Figure 4-1, not all passivating control inputs are safe and vice versa, but a feasible solution exists at each state in the safe set.

If the $\overline{\nu}$ term was not included in the design of the CBF as in [129], the safe set of control inputs K_c would be shifted to the right, and the CBF would be unable to keep the state inside the safe set for certain values of the external disturbance. Another key advantage of the developed approach over previous results is its ability to minimize the control input that will achieve both objectives.

4.6 Simulation Study

A numerical simulation was performed to provide an example of the effectiveness of the developed control scheme in ensuring both passivity of the closed-loop system as well as satisfaction of some state constraints required for safety. Consider a frictionless two-link planar and revolute robot modeled by Euler-Lagrange dynamics in the form

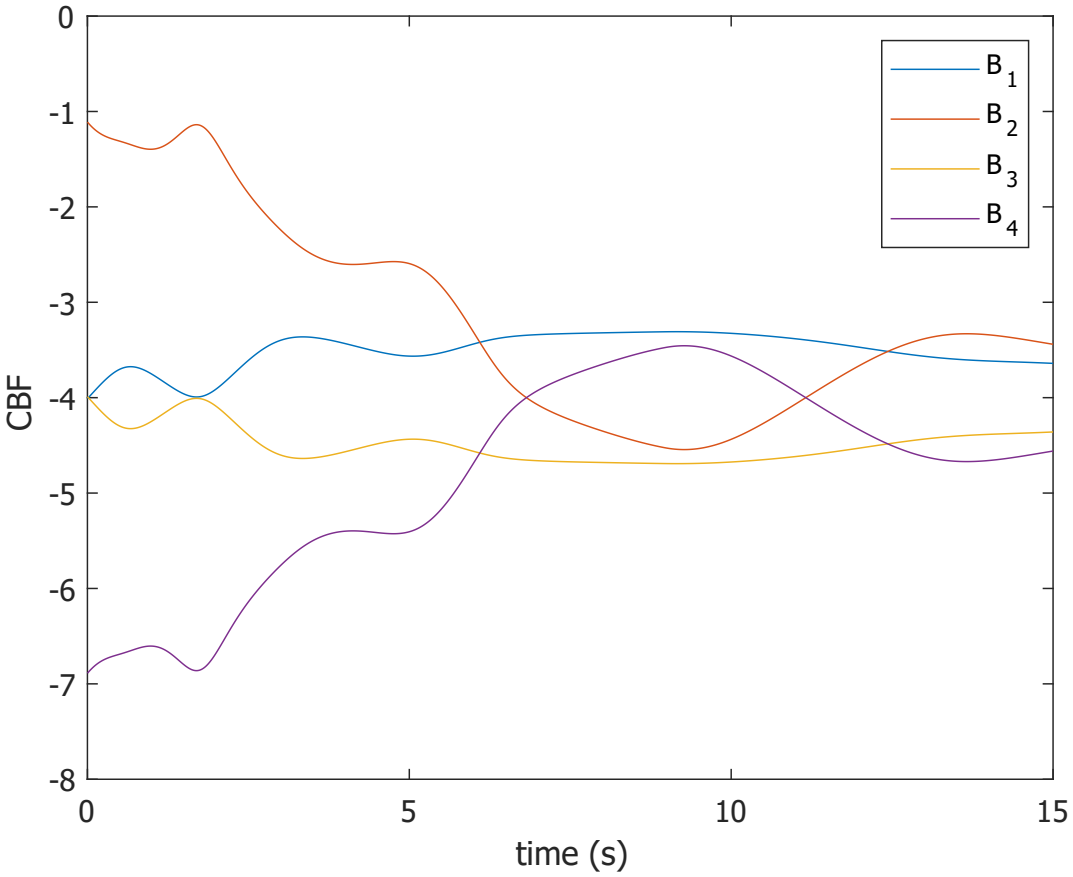

Figure 4-3. The value of each of the CBFs over time. None of the CBFs reach a positive value, meaning that the state never reaches an unsafe region of the state space.

of [173]

$$M(q)\ddot{q} = -C(q,\dot{q})\dot{q} + \tau_e + \tau_h, \tag{4–10}$$

where $q \triangleq [q_1\ q_2]^\top \in \mathbb{R}^2$, $\dot{q} \triangleq [\dot{q}_1\ \dot{q}_2]^\top \in \mathbb{R}^2$, and $\ddot{q} \triangleq [\ddot{q}_1\ \ddot{q}_2]^\top$ denote the angular position, velocity, and acceleration of each of the links, respectively. The inertia matrix and centripetal-Coriolis matrix are denoted by $M(q) : \mathbb{R}^2 \to \mathbb{R}^{2\times 2}$ and $C(q,\dot{q}) : \mathbb{R}^2 \times \mathbb{R}^2 \to \mathbb{R}^{2\times 2}$, respectively, and are defined as

$$M(q) \triangleq \begin{bmatrix} p_1 + 2p_3\cos(q_2) & p_2 + p_3\cos(q_2) \\ p_2 + p_3\cos(q_2) & p_2 \end{bmatrix},$$

$$C(q_1,q_2) \triangleq \begin{bmatrix} -p_3\sin(q_2)\dot{q}_2 & -p_3\sin(\dot{q}_1+\dot{q}_2) \\ p_3\sin(q_2)\dot{q}_1 & 0 \end{bmatrix},$$

where $p_1 = 3.473$ kg $\cdot$ m^2, $p_2 = 0.196$ kg $\cdot$ m^2, and $p_3 = 0.242$ kg $\cdot$ m^2. The electric motor torque inputs are denoted by $\tau_e \in \Psi(q) \subset \mathbb{R}^2$, where $\Psi(q) \triangleq \left\{\tau_e \in \mathbb{R}^2 : \left\|\tau_e\right\| \leq \overline{\tau}_e\right\}$ and $\overline{\tau}_e \in \mathbb{R}_{>0}$ is a user-selected upper-bound on the magnitude of the control input. The inertia and centripetal-Coriolis matrix satisfy the skew-symmetric relation: $q^\top\left(\frac{1}{2}\dot{M}(q) - C(q,\dot{q})\right)q = 0$ for all $q \in \mathbb{R}^2$. The external disturbance $\tau_h \in \Phi(q) \subset \mathbb{R}^2$ can be thought of as a torque input from a human operator coming into contact with the robotic system, where $\Phi(q) \triangleq \left\{\tau_h \in \mathbb{R}^2 : \left\|\tau_h\right\| \leq \overline{\tau}_h\right\}$ and $\overline{\tau}_h \in \mathbb{R}_{>0}$ is a known upper-bound on the external disturbance term. The robot needs to remain passive with respect to the human disturbance, while remaining inside some velocity bounds enforced through the use of a CBF.

The output of the system $y \in \mathbb{R}^2$ is considered to be $y = \dot{q}$, and the system's storage function is

$$V(q) = \frac{1}{2}\dot{q}^\top M(q)\dot{q}. \tag{4–11}$$

Invoking the skew symmetry property, the derivative of the storage function is given by $\dot{V} = \text{sgn}\left(q\right)^{\top} \dot{q} + \dot{q}^{\top}\left(\tau_e + \tau_h\right)$, where sgn $(\cdot)$ denotes the signum function. The storage function in (4–11) results in

$$P\left(q\right) = \sup_{\tau_h \in \Phi(x)} \left\{\dot{q}^{\top}\tau_h - \tau_h^{\top}\dot{q}\right\} = 0.$$

By the Definition 4.2, any control input in the set

$$K_p\left(q, \dot{q}\right) \triangleq \left\{\tau_e \in \Psi\left(q\right) : \dot{q}^{\top}\tau_e \leq 0\right\}, \tag{4–12}$$

renders the system passive from disturbance τ_h to output $\dot{q}$.

In addition to the passivity requirement, suppose also that each link of the robot arm must comply to some energy (i.e., velocity) constraints. If procedures such as those in [129] were followed, there would be no way to guarantee forward invariance of the safe set if there is an external disturbance from the operator; however, using the developed approach, it can be guaranteed that the state trajectories will not reach an unsafe region of the state space despite the unknown disturbance from the person. Because of physical limitations of the operator, the torque disturbance from the person τ_h can be bounded by known constants. Considering the bound of the external disturbance in the design of the CBF constraint provides robustness to the torque supplied by the operator, insuring that the operator will not push the state outside of the safe set.

We consider a CBF candidate designed to limit the velocities of each of the links defined as $B\left(q, \dot{q}\right) \triangleq \left[-M(q)(\dot{q} + \bar{\dot{q}}),\ M(q)(\dot{q} - \bar{\dot{q}})\right]^{\top}$, where $\bar{\dot{q}} \in \mathbb{R}^2$ is the user-selected boundary of the safe set (i.e., the maximum allowable magnitude of the velocities of each of the links). The set of safety ensuring control inputs is defined as

$$\begin{aligned} K_c\left(q, \dot{q}\right) \triangleq \Big\{\tau_e \in \mathbb{R}^2 : \nabla B\left(q, \dot{q}\right)^{\top}\left(-C\left(q, \dot{q}\right)\dot{q} + \tau_e\right) \\ + \left\|\nabla B\left(q, \dot{q}\right)\right\| \overline{\tau}_h \leq -\gamma\left(q, \dot{q}\right)\Big\}, \end{aligned} \tag{4–13}$$

where the function γ is chosen as $\gamma\left(q,\dot{q}\right) = k_b B\left(q,\dot{q}\right)$ and $k_b = 10$. The set K_c is nonempty when both components of the CBF are simultaneously feasible. The first component of the CBF, $B_1\left(q,\dot{q}\right) = -M(q)(\dot{q}+\bar{\dot{q}})$, imposes the condition on the control input $\tau_e \geq -M\left(q\right)k_b\left(\dot{q}+\bar{\dot{q}}\right) + C\left(q,\dot{q}\right)\dot{q} - \dot{M}\left(q\right)\left(\dot{q}+\bar{\dot{q}}\right) + \overline{\tau}_h$. The second component of the CBF, $B_2\left(q,\dot{q}\right) = M\left(q\right)\left(\dot{q}-\bar{\dot{q}}\right)$, imposes the condition on the control input $\tau_e \leq -M\left(q\right)k_b\left(\dot{q}-\bar{\dot{q}}\right) + C\left(q,\dot{q}\right)\dot{q} - \dot{M}\left(q\right)\left(\dot{q}-\bar{\dot{q}}\right) - \overline{\tau}_h$. It is possible for τ_e to satisfy both inequalities only if $-M\left(q\right)k_b\left(\dot{q}+\bar{\dot{q}}\right) + C\left(q,\dot{q}\right)\dot{q} - \dot{M}\left(q\right)\left(\dot{q}+\bar{\dot{q}}\right) + \overline{\tau}_h \leq -M\left(q\right)k_b\left(\dot{q}-\bar{\dot{q}}\right) + C\left(q,\dot{q}\right)\dot{q} - \dot{M}\left(q\right)\left(\dot{q}-\bar{\dot{q}}\right) - \overline{\tau}_h$. Therefore, (4–13) is nonempty for all $q \in \mathbb{R}^2$ if k_b is selected such that $M\left(q\right)k_b\bar{\dot{q}} \geq \bar{\tau}_h$.

In this example, the QP-based control law is defined as in (4–9), where the cost function is defined as $Q\left(q,u\right) \triangleq \left\|\tau_e - u_{\text{nom}}\right\|^2$ and the two constraints correspond to the passivity and safety conditions in (4–12) and (4–13), respectively, and the third constraint corresponds to a limit on the magnitude on the designable control input u. By defining the cost function in this way, the nominal nonpassivating controller is minimally modified such that it satisfies each constraint in the QP. We define the nominal control input as $u_{\text{nom}} = \left[-0.1\cos\left(0.5t\right)q,\ 0\right]^\top$, which can be thought of as a variable stiffness spring acting on the first link and would not always result in passivity with respect to input-output pair $(\tau_h,\dot{q})$ and storage function (4–11). When $\Psi\left(q\right) = \mathbb{R}^2$, the feasibility of the control law κ^* in this problem can be verified analytically. The intersection of K_p and K_c is nonempty for all $q \in \mathbb{R}^2$, provided k_b is selected such that K_c is nonempty. Because the passivity and stability constraints are both imposing conditions on $\dot{q}$ in this simulation, the feasibility analysis is simpler compared to the case of the system being rendered passive with respect to a different input-output pair. For more complex problems, the nonemptiness of K can be verified using the sum of squares programming approach developed in [65].

The two top plots of Figure 4-2 show a simulation of the state and control input of the mechanical system in (4–10) with $\tau_h = \begin{bmatrix} 0 & 0 \end{bmatrix}^\top$, i.e., the human disturbance was

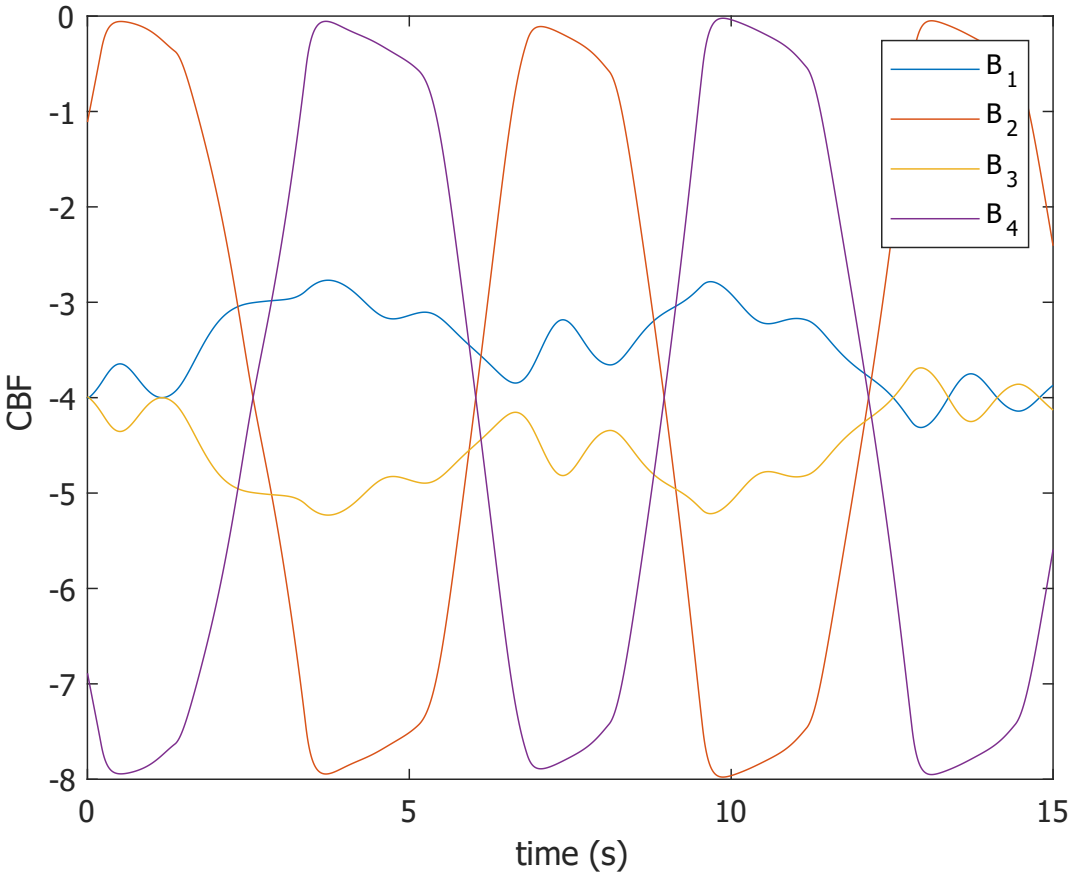

Figure 4-4. The value of each of the CBFs over time with the added human input. None of the CBFs reach a positive value, meaning that the state never reaches an unsafe region of the state space.

set to zero. Both links started from rest, and the initial position of each of the links were randomized between $-\pi$ and π. The state trajectory stays within the desired range while remaining passive to the disturbance. The top right plot of Figure 4-2 shows how the QP modifies the control input to achieve the desired behavior. Figure 4-3 shows the value of each of the CBFs over the 15 second simulation. The CBFs remain less than zero, reaching a maximum value of -1.111, meaning that the states do not leave their safe ranges.

The two bottom plots of Figure 4-2 show the simulation repeated for a disturbance τ_h chosen as $\tau_h = \begin{bmatrix} 3\sin(3t) & 4\sin(2t) \end{bmatrix}^\top$, where τ_h has an upper bound of $\overline{\tau}_h = 5$. Again, the state trajectory never exits the safe set, despite the unknown disturbance from the operator. The result is supported in Figure 4-4 which shows the value of the CBF over time. For the simulated operator disturbance, the CBF reaches a maximum value of -0.023 which is closer to zero than in the case when $\tau_h = \begin{bmatrix} 0 & 0 \end{bmatrix}^\top$. This outcome is due to the use of the upper bound of the disturbance in the design of the CBF which introduces some conservativeness in the absence of disturbance

4.7 Conclusion

In this chapter, the concepts of PBC and CBFs are combined to produce a controller that renders the system passive with respect to an external disturbance and the safe set forward invariant. Theoretical results usually reserved for multiple CBF constraints are used to develop an optimization-based controller that enforces both passivity and state constraints. Unlike typical previous results, the external disturbance is considered during the design of the CBF to ensure the state does not reach an unsafe region of the state space at any time. The developed method was demonstrated on a two-link robotic system, yielding passivity and safety despite the unknown external disturbance by a person making contact by the robot.

CHAPTER 5
SUMMARY AND FUTURE WORK

Historically, much attention has been given to Lyapunov-derived control laws to ensure the stability of nonlinear systems. Stability can be thought of as a liveness property, where it is guaranteed that a good thing, in this case convergence, will eventually happen. A counterpart of liveness, safety, is a property that guarantees some bad event will not occur. Safety is of great significance in control systems, especially for those control systems that come in close contact with people. This dissertation investigated different ways to define safety in the context of control systems and methods to achieve the desired safety properties. Forward invariance of some safe set is commonly used in the literature as a metric of safety. Using CBFs, constraints on the state can be used to find control inputs that render the safe set forward invariant. In PBC works, safety refers to a more general notion of robust stability with respect to the environment, where the system does not generate energy but instead only dissipates the energy provided to it. Each of these notions of safety are considered to be weaker results than asymptotic stability. As a result, each of these methods can provide more flexibility in control design than Lyapunov-based methods.

Chapter 1 presented background on safety, CBFs, and PBC. It also explored some of the shortcomings of the two methods in the current literature. The main limitations of the approaches are that CBFs are general only useful for systems of relative degree one, uncertainty in the model dynamics or loss of state feedback can disrupt forward invariance guarantees or restrict the state to an operating region that is a subset of the safe set, CBFs are not well defined for control systems with hybrid dynamics, and state and passivity constraints cannot be incorporated into one optimization-based controller. Chapters 2, 3, and 4 of this dissertation developed methods to overcome three of the four limitations listed above.

In Chapter 2 a HOCBF method was developed to for systems that can be modeled by differential inclusions. The developed method can be applied to a more general class of systems than previous works with an arbitrarily high relative degree. The approach is then demonstrated on a rehabilitative cycling system to constrain the cycle crank position to some range about the desired position, representative of a constraint of relative degree two. Experimental results show that the developed approach is effective in maintaining the cycle crank's position between ± 30 degrees from the desired position while minimizing the control input. Minimizing the control input returns control authority back to the rider which helps to facilitate more effective therapy for individuals with NDs.

aDCBFs were introduced in Chapter 3, where an adaptive DNN is used to learn the unknown system dynamics in real time to render the safe set forward invariance while reducing conservative behavior by expanding the state's operating region. Updating the DNN weights in real-time, eliminates the need for pre-training. A least squares weight adaptation law is based on the error between the DNN estimate of the dynamics and a secondary observer's estimate of the dynamics. A Lyapunov-based analysis yields a convergent upper-bound of the parameter estimation error is used in the CBF constraint which expands the operating region as the DNN learns the system dynamics. The DNN can then be used to generate the estimate of the dynamics during intermittent loss of feedback. Based on the worst-case difference between the estimate of the state and the true state, the CBF constraint was reformulated to keep the state inside the safe set even if feedback is temporarily lost. Two simulation studies were provided with comparisons to baseline results in [25] and [48].

Chapter 4 unites PBC and CBFs by ensuring the closed-loop system is both passive with respect to an external disturbance and the safe set of states is forward invariant. The developed approach provides a set of controllers that will satisfy both the passivity and state constraints, without the design of an initially passivating nominal controller. From there, at each time step, a single controller is chosen from the set of

possible control inputs while minimizing some cost function. The developed approach is especially useful in human-machine interaction, where the robot controller should be designed to be both compliant to the person it is interacting with while satisfying some state constraints for safe operation. A simulation is provided to demonstrate how the developed approach works for this problem.

There are several potential avenues for future work. The results in Chapters 2 and 3 could be combined to design an adaptive DNN-based HOCBF. This would reduce the conservative behavior seen in Chapter 2, while allowing for systems of higher relative degree to be considered, unlike in Chapter 3. Extending the aDCBF approach to systems of higer relative degree would introduce additional challenges in the design of the DNN and weight adaptation law due to the potentially more complex higher-order dynamics. A high-order aDCBF approach could be applied to a variety of control problems, including the cycling position constraint investigated in Chapter 2, obstacle avoidance for air or ground robots, or a modified version of the ACC problem in Chapter 3.

Another potential future effort includes the extension of [65] to hybrid control systems such as the one in Section 1.8.2, which would be an especially impactful result. As discussed in Chapter 1, the work in [65] provides conditions on the control input that will result in the forward invariance and asymptotic stability of the safe set for a continuous closed-loop system, and the work in [69] provides a method of verifying the forward invariance and asymptotic stability of uncontrolled hybrid systems. There is a gap in the literature for the development of safety-ensuring controllers for hybrid dynamical systems. The hybrid control system case will require the consideration of discrete dynamics (that were not considered in [65]) and the design of a hybrid controller, which will broaden the application possibilities of the CBFs but complicate the theoretical development. The forward invariance guarantees will have to hold on both the flow and jump sets, so separate analyses will have to be done for each case. The

hybrid controller will not only need to ensure that $\sup_{f \in F(x,u)} \langle \nabla B(x), f \rangle \leq -\gamma_C(x)$ in the jump set C_u, but also that $\sup_{g \in G(x,u)} B(g) \leq -\gamma_D(x)$ in the jump set D_u. Furthermore, while there will be separate control laws on the flow and jump sets, the overall controller will need to be continuous to satisfy the hybrid basic conditions that enable the use of the results in [68] in the analysis. Once the theoretical results for CBFs are developed for hybrid control systems, the topics in Chapters 2, 3, and 4 for continuous control systems can be investigated for hybrid control systems.

This dissertation provided solutions for several limiting factors in the safe control systems literature. The dissertation provides a HOCBF method for general systems with constraints of arbitrarily high relative degree. It also provided the first result combining PBC and CBFs into one optimization-based controller, without the design of an initially passivitating controller, and the first result that uses CBFs with an adaptive DNN for system identification. Experimental and simulation results demonstrate the effectiveness of each of the developed methods. Future work should investigate the remaining limitations in these methods.

REFERENCES

[1] L. Lamport, “Proving the correctness of multiprocess programs,” *IEEE Trans. on Softw. Eng.*, vol. SE-3, no. 2, 1977.

[2] L. Lamport, “Basic concepts.” Advanced Course on Distributed Systems- Methods and Tools for Specification, ser. Lecture Notes in Computer Science, 1984.

[3] B. Alpern and F. B. Schneider, “Defining liveness,” *Inf. Process. Lett.*, 1985.

[4] M. Nagumo, “Ubeer die lage der intergrakurven gewhnlicher differentialgleichungen,” 1942.

[5] H. Brezis, “On a Characerization of Flow-Invariant Sets,” *Comm. P. Appl. Math.*, vol. XXIII, pp. 261–263.

[6] F. Blanchini, “Set Invariance in Control,” *Automatica*, vol. 35, no. 11, pp. 1747–1767, 1999.

[7] R. Abraham, J. E. Marsden, and T. Ratiu, *Manifolds, Tensor Analysis, and Applications*, vol. 75. Springer Science & Business Media, 2012.

[8] J.-M. Bony, “Principe du maximum, inégaliteé de Harnack et uniceité du problème de Cauchy pour les opérateurs elliptiques dégénérés,” *Annales de l´institut Fourier*, vol. 19, no. 1, pp. 277–304.

[9] S. Stramigioli, “Energy-aware robotics.” Mathematical Control Theory I ser. Lecture Notes in Control and Information Sciences, 2015.

[10] J. Zhang and C. C. Cheah, “Passivity and stability of human-robot interaction control for upper-limb rehabilitation robots,” *IEEE Trans. on Robot.*, vol. 31, no. 2, pp. 233–245, 2015.

[11] S. Prajna and A. Jadbabaie, “Safety verification of hybrid systems using barrier certificates,” in *International Workshop on Hybrid Systems: Computation and Control*, pp. 477–492, Springer, 2004.

[12] S. Prajna, “Barrier certificates for nonlinear model validation,” *Automatica*, 2006.

[13] S. Prajna, A. Jadbabaie, and G. J. Pappas, “A framework for worst-case and stochastic safety verification using barrier certificates,” *IEEE Transactions on Automatic Control*, vol. 52, no. 8, pp. 1415–1428, 2007.

[14] S. Prajna and A. Rantzer, “On the necessity of barrier certificates,” in *IFAC Proceedings Volumes*, vol. 38, pp. 526–531, 2005.

[15] S. Prajna, A. Jadbabaie, and G. J. Pappas, “A framework for worst-case and stochastic safety verification using barrier certificates,” *IEEE Trans. Automat. Cont.*, 2009.

[16] K. P. Tee, S. S. Ge, and E. H. Tay, “Barrier Lyapunov functions for the control of output-constrained nonlinear systems,” *Automatica*, vol. 45, no. 4, pp. 918–927, 2009.

[17] J.-P. Aubin, “A survey of viability theory,” *SIAM J. Control Optim.*, 1990.

[18] J.-P. Aubin, *Viability Theory*. Springer, 2009.

[19] J.-P. Aubin, A. M. Bayen, and P. Saint-Pierre, *Viability theory: new directions*. Springer Berlin, Heidelberg, 2011.

[20] P. Wieland and F. Allgöwer, “Constructive safety using control barrier functions,” *IFAC Proc. Vol.*, vol. 40, no. 12, pp. 462–467, 2007.

[21] M. Z. Romdlony and B. Jayawardhana, “Stabilization with guaranteed safety using control Lyapunov–barrier function,” *Automatica*, vol. 66, pp. 39–47, 2016.

[22] M. Z. Romdlony and B. Jayawardhana, “Uniting control lyapunov and control barrier functions,” in *53rd IEEE Conf. Decis. Control*, pp. 2293–2298, 2014.

[23] A. D. Ames, X. Xu, J. W. Grizzle, and P. Tabuada, “Control barrier function based quadratic programs for safety critical systems,” *IEEE Trans. Autom. Control*, vol. 62, no. 8, pp. 3861–3876, 2016.

[24] X. Xu, P. Tabuada, J. W. Grizzle, and A. D. Ames, “Robustness of control barrier functions for safety critical control,” *IFAC-PapersOnLine*, vol. 48, no. 27, pp. 54–61, 2015.

[25] A. D. Ames, J. W. Grizzle, and P. Tabuada, “Control barrier function based quadratic programs with application to adaptive cruise control,” in *IEEE Conf. Decision and Control*, pp. 6271–6278, IEEE, 2014.

[26] M. Jankovic, “Robust control barrier functions for constrained stabilization of nonlinear systems,” *Automatica*, vol. 96, pp. 359–367, 2018.

[27] U. Borrmann, L. Wang, A. D. Ames, and M. Egerstedt, “Control barrier certificates for safe swarm behavior,” *IFAC-PapersOnLine*, vol. 48, no. 27, pp. 68–73, 2015.

[28] L. Wang, A. D. Ames, and M. Egerstedt, “Safety barrier certificates for collisions-free multirobot systems,” *IEEE Trans. Robot.*, vol. 33, no. 3, pp. 661–674, 2017.

[29] P. Glotfelter, J. Cortés, and M. Egerstedt, “Nonsmooth barrier functions with applications to multi-robot systems,” *IEEE Control Syst. Lett.*, vol. 1, no. 2, pp. 310–315, 2017.

[30] A. Agrawal and K. Sreenath, “Discrete control barrier functions for safety-critical control of discrete systems with application to bipedal robot navigation,” *Robotics: Science and Systems*, 2017.

[31] A. Isaly, B. C. Allen, R. G. Sanfelice, and W. E. Dixon, “Encouraging volitional pedaling in FES-assisted cycling using barrier functions,” *Front. Robot. AI*, vol. 8, pp. 1–13, 2021. Special Issue on Safety in Collaborative Robotics and Autonomous Systems.

[32] S.-C. Hsu, X. Xu, and A. D. Ames, “Control barrier function based quadratic programs with application to bipedal robotic walking,” in *Proc. Am. Control Conf.*, pp. 4542–4548, 2015.

[33] G. Wu and K. Sreenath, “Safety-critical and constrained geometric control synthesis using control Lyapunov and control barrier functions for systems evolving on manifolds,” in *Proc. Am. Control Conf.*, pp. 2038–2044, 2015.

[34] W. Xiao and C. Belta, “High order control barrier functions,” *IEEE Trans. Automat. Contr.*, early access, 2021.

[35] T. Johnston, B. Smith, O. Oladeji, R. Betz, and R. Lauer, “Outcomes of a home cycling program using functional electrical stimulation or passive motion for children with spinal cord injury: a case series,” *J. Spinal Cord Med.*, vol. 31, no. 2, pp. 215–21, 2008.

[36] S. P. Hooker, S. F. Figoni, M. M. Rodgers, R. M. Glaser, T. Mathews, A. G. Suryaprasad, and S. C. Gupta, “Physiologic effects of electrical stimulation leg cycle exercise training in spinal cord injured persons,” *Arch. Phys. Med. Rehabil.*, vol. 73, no. 5, pp. 470–476, 1992.

[37] C. Rouse, C. A. Cousin, V. Duenas, and W. E. Dixon, “FES and motor assisted cycling to track power and cadence to desired voluntary bounds,” in *Proc. IFAC Conf. Cyber. Phys. Hum. Syst.*, pp. 34–39, 2018.

[38] A. Isaly, B. C. Allen, R. Sanfelice, and W. E. Dixon, “Zeroing control barrier functions for safe volitional pedaling in a motorized cycle,” in *IFAC Conf. Cyber-Phys. Hum.-Syst.*, 2020.

[39] K. J. Stubbs, A. Isaly, and W. E. Dixon, “Control barrier functions for safe teleoperation of a functional electric stimulation enabled rehabilitation system,” in *Proc. Am. Control Conf.*, pp. 4347–4352, June 2022.

[40] C. Rouse, C. Cousin, B. C. Allen, and W. E. Dixon, “Split-crank cadence tracking for switched motorized FES-cycling with volitional pedaling,” in *Proc. Am. Control Conf.*, pp. 4393–4398, 2019.

[41] A. J. Taylor and A. D. Ames, “Adaptive safety with control barrier functions,” in *Proc. Am. Control Conf.*, pp. 1399–1405, 2020.

[42] B. T. Lopez, J.-J. E. Slotine, and J. P. How, “Robust adaptive control barrier functions: An adaptive and data-driven approach to safety,” *IEEE Control Syst. Lett.*, vol. 5, no. 3, pp. 1031–1036, 2020.

[43] M. H. Cohen and C. Belta, “High order robust adaptive control barrier functions and exponentially stabilizing adaptive control Lyapunov functions,” in *Proc. Am. Control Conf.*, 2022.

[44] W. Xiao, C. A. Belta, and C. G. Cassandras, “Sufficient conditions for feasibility of optimal control problems using control barrier functions,” *Automatica*, vol. 135, p. 109960, 2022.

[45] A. Isaly, O. Patil, R. G. Sanfelice, and W. E. Dixon, “Adaptive safety with multiple barrier functions using integral concurrent learning,” in *Proc. Am. Control Conf.*, pp. 3719–3724, 2021.

[46] M. Srinivasan, A. Dabholkar, S. Coogan, and P. A. Vela, “Synthesis of control barrier functions using a supervised machine learning approach,” in *Int. Conf. Intell. Robots and Syst.*, pp. 7139–7145, 2020.

[47] R. Cheng, G. Orosz, R. M. Murray, and J. W. Burdick, “End-to-end safe reinforcement learning through barrier functions for safety-critical continuous control tasks,” in *Proc. AAAI Conf. Artif. Intell.*, vol. 33, pp. 3387–3395, 2019.

[48] A. Isaly, O. Patil, H. Sweatland, R. Sanfelice, and W. E. Dixon, “Adaptive safety with a RISE-based disturbance observer,” *IEEE Trans. Autom. Control*, vol. 69, no. 7, pp. 4883–4890, 2024.

[49] D. R. Agrawal and D. Panagou, “Safe and robust observer-controller synthesis using control barrier functions,” *IEEE Control Syst. Lett.*, vol. 7, pp. 127–132, 2010.

[50] A. Alan, T. G. Molnar, E. Das, A. D. Ames, and G. Orosz, “Disturbance observers for robust safety-critical control with control barrier functions,” *IEEE Control Syst. Lett.*, vol. 7, pp. 1123–1128, 2023.

[51] J. Sun, J. Yang, and Z. Zeng, “Safety-critical control with control barrier function based on disturbance observer,” *IEEE Trans. Autom. Control*, pp. 1–8, 2024.

[52] O. Patil, D. Le, M. Greene, and W. E. Dixon, “Lyapunov-derived control and adaptive update laws for inner and outer layer weights of a deep neural network,” *IEEE Control Syst Lett.*, vol. 6, pp. 1855–1860, 2022.

[53] E. Vacchini, N. Sacchi, G. P. Incremona, and A. Ferrara, “Design of a deep neural network-based integral sliding mode control for nonlinear systems under fully unknown dynamics,” *IEEE Control Syst. Lett.*, 2023.

[54] S. Li, H. T. Nguyen, and C. C. Cheah, “A theoretical framework for end-to-end learning of deep neural networks with applications to robotics,” *IEEE Access*, vol. 11, pp. 21992–22006, 2023.

[55] O. S. Patil, E. J. Griffis, W. A. Makumi, and W. E. Dixon, “Composite adaptive Lyapunov-based deep neural network (Lb-DNN) controller,” *arXiv preprint arXiv:1306.3432*, 2023.

[56] E. Griffis, O. Patil, W. Makumi, and W. E. Dixon, “Deep recurrent neural network-based observer for uncertain nonlinear systems,” in *IFAC World Congr.*, pp. 6851–6856, 2023.

[57] J. Breeden and D. Panagou, “High relative degree control barrier functions under input constraints,” in *Proc. IEEE Conf. Decis. Control*, 2021.

[58] W. S. Cortez and D. V. Dimarogonas, “Correct-by-design control barrier functions for Euler-Lagrange systems with input constraints,” in *Proc. Am. Cont. Conf.*, 2020.

[59] D. R. Agrawal and D. Panagou, “Safe control synthesis via input constrained control barrier functions,” in *2021 60th IEEE Conference on Decision and Control (CDC)*, pp. 6113–6118, IEEE, 2021.

[60] W. S. Cortez, X. Tan, and D. Dimarogonas, “A robust, multiple control barrier function framework for input constrained systems,” *IEEE Control Sys. Lett.*, 2021.

[61] T. Gurriet, A. Singletary, J. Reher, L. Ciarletta, E. Feron, and A. Ames, “Towards a framework for realizable safety critical control through active set invariance,” in *Proc ACM/IEEE Int. Conf. Cyber Phys. Syst.*, pp. 98–106, 2018.

[62] G. Blekherman, P. A. Parrilo, and R. R. Thomas, “Semidefinite optimization and convex algebraic geometry,” *SIAM*, 2012.

[63] X. Xu, J. W. Grizzle, P. Tabuada, and A. D. Ames, “Correctness guarantees for the composition of lane keeping and adaptive cruise control,” *IEEE Trans. Automat. Cont.*, 2018.

[64] P. Glotfelter, J. Cortes, and M. Egerstedt, “A nonsmooth approach to controller synthesis for boolean specifications,” *IEEE Trans. Autom. Control*, 2020.

[65] A. Isaly, M. Mamaghani, R. G. Sanfelice, and W. E. Dixon, “On the feasibility and continuity of feedback controllers defined by multiple control barrier functions,” *IEEE Trans. Autom. Control*, vol. 69, no. 11, pp. 7326 – 7339, 2024.

[66] A. Isaly, M. Ghanbarpour, R. G. Sanfelice, and W. E. Dixon, “On the feasibility and continuity of feedback controllers defined by multiple control barrier functions,” in *Proc. Am. Control Conf.*, pp. 5160–516, June 2022.

[67] R. Goebel, R. G. Sanfelice, and A. R. Teel, *Hybrid Dynamical Systems*. Princeton University Press, 2012.

[68] R. G. Sanfelice, *Hybrid Feedback Control*. Princeton University Press, 2021.

[69] M. Maghenem and R. G. Sanfelice, “Sufficient conditions for forward invariance and contractivity in hybrid inclusions using barrier functions,” *Automatica*, vol. 124, 2021.

[70] E. Guillemin, “Transformation theory applied to linear active and/or nonbilateral networks,” *IRE Trans. Circuit Theory*, 1957.

[71] L. Weinberg, “Progress in circuit theory - 1960-1963,” *IEEE Trans. Circuit Theory*, 1964.

[72] R. E. Kalman, “Lyapunov functions for the problem of lur’e in automatic control,” in *Proceedings of the national academy of sciences*, vol. 49, pp. 201–205, 1963.

[73] V. A. Yakubovich, “Absolute stability of nonlinear control in critical cases-part I,” *Automat. Remote Contr.*, 1963.

[74] V. M. Popov, “Hyperstability and optimality of automatic systems with several control functions,” *Re. Roum. Sci. Tech., Ser. Electrotech. Energ.*, 1964.

[75] N. Kottenstette, M. J. McCourt, M. Xia, V. Gupta, and P. J. Antsaklis, “On relationships among passivity, positive realness, and dissipativity in linear systems,” *Automatica*, vol. 50, no. 4, pp. 1003–1016, 2014.

[76] J. C. Willems, “Dissipative dynamical systems part I: General theory,” *Arch. Rational Mech. Anal.*, vol. 45, pp. 321–351, Jan. 1972.

[77] J. C. Willems, “Dissipative dynamical systems part II: Linear systems with quadratic supply rates,” *Arch. Rational Mech. Anal.*, vol. 45, no. 5, pp. 352–393, 1972.

[78] P. Moylan, “Implications of passivity in a class of nonlinear systems,” *IEEE Trans. Autom. Control*, 1974.

[79] H. K. Khalil, *Nonlinear Systems*. Prentice Hall, 3 ed., 2002.

[80] D. Hill and P. Moylan, “The stability of nonlinear dissipative systems,” *IEEE Trans Autom. Contol*, vol. 21, pp. 708–711, Oct. 1976.

[81] J. E. Colgate, “Coupled stability of multiport systems- theory and experiments,” *J. Dyn. Sys., Meas., Control.*, pp. 419–428, Sept. 1994.

[82] C.-Y. Su, T. P. Leung, and Q.-J. Zhou, “A novel variable structure control scheme for robot trajectory control,” in *Proc. IFAC World Congress*, vol. 9, pp. 121–124, 1990.

[83] M. W. Spong, “On the robust control of robot manipulators,” *IEEE Trans. Aut. Cont.*, vol. 37, no. 11, pp. 1782–1786, 1992.

[84] J.-J. Slotine and W. Li, “Adaptive robot control: A new perspective,” in *Proc. IEEE Conf. Decis. Control*, pp. 192–198, Dec. 1987.

[85] I. Landau and R. Horowitz, “Synthesis of adaptive controllers for robot manipulators using a passive feedback systems approach,” in *Proc. IEEE Int. Conf. Robot. Autom.*, pp. 1028–1033, Apr. 1988.

[86] S. Arimoto and T. Naniwa, “Learnability and adaptability from the viewpoint of passivity analysis,” *Intelligent Automation and Soft Computing*, vol. 8, no. 2, pp. 71–94, 2002.

[87] R. Ortega and M. W. Spong, “Adaptive control of robot manipulators: a tutorial,” *Automatica*, 1989.

[88] R. Ortega, A. Loría, P. J. Nicklasson, and H. J. Sira-Ramirez, *Passivity-based Control of Euler-Lagrange Systems: Mechanical, Electrical and Electromechanical Applications*. Springer, 1998.

[89] A. van der Schaft, “Port-Hamiltonian systems: an introductory survey,” in *Proc. Int. Congr. Math.*, 2006.

[90] W. Chen and M. Saif, “Passivity and passivity based controller design of a class of switched control systems,” in *Proc. Preprints 16th IFAC World Congress*, pp. 143–147, July 2005.

[91] P. J. Nicklasson, R. Ortega, G. Espinosa-Perez, and C. G. J. Jacobi, “Passivity-based control of a class of Blondel-Park transformable electric machines,” *IEEE Trans. Autom. Control*, 1997.

[92] G. Espinosa-Perez, P. Maya-Ortiz, M. Velasco-Villa, and H. Sira-Ramirez, “Passivity-based control of switched reluctance motors with nonlinear magnetic circuits,” *IEEE Trans. Control Syst. Technol.*, 2004.

[93] H. Sira-Ramirez and M. I. Angulo-Nunez, “Passivity-based control of nonlinear chemical processes,” *Int. J. Control*, 2010.

[94] Z. Liu, R. Ortega, and H. Su, “Stabilisation of nonlinear chemical processes via dynamic power-shaping passivity-based control,” *Int. J. Control*, 2009.

[95] M. W. Spong, J. K. Holm, and D. Lee, “Passivity-based control of bipedal locomotion,” *IEEE Robot. Autom. Mag.*, 2007.

[96] M. Franken, S. Stramigioli, S. Misra, C. Secchi, and A. Macchelli, “Bilateral telemanipulation with time delays: a two-layer approach combining passivity and transparency,” *IEEE Trans. Robot.*, 2011.

[97] C. I. Byrnes, A. Isidori, and J. C. Willems, “Passivity, feedback equivalence, and the global stabilization of minimum phase nonlinear systems,” *IEEE Trans Autom. Contol*, vol. 36, no. 11, pp. 1228–1240, 1991.

[98] R. Ortega, A. J. V. der Schaft, I. Mareels, and B. Maschke, “Putting energy back in control,” *IEEE Control Sys.*, vol. 21, no. 2, pp. 18–33, 2001.

[99] S. Arimoto and M. Takegaki, “A new feedback method for dynamic control of manipulators,” *J. Dyn. Sys., Meas., Control*, vol. 102, pp. 119–125, 1981.

[100] A. Ailon and R. Ortega, “An observer-based controller for robot manipulators with flexible joints,” *Syste. Control Lett.*, 1993.

[101] R. Kelly, “Regulation of manipulators in generic task space: An energy shaping plus damping injection approach,” *IEEE Trans. Robot. Autom.*, vol. 15, no. 2, pp. 381–386, 1999.

[102] E. Nuño, R. Ortega, B. Jayawardhana, and L. Basañez, “Coordination of multi-agent Euler-Lagrange systems via energy-shaping: Networking improves robustness,” *Automatica*, vol. 49, pp. 3065–3071, Oct. 2013.

[103] R. Sipahi, S.-i. Niculescu, C. T. Abdallah, W. Michiels, and K. Gu, “Stability and stabilization of systems with time delay,” *IEEE Cont. Syst. Mag.*, vol. 31, no. 1, pp. 38–65, 2011.

[104] R. Anderson and M. Spong, “Bilateral control of teleoperators with time delay,” *IEEE Trans. Autom. Control*, vol. 34, pp. 494–501, May 1989.

[105] G. Niemeyer and J.-J. Slotine, “Stable adaptive teleoperation,” *IEEE J. Oceanic. Eng.*, vol. 16, pp. 152–162, 1991.

[106] M. Mahmoud and A. Ismail, “Passivity and passification of time-delay systems,” *J. Math. Anal. Appl.*, 2004.

[107] C. Li and X. Liao, “Passivity analysis of neural networks with time delay,” *IEEE Trans. Circuits Syst. II*, 2005.

[108] T. Hulin, A. Albu-Schaffer, and G. Hirzinger, “Passivity and stability boundaries for haptic systems with time delay,” *IEEE Trans. Control Syst. Technol.*, 2014.

[109] G. Niemeyer and J.-J. Slotine, “Telemanipulation with time delays,” *Int. J. Robot. Res.*, vol. 23, pp. 873–890, 2004.

[110] P. F. Hokayem and M. W. Spong, “Bilateral teleoperation: An historical survey,” *Automatica*, vol. 42, pp. 2035–2057, Dec. 2006.

[111] N. Chopra, M. Spong, and R. Lozano, “Synchronization of bilateral teleoperators with time delay,” *Automatica*, vol. 44, no. 8, pp. 2142–2148, 2008.

[112] N. Chopra and M. W. Spong, “Passivity-based control of multi-agent systems,” *Advances in Robot Control*, 2008.

[113] A. L. Fradkov and D. J. Hill, “Exponential feedback passivity and stabilizability of nonlinear systems,” *Automatica*, vol. 34, no. 6, pp. 697–703, 1998.

[114] J. Zhao and D. J. Hill, “A notion of passivity for switched systems with state-dependent switching,” *Journal of Control Theory and Applications*, vol. 4, no. 1, pp. 70–75, 2006.

[115] J. Zhao and D. J. Hill, “Passivity and stability of switched systems: A multiple storage function method,” *Syst. Control Lett.*, vol. 57, no. 2, pp. 158–164, 2008.

[116] B. Brogliato, R. Lozano, B. Maschke, and O. Egeland, *Dissipative Systems Analysis and Control: Theory and Applications*. Springer-Verlag London Ltd, 2nd ed., 2007.

[117] J. Mareczek, M. Buss, and M. W. Spong, “Invariance control for a class of cascade nonlinear systems,” *IEEE Trans. Autom. Control*, 2002.

[118] W. M. Haddad, V. Chellaboina, and N. A. Kablar, “Non-linear impulsive dynamical systems. part i: Stability and dissipativity,” *Int. J. Control*, vol. 74, no. 17, pp. 1631–1658, 2001.

[119] W. M. Haddad and Q. Hui, “Energy dissipating hybrid control for impulsive dynamical systems,” *Nonlinear Anal.*, 2008.

[120] M. Zefran, F. Bullo, and M. Stein, “A notion of passivity for hybrid systems,” in *Proc. IEEE Conf. Decis. Control*, 2001.

[121] R. Naldi and R. G. Sanfelice, “Passivity-based control for hybrid systems with applications to mechanical systems exhibiting impacts,” *Automatica*, 2013.

[122] A. R. Teel, “Asymptotic stability for hybrid systems via decomposition, dissipativity, and detectability,” in *Proc. IEEE Conf. Decis. Control*, 2010.

[123] M. Spong and F. Bullo, “Controlled symmetries and passive walking,” *IEEE Trans. Automat. Control*, vol. 50, no. 7, pp. 1025–1031, 2005.

[124] A. Bemporad, G. Bianchini, and F. Brogi, “Passivity analysis and passification of discrete-time hybrid systems,” *IEEE Trans. on Automat. Control*, vol. 53, no. 4, pp. 1004–1009, 2008.

[125] A. D. Ames, S. Coogan, M. Egerstedt, G. Notomista, K. Sreenath, and P. Tabuada, “Control barrier functions: Theory and applications,” in *Proc. Eur. Control Conf.*, pp. 3420–3431, 2019.

[126] F. Califano, R. Rashad, C. Secchi, and S. Stramigioli, “On the use of energy tanks for robotic systems,” in *Int. Workshop Hum.-Friendly Robot.*, 2023.

[127] B. Capelli, C. Secchi, and L. Sabattini, “Passivity and control barrier functions: optimizing the use of energy,” *IEEE Robot. Autom. Lett.*, 2022.

[128] G. Notomista, X. Cai, J. Yamauchi, and M. Egerstedt, “Passivity-based decentralized control of multi-robot systems with delays using control barrier functions,” in *Proc. Int. Symp. Multi-Robot. Multi-Agent Syst.*, 2019.

[129] F. Califano, “Passivity-preserving safety-critical control using control barrier functions,” *IEEE Control Syst. Lett.*, vol. 7, pp. 1742–1747, 2023.

[130] Z. Dong and D. Angeli, “Analysis of economic model predictive control with terminal penalty functions on generalized optimal regimes of operation,” *International Journal of Robust and Nonlinear Control*, vol. 28, no. 16, pp. 4790–4815, 2018.

[131] M. Lazar, “Stabilization of discrete time nonlinear systems based on control dissipation functions,” in *2021 60th IEEE Conference on Decision and Control (CDC)*, pp. 3179–3185, 2021.

[132] C. T. Landi, F. Ferraguti, S. Costi, M. Bonfe, and C. Secchi, “Safety barrier functions for human-robot interaction with industrial manipulators,” in *Proc. European Control Conference*, 2019.

[133] F. Ferraguti, C. T. Landi, S. Costi, M. Bonfè, S. Farsoni, C. Secchi, and C. Fantuzzi, “Safety barrier functions and multi-camera tracking for human–robot shared environment,” *Rob. Auton. Syst.*, vol. 124, p. 103388, 2020.

[134] T. Gurriet, M. Tucker, A. Duburcq, G. Boeris, and A. Ames, “Towards variable assistance for lower body exoskeletons,” *IEEE Robot. Autom. Lett.*, 2019.

[135] D.-P. Tan, G.-Z. Cao, Y.-P. Zhang, J.-C. Chen, and L.-L. Li, “Safe movement planning with DMP and CBF for lower limb rehabilitation,” in *Proc. Int. Conf. Ubiquitous Robot.*, 2022.

[136] E. Griffis, W. Makumi, H. Sweatland, K. Stubbs, T. Taivassalo, D. Lott, and W. E. Dixon, “Control barrier functions for safe admittance control of a rehabilitation cycle for dmd,” in *Proc. IEEE Conf. Control Tech. Appl.*, pp. 1074–1079, Aug. 2022.

[137] I. Tezuka and H. Nakamura, “Strict zeroing control barrier function for continuous safety assist control,” *IEEE Cont. Syst. Lett.*, 2022.

[138] W. S. Cortez, C. K. Verginis, and D. Dimarogonas, “Safe, passive control for mechanical systems with application to physical human-robot interactions,” in *IEEE International Conference on Robotics and Automation*, 2021.

[139] P. J. Antsaklis, B. Goodwine, V. Gupta, M. J. McCourt, Y. Wang, P. Wu, M. Xia, H. Yu, and F. Zhu, “Control of cyberphysical systems using passivity and dissipativity based methods,” *Europ. J. Control*, vol. 19, no. 5, pp. 379–388, 2013.

[140] B. Siciliano and L. Villani, “A passivity-based approach to force regulation an motion control of robot manipulators,” *Automatica*, 1996.

[141] C. T. Landi, F. Ferraguti, C. Fantuzzi, and C. Secchi, “A passivity-based strategy for coaching human robot interaction,” in *Proc. IEEE Conf. Robot. Autom.*, 2018.

[142] D. Papageorgiou, T. Kastritsi, Z. Doulgeri, and G. A. Rovithakis, “A passive pHRI controller for assisting the user in partially known tasks,” *IEEE Trans. Robot.*, 2020.

[143] S. Music and S. Hirche, “Passive noninteracting control for human-robot team interaction,” in *Proc. IEEE Conf. Dec. Cont.*, 2018.

[144] A. van der Schaft, *L2-gain and passivity techniques in nonlinear control*. Springer International Publishing, 2017.

[145] A. Zacharaki, I. Kostavelis, A. Gasteratos, and I. Dokas, “Safety bounds in human robot interaction: a survey,” *Safety Sci.*, 2020.

[146] A. J. del Ama, Á. Gil-Agudo, J. L. Pons, and J. C. Moreno, “Hybrid fes-robot cooperative control of ambulatory gait rehabilitation exoskeleton,” *J. Neuroeng. Rehabil.*, vol. 11, no. 1, p. 27, 2014.

[147] A. Q. Keemink, H. van der Kooij, and A. H. Stienen, “Admittance control for physical human–robot interaction,” *Int. J. Rob. Res.*, vol. 37, no. 11, pp. 1421–1444, 2018.

[148] S. Banala, S. Agrawal, and A. Fattah, “Gravity-balancing leg orthosis and its performance evaluation,” *IEEE Trans. Robot.*, 2007.

[149] S. Banala, S. Kim, S. Agrawal, and J. Scholz, “Robot assisted gait training with active leg exoskeleton (ALEX),” *IEEE Trans. Neural Syst. Rehabil. Eng.*, vol. 17, pp. 2–8, Feb 2009.

[150] J. Lin, N. V. Divekar, G. C. Thomas, and R. D. Gregg, “Optimally biomimetic passivity-based control of a lower-limb exoskeleton over the primary activities of daily life,” *IEEE Open J. Control Syst.*, vol. 1, pp. 15–28, 2022.

[151] C. Rouse, C. A. Cousin, B. C. Allen, and W. E. Dixon, “Shared control for switched motorized FES-cycling on a split-crank cycle accounting for muscle control input saturation,” *Automatica*, vol. 123, pp. 1–11, 2021.

[152] C. Rouse, R. Downey, C. Gregory, C. Cousin, V. Duenas, and W. E. Dixon, “FES cycling in stroke: Novel closed-loop algorithm accommodates differences in functional impairments,” *IEEE Trans. Biomed. Eng.*, vol. 67, no. 3, pp. 738–749, 2020.

[153] C. Rouse, C. Cousin, V. H. Duenas, and W. E. Dixon, “Cadence tracking for switched FES cycling combined with voluntary pedaling and motor resistance,” in *Proc. Am. Control Conf.*, pp. 4558–4563, 2018.

[154] D. S. Bernstein, *Matrix Mathematics*. Princeton university press, 2009.

[155] J. Chai and R. G. Sanfelice, "On notions and sufficient conditions for forward invariance of sets for hybrid dynamical systems," in *2015 54th IEEE Conference on Decision and Control (CDC)*, pp. 2869–2874.

[156] O. S. Patil, D. M. Le, E. Griffis, and W. E. Dixon, "Deep residual neural network (ResNet)-based adaptive control: A Lyapunov-based approach," in *Proc. IEEE Conf. Decis. Control*, pp. 3487–3492, 2022.

[157] E. Griffis, O. Patil, Z. Bell, and W. E. Dixon, "Lyapunov-based long short-term memory (Lb-LSTM) neural network-based control," *IEEE Control Syst. Lett.*, vol. 7, pp. 2976–2981, 2023.

[158] J. P. Aubin and H. Frankowska, *Set-valued analysis*. Birkhäuser, 2008.

[159] M. J. Bellman, R. J. Downey, A. Parikh, and W. E. Dixon, "Automatic control of cycling induced by functional electrical stimulation with electric motor assistance," *IEEE Trans. Autom. Science Eng.*, vol. 14, pp. 1225–1234, April 2017.

[160] J. Raymond, G. Davis, M. Climstein, and J. Sutton, "Cardiorespiratory responses to arm cranking and electrical stimulation leg cycling in people with paraplegia," *Med. Sci. Sports Exerc.*, vol. 31, pp. 822–28, June 1999.

[161] P. Kidger and T. Lyons, "Universal approximation with deep narrow networks," in *Conf. Learn. Theory*, pp. 2306–2327, 2020.

[162] F. L. Lewis, A. Yesildirek, and K. Liu, "Multilayer neural-net robot controller with guaranteed tracking performance," *IEEE Trans. on Neural Netw.*, vol. 7, no. 2, pp. 388–399, 1996.

[163] K. Kawaguchi, "Deep learning without poor local minima," *NeurIPS*, vol. 29, 2016.

[164] H. Lu and K. Kawaguchi, "Depth creates no bad local minima," *arXiv preprint arXiv:1702.08580*, 2017.

[165] S. Du, J. Lee, Y. Tian, A. Singh, and B. Poczos, "Gradient descent learns one-hidden-layer CNN: Dont be afraid of spurious local minima," in *Proc. 35th Int. Conf. Mach. Learn.*, vol. 80, pp. 1339–1348, Jul 2018.

[166] K. Kawaguchi and Y. Bengio, "Depth with nonlinearity creates no bad local minima in resnets," *Neural Netw.*, vol. 118, pp. 167–174, 2019.

[167] I. Goodfellow, Y. Bengio, A. Courville, and Y. Bengio, *Deep Learning*, vol. 1. MIT press Cambridge, 2016.

[168] R. Hart, O. Patil, E. Griffis, and W. E. Dixon, "Deep Lyapunov-based physics-informed neural networks (DeLb-PINN) for adaptive control design," in *Proc. IEEE Conf. Decis. Control*, pp. 1511–1516, 2023.

[169] M. Krstic, I. Kanellakopoulos, and P. V. Kokotovic, *Nonlinear and Adaptive Control Design*. New York: John Wiley & Sons, 1995.

[170] J. J. Slotine and W. Li, "Composite adaptive control of robot manipulators," *Automatica*, vol. 25, pp. 509–519, July 1989.

[171] H.-Y. Chen, Z. Bell, P. Deptula, and W. E. Dixon, "A switched systems approach to path following with intermittent state feedback," *IEEE Trans. Robot.*, vol. 35, no. 3, pp. 725–733, 2019.

[172] A. Parikh, T.-H. Cheng, H.-Y. Chen, and W. E. Dixon, "A switched systems framework for guaranteed convergence of image-based observers with intermittent measurements," *IEEE Trans. Robot.*, vol. 33, pp. 266–280, April 2017.

[173] A. Parikh, R. Kamalapurkar, and W. E. Dixon, "Integral concurrent learning: Adaptive control with parameter convergence using finite excitation," *Int J Adapt Control Signal Process*, vol. 33, pp. 1775–1787, Dec. 2019.

BIOGRAPHICAL SKETCH

Hannah Marie Sweatland grew up in Green Cove Springs, Florida. She received her Bachelor of Science (B.S.) degree from the Department of Mechanical and Aerospace Engineering at the University of Florida in May 2020. In August 2020, Hannah joined the Nonlinear Controls and Robotics Laboratory at the University of Florida under the supervision of Dr. Warren Dixon to pursue her Ph.D. She received her Master of Science (M.S.) degree in mechanical engineering in May 2022. Hannah's research focuses on ensuring the safety of nonlinear and uncertain dynamical systems through the use of control barrier functions and passivity-based control.